9-1-1992

Evaluation of Mechanical Properties of Welded TMCP Jumbo Sections

E. J. Kaufmann

John W. Fisher

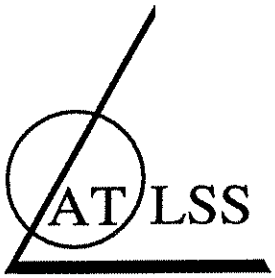

ADVANCED TECHNOLOGY FOR
LARGE
STRUCTURAL SYSTEMS

Lehigh University

Evaluation of Mechanical Properties of Welded TMCP Jumbo Sections

AWI 9126
Weldability of QST Jumbo Sections

Final Report

Prepared for
American Welding Institute
Project #9126
Sub-Contract #30-007-90

by

E. J. Kaufmann
Research Engineer

J. W. Fisher
Director, ATLSS

ATLSS Report No. 92 -06

September 1992

ATLSS Engineering Research Center
Lehigh University
117 ATLSS Dr., Imbt Laboratories
Bethlehem, PA 18015-4729
(215) 758-3525

An NSF Sponsored Engineering Research Center

ABSTRACT

As part of a study by the American Welding Institute to evaluate the weldability of quenched and self tempered (QST) rolled beams manufactured by ARBED S.A. in Luxembourg, the mechanical properties of a series of full section weld splices fabricated from W14 X 730 jumbo sections were examined. Although the QST produced Grade 65 material satisfies the composition and mechanical property requirements of ASTM A572 Grade 65 for all thicknesses, the current specification does not include Group 4 and 5 shapes at this strength level. Also construction codes exclude Grade 65 from use in certain seismic applications. Finally the AWS D1.1 Structural Welding Code does not recognize the no-preheat option of QST produced material. The study aimed at providing test data which can be used by code writing bodies.

Six weld splices were fabricated by a structural steel fabricator using several weld processes including SMAW, FCAW, and SAW over a range of heat inputs from 38 KJ/in. (1.5 KJ/mm) to 200 KJ/in. (7.9 KJ/mm). Weld joint preparation followed AISC Requirements for Heavy Shapes. All welding was performed without the use of preheat.

Evaluation of the weld joints followed AWS and AISC for procedure qualification and included full flange thickness tensile tests, side bend tests, and Charpy V-Notch tests of the weld metal, base metal, and heat-affected zone at the test position specified in the AISC Requirements for Heavy Shapes and at locations throughout the flange cross-section. A microstructure and hardness survey of the flange at each test position was also obtained.

No evidence of cracking was found in any of the weld splices welded without preheat. All of the weld splices satisfied the AWS procedure qualification requirements. Charpy V-Notch tests of the weld metal, base metal, and HAZ in all of the weld joints satisfied the AISC requirement. Absorbed energies in the base metal ranged from 62 ft-lbs @ 0°C (84 J) at the web-flange intersection to as high as 239 ft-lbs @ 0°C (324 J) near the flange surface. Charpy V-Notch energies in the HAZ were reduced, particularly at the highest heat inputs, but well in excess of base metal requirements.

The test results show that QST jumbo sections can be welded without preheat and produce weld joints with adequate mechanical properties. Results also show that the fracture toughness of QST rolled beams is high and should significantly reduce the possibility of fracture in these members.

TABLE OF CONTENTS

	Page
Abstract	
Introduction	1
Background	2
Base Material	3
Weld Joints	3
Test Specimen Layout	3
Test Results	
Tension Tests	4
Side Bend Tests	5
Weld Metal Charpy V-Notch Tests	5
Base Metal Charpy V-Notch Tests	5
Base Metal Microstructure and Hardness	6
HAZ Charpy V-Notch Tests	6
Summary	7
References	9
Tables	
Figures	
Appendix A	
Microstructures	

I. Introduction

As part of a study by the American Welding Institute (AWI 9126) to evaluate the weldability of quenched and self-tempered (QST) jumbo sections currently produced by ARBED in Luxembourg, the ATLSS Center at Lehigh University was requested to perform an evaluation of the mechanical properties of a series of full section weld splices fabricated from W14 X 730 rolled sections. The thermomechanical controlled process (TMCP) material satisfied the physical property requirements of ASTM A572 Grade 65 although the current specification does not include Group 4 and 5 shapes at this strength level. The advantages of thermomechanical controlled processing of steels have become increasingly recognized in recent years due primarily to the reduction in carbon content which is possible without sacrificing strength and the corresponding improvement in weldability and fracture toughness. The weld splices evaluated in this study were fabricated by a structural steel fabricator using several weld processes which fabricators would likely consider for joining these members including SMAW, FCAW, and SAW and encompassed a range of heat inputs from 38 KJ/in. (1.5 KJ/mm) to 200 KJ/in. (7.9 KJ/mm). The five inch thick flange splices and three inch thick web splices were fabricated without the application of preheat and were welded under a moderate degree of restraint. Details of the joint design, welding procedure, and fabrication sequence are covered in AWI Report 91-002.

Evaluation of the weld joints followed AWS D1.1[1] and AISC[2] for procedure qualification and included full flange thickness tensile tests, side bend tests, and Charpy V-Notch fracture toughness tests of the weld metal, base metal, and the heat-affected zone (HAZ) at the position specified in the requirements for heavy shapes subject to primary tensile stresses of Supplement No. 1 to the AISC LRFD Specification, First Edition and Section 5.A3.1.c of the AISC ASD Specification, Ninth Edition (subsequently referred to as the AISC Requirements for Heavy Shapes). This position is specified as the intersection of the flange quarter thickness (measured from the inner flange surface) and the web mid-thickness. As the study proceeded, a more extensive evaluation of the fracture characteristics of the base metal and HAZ of the weld joints was undertaken. Due to the nature of the QST process whereby the thermomechanical controlled rolled shape is first selectively cooled in the vicinity of the web-flange intersection followed by in-line quenching and self-tempering, a variety of microstructures and properties could be obtained throughout the beam cross-section. Consequently the fracture characteristics of a total of twenty locations within the flange (five positions across the flange width and four depths beneath the flange surface) were evaluated by generating CVN data in the transition region at each location. This effectively mapped the fracture characteristics over the full flange cross-section. To supplement this data, a microstructural and hardness survey of the material at each position was also obtained.

II. Background

With the increased use of jumbo rolled sections in building columns and trusses during the past decade, a number of instances of cracking were observed as well. The cracking, which in some cases resulted in complete fracture of the member, tended to occur in the heavier W12 and W14 sections of A572 Grade 50 (as large as 730 lb/ft) but was also observed in sections as light as 370 lb/ft. Similar cracking has also been observed in built-up members fabricated from thick plate. The cracking has been associated with both complete penetration and partial penetration groove welded splices in column and truss members. Investigations of the cracking, and toughness tests performed on a variety of other jumbo member sizes, has shown that the notch toughness of these members in the region of the web-flange intersection and at the mid-thickness of the flange and web can be low.[3,4] Charpy V-notch impact energies in the core region (web-flange intersection) have been measured under 20 ft-lbs @ 20°C and in some cases below 10 ft-lbs at 20°C. Static fracture toughness tests have shown K_{IC} in the core region can be in the range of 40-60 Ksi(in)$^{1/2}$ (44-66 MPa(m)$^{1/2}$) in the temperature range of 50-100°F (10-38°C). Welding defects and discontinuities associated with flame cut surfaces or weld terminations in this region were found to initiate fracture which propagated into the low toughness region under the combination of welding residual stress and applied load or residual stress alone.

Fracture mechanics analyses show[4] that with this low level of fracture toughness in the core region and welding residual stresses approaching the yield point of the material, tolerable defect sizes in this area are too small to be readily detected by NDE, particularly in a large thickness member, but are within the allowable sizes permitted by AWS D1.1. Thus it is possible that defects unacceptable in size from a fracture safety viewpoint would be permitted after even careful inspection, provided they were not identified as cracks.

The metallurgical reasons for poor toughness in the core region of conventionally hot rolled jumbo shapes stems from their size and method of fabrication as well as from compositional and segregation effects. The limited hot work which the core region undergoes in such heavy sections and high rolling temperatures can leave this region with a coarse, low toughness, prior austenite microstructure even if the material is manufactured to fine grain practice. Ingot segregation also results in different compositions and properties at different ends of the rolled shape which can result in low toughness at the ends of some members.[5]

Recognition of these factors led to Supplement No. 2 to the AISC Steel Construction Manual in 1989 where minimum CVN energies at the web-flange intersection (20 ft-lbs @ 70° F) were established in addition to requirements for cope hole geometries and thermal cut surfaces. Although a good welding procedure and adequate inspection are essential ingredients in producing sound weldments and will have the effect of reducing defect size, they will have little effect on the inherent low toughness of the base material. Thermomechanical controlled processing offers the possibility of improving the fracture properties of jumbo sections, particularly in the core region, by accelerating the cooling rates in this area resulting in a finer grained, higher toughness microstructure. The elevation in strength resulting from this processing also permits lower carbon content and hence improves weldability as well.[6]

III. Base Material

Material for the beam splices consisted of rolled W14 X 730 wide flange sections, each segment cut to approximately 6.5 feet (2m) in length. The segments were rolled from two heats of material, the identification of which was maintained throughout the beam splice fabrication stage. Table I shows the composition and mechanical properties of the two heats (Heat No. 89322-9009 and 89322-9041). Both heats of material satisfy the compositional and mechanical property requirements of ASTM A572 Grade 65. The carbon equivalent of the material calculates (IIW formula) to be 0.40 (Heat 89322-9009) and 0.39 (Heat 89322-9041). The relatively low CE is largely due to the low carbon contents seen in Table I.

IV. Weld Joints

Six full section splices were fabricated from the beam segments using the SMAW, FCAW, and SAW processes at several heat inputs. Material from Heat No. 89322-9009 was used for the SMAW and FCAW splices. Material from Heat No. 89322-9041 was used for the SAW beam splices. This provided two duplicate flanges for each weld process/heat input.Table II provides a listing of the weld joint designations as well as the base metal heat number, weld process, heat input, and filler metal used to fabricate the beam splice. Due to material shortage, a web splice (8W) was later substituted for one of the 50 KJ/in. (2 KJ/mm) SAW splices. Tensiles, side bends, and weld metal Charpy V-Notch specimens were fabricated from one flange weld joint and the other was used entirely for CVN fracture toughness testing of the base metal and HAZ at various positions across the flange cross-section. Details of the welding procedure are provided in AWI Report 91-002.

After completion of the beam splices and NDE tests, the flanges and webs were cut from the beams and delivered to Lehigh University for fabrication and testing of test specimens. Figures 1-5 show etched cross-sections of each type of flange splice weld. Insufficient material prevented preparation of a cross-section for the web splice (8W). The cross-sections appear sound and show few weld defects and no evidence of HAZ cracking. The full thickness tensile tests further verified the soundness of the weld joint.

V. Test Specimen Layout

Full flange thickness tensiles, side bends, and weld metal Charpy V- notch specimens were fabricated from one of each of the types of weld joints as sketched in Figure 6. The layout of specimens for the SAW 50 KJ/in. (2 KJ/mm) weld joint, fabricated from a web splice, is shown in Figure 7. The test specimen design and layout followed the AWS D1.1 procedure qualification guidelines.

As indicated earlier, an expanded test program for the evaluation of the fracture characteristics of the base metal and HAZ was initiated after the study commenced. In addition to testing Charpy V-notch specimens at the position specified in the AISC Requirements for Heavy Shapes (the intersection of the flange mid-width and the 1/4 thickness measured from the inside flange surface), additional testing was performed at 19 other positions within the flange cross-section as shown in Figure 8. Five positions across the flange width (1/6W, 1/4W, 1/2W, 1/4W, 1/6W) and four positions below the outside flange surface (Near Surface, 1/4T, 1/2T, 3/4T) were chosen. The position specified in the AISC Requirements for Heavy Shapes corresponds to the 1/2W - 3/4T position. To distinguish between identical positions with respect to the web centerline, the test positions were further identified as Pos.1 or Pos.2. Twelve base metal CVN specimens were fabricated at each of the 20 positions which provided sufficient specimens to construct a base metal transition curve at each position. Since two heats of material were used (Heat No. 89322-9009 and 89322-9041),an identical series of base metal CVNs were tested from a beam rolled from each heat. Because of the uniqueness of each test location, a maximum of three HAZ specimens could be fabricated at each position. Specimens were notched 0.25-0.50 mm from the fusion line corresponding to the coarse grained HAZ. Specimens were fabricated at each of the twenty positions for five types of weld joints (FCAW-40KJ/in.,FCAW-75KJ/in.,SAW-50KJ/in.,SAW-100KJ/in.,SAW-200KJ/in.).

VI. Test Results

A. Tension Tests

The two full flange thickness tensile test specimens fabricated from each flange splice were tested in an 800 kip capacity testing machine. The smaller web splice test specimens (8W-1,8W-2) were tested in a 300 kip capacity testing machine. Figure 9 shows completed test specimens prior to installing in the testing machine (see Figure 10). Ultimate load was recorded in each test. An approximate yield load was recorded, when observable, as indicated by a momentary drop in load.

The results of tests on the six types of weld joints are given in Table III. In all cases, the ultimate strength of the joint exceeded 80 ksi and reached a maximum of 87 ksi in the SMA weld joint (1A). Although the yield strengths shown in Table III are approximate, the test data indicate weld yield strengths in the range of 70-78 ksi.

Fracture of the test specimens generally occurred within the weld metal (see Figure 11) although four test specimens (7B-1, 8A-2, 8B-1, 8B-2) fractured within the base metal adjacent to the weld (see Figure 12). In both cases the fractures exhibited extensive ductility and few weld defects. The variation in fracture location and the close similarity in ultimate strengths is clear evidence of the very close match of strength which was achieved between the weld metal and the base material.

B. Side Bend Tests

Side bend test specimens were fabricated, tested, and evaluated as per AWS D1.1 Sec. 5.28. Three 1-1/2 in. wide specimens were required to cover the full thickness of the flange weld as shown in Figure 6. A total of twelve specimens were therefore required to test each weld joint at four locations. Web splice 8W required two specimens to cover the web thickness. This resulted in only eight specimens to be tested. Figure 13 shows a specimen under test.

With the exception of two specimens machined near the weld root of Flange Splice 1A (SMAW @ 50 KJ/in.), all specimens tested were found to be acceptable. Table IV gives a summary of the test results. Figures 14-19 show a typical set of test specimens covering the full thickness of each type of weld splice. All specimens showed adequate ductility and few defects. The unacceptable defects located at the weld root in Flange Splice 1A are clearly seen in Figure 14. A close examination of the largest defect showed it to be due to a slag inclusion. Smaller defects along the fusion line also appear to be associated with slag inclusions. No indication of HAZ cracking was seen in any of the tests.

C. Weld Metal Charpy V-Notch Tests

Weld metal Charpy V-Notch specimens were fabricated from each type of weld joint as shown in Figure 6. Specimens were fabricated and tested over a range of temperature in the transition range in accordance with ASTM E-23. Five specimens were tested at 0°C. Table V shows the test data for each type of weld joint tested. Figure 20 shows a plot of the combined weld metal test data. In computing the average energy absorbed at 0°C in Table V, the highest and lowest test result in each set were discarded.

The test data indicate a more than adequate level of weld metal toughness for all weld processes and heat input combinations examined. At the highest heat input tested (SAW 200 KJ/in.) the weld metal toughness shows a significant reduction as would be expected at very high heat inputs. The 66 ft-lbs average energy absorbed at 0°C is still well in excess of the AISC Requirements for Heavy Shapes of 20 ft-lbs at 70°F.

D. Base Metal Charpy V-Notch Tests

Tables VI and VII provide a compilation of the base metal CVN test results for the two heats of material used in the beam splices. Twelve specimens were tested at each of the twenty locations within the flange cross-section as described in Section IV. Each set of specimens were tested over a range of temperatures within the transition temperature range for the material at the specific location. Figures 21-32 show the test data plotted for each flange test location (identical positions with respect to the web centerline are shown on the same plot for comparison i.e. Pos.1 and Pos.2) and heat of material.

Several observations can be made from the test data:

1. The fracture toughness of the base material varies considerably over the flange cross-section. The two heats of material have very similar fracture characteristics at all flange test locations. Both heats of material show upper shelf energies ranging from 100-240 ft-lbs and transition temperatures (15 ft-lb) ranging from below -100°C to -10°C depending upon test location. As might be expected, the lowest transition temperatures occur at surface locations and rise with increasing depth below the surface.

2. The average absorbed energy at 0°C for all locations tested in both heats of material ranges from 62 ft-lbs to 239 ft-lbs (see Table VIII). The absorbed energy at the 1/2W-3/4T location (AISC Requirements for Heavy Shapes) in both heats is well in excess of the code requirements.

3. There is a small but discernible difference between Pos.1 and Pos.2 test data at mirror image locations about the web centerline. This is thought to be due to the orientation of the beam (which flange tip faced upward) when it was processed.

E. Base Metal Microstructure and Hardness

A metallographic sample was prepared at each of the twenty test locations in the flange cross-section to identify the microstructure of the material tested in the CVN tests. This was performed on one of the heats (Heat No. 89322-9009) of material since the test results were similar. Figure 33 shows a collage of microstructures (100X) at the twenty locations. The figure shows the microstructure varies across the cross-section of the flange ranging from a fine bainitic structure near the flange surface to a coarser ferritic-pearlitic structure toward the web-flange intersection. Intermediate locations contain a mixture of bainite-ferrite-pearlite with a decreasing fraction of bainite toward the web-flange intersection. Although the microstructure coarsens toward the web-flange intersection, the ferrite grain size (Ferrite G.S. No. 5-6) and austenite grain size appear fine. Larger aereal views of the microstructure at the twenty locations appear in Appendix A of this report.

Hardness measurements were also taken at the twenty test locations. Figure 34 shows a schematic representation of the flange cross-section and the corresponding RB hardness obtained at the test locations. The hardness ranges from a minimum of RB 80-83 at the flange mid-width and mid-thickness region to a maximum of RB 94-96 at the flange tip surfaces.

F. HAZ Charpy V-Notch Tests

Since the fracture toughness of the base material varied considerably with test location

and only a limited number of HAZ CVN specimens could be extracted at each location (three specimens), it was decided to test the group of specimens at each location at a temperature which was approximately in the middle of the transition temperature range for the base material at this location. This corresponded to test temperatures from -80°C in the toughest locations to 0°C at the web-flange intersection (location as specified in the AISC Requirements for Heavy Shapes).

A compilation of test results for the five weld joint types tested (SAW 50 KJ/in., SAW 100 KJ/in., SAW 200 KJ/in., FCAW 40 KJ/in.,FCAW 75 KJ/in.) is given in Table IX. A comparison between the test results and the corresponding average base metal toughness at each test location is shown graphically in Figures 35-46. Although the results show some scatter typical of HAZ CVN testing due to difficulty in placing of the machined notch entirely within the same HAZ microstructure,the trend is clear. There is a loss of toughness seen in the CGHAZ which is seen more clearly in the SAW weld joints than in the FCAW welds. The observed increase in toughness in some of the FCAW tests suggests that the notch was likely outside the CGHAZ and probably in the FGHAZ or unaffected base metal. This may be due to a wider HAZ in the higher heat input SAW welds which was more forgiving of errors in notch placement. In general, Figures 35-46 show a loss of toughness which increases with increased heat input. Tests performed at the position specified in the AISC Requirements for Heavy Shapes (see Figure 46) at 0°C indicate a loss of toughness, however the level of fracture toughness still exceeds the base metal requirements at this location.

VII. Summary

1. None of the W14 X 730 weld splices made without preheat exhibited any evidence of cracking in the weld metal or HAZ.

2. The filler metals used were found to be closely matching in tensile strength to the base material for all weld processes and heat inputs examined. The weld joint tensile strength exceeded the minimum tensile strength requirements for ASTM A572 Grade 65 (80 ksi min. T.S) in all six weld joint types. Weld joint ductility was also found to be good in all weld joints examined.

3. The toughness of the weld metal in all six types of weld joints including the highest heat input submerged arc weld joint (200 KJ/in.) was well in excess of the specification requirements.

4. Charpy V-Notch tests performed on two heats of base material tested at the position specified in the AISC Requirements for Heavy Shapes near the web-flange intersection and at other locations across the flange cross-section showed very high levels of fracture toughness. The

average absorbed energy at 0°C for specimens tested at the AISC test position were 62 ft-lbs and 125 ft-lbs for the two heats of material tested.Fracture toughness at other locations in the flange cross-section was greater.

5. Charpy V-Notch tests performed in the CGHAZ of welds deposited over a range of heat inputs from 40 KJ/in. (1.5 KJ/mm) to 200 KJ/in. (7.9 KJ/mm) possessed reduced (particularly at the highest heat inputs) but adequate toughness. The toughness in the HAZ at the position specified in the AISC Requirements for Heavy Shapes was in excess of the base metal requirements at this position for all weld processes and heat inputs examined.

References

1. American Welding Society, Structural Welding Code, Ninth Edition,1985.

2. American Institute of Steel Construction, Steel Construction Manual, Ninth Edition,1989.

3. Fisher,J.W.,Pense,A.W.,"Experience With Use of Heavy W-Shapes in Tension", AISC Engineering Journal,2nd Quarter,1987,Chicago,IL

4. Fisher,J.W.,Pense,A.W.,Kaufmann,E.J.,"Cracking and Toughness Problems in Jumbo Rolled Sections:Occurrence and Avoidance", ATLSS Report No. 88-03, 1988.

5. Barsom,J.M.,Reisdorf,B.G.,"Characteristics of Heavy Weight Wide-Flange Structural Shapes",Welding Research Council,Bulletin No. 331, February 1988.

6. Reuter,E., "HISTAR - A New Generation of Rolled Sections for Economical Steel Construction",Proceedings of the International Conference on Steel and Aluminum Structures, ICSAS 91,Elsevier Applied Science,New York.

TABLE I

COMPOSITION AND MECHANICAL PROPERTIES OF THE BASE MATERIALS

Wt %

	C	Mn	P	S	Si	Ni	Cr	Cu	Nb	Al
Heat 89322-9009	0.091	1.49	0.008	0.005	0.301	0.054	0.031	0.056	0.044	0.032
Heat 89322-9041	0.089	1.48	0.010	0.004	0.290	0.048	0.017	0.056	0.045	0.036
ASTM A572	0.23 max.	1.65 max.	0.04 max.	0.05 max.	-	-	-	-	-	-

	Yld. Strength,ksi (MPa)	Ten. Strength,ksi (MPa)	Elongation, %
Heat 89322-9009	65.5 (452)	83.8 (578)	22.4
Heat 89322-9041	66.3 (457)	83.5 (576)	20.1
ASTM A572 Grade 65	65.0 min. (450)	80.0 min (550)	15.0 min.

TABLE II

WELD JOINT IDENTIFICATION

Weld Joint Designation	Heat No.	Weld Process(Heat Input	Filler Metal
1A	89322-9009	SMAW (50 KJ/in.)	E8018-C3
2B 8W*	89322-9041	SAW (50 KJ/in.)	1/8 F7A6-EH11K
3B 8A	89322-9041	SAW (100 KJ/in.)	1/8 F7A6-EH11K
4B 8B	89322-9041	SAW (200 KJ/in.)	1/8 F7A6-EH11K
5A 7A	89322-9009	FCAW (40 KJ/in.) FCAW (38 KJ/in.)	0.045 E81T1-Ni1
6A 7B	89322-9009	FCAW (75 KJ/in.) FCAW (42 KJ/in.)	0.062 E81T1-Ni1

* Web Splice

TABLE III

TENSILE TEST RESULTS

Weld Joint	Weld Process	Yield Load (kips)	Ult. Load (kips)	Yld. Strength ksi (MPa)	Ult. Strength ksi (MPa)	Failure Location
1A-1	SMAW	-	427.0	-	87.1 (601)	Weld Metal
1A-2	50 KJ/in.	-	422.2	-	86.1 (594)	Weld Metal
7B-1	FCAW	373.6	403.2	77.7 (536)	83.9 (578)	Base Metal
7B-2	42 KJ/in.	374.5	405.8	77.9 (537)	84.4 (582)	Weld Metal
7A-1	FCAW	365.3	399.5	76.6 (528)	83.7 (577)	Weld Metal
7A-2	38 KJ/in.	370.2	400.6	78.1 (539)	84.6 (583)	Weld Metal
8A-1	SAW	-	399.1	-	82.5 (569)	Weld Metal
8A-2	100 KJ/in.	-	402.4	-	83.4 (575)	Base Metal
8B-1	SAW	-	401.0	-	83.0 (572)	Base Metal
8B-2	200 KJ/in.	-	401.2	-	82.4 (568)	Base Metal
8W-1	SAW	205.0	240.2	69.8 (481)	81.8 (564)	Weld Metal
8W-2	50 KJ/in.	210.0	241.5	71.2 (491)	81.9 (565)	Weld Metal

TABLE IV

SIDE BEND TEST RESULTS

Weld Joint	Total Tests	Acceptable	Rejectable
1A SMAW 50 KJ/in.	12	10	2
8W SAW 50 KJ/in.	8	8	-
8A SAW 100 KJ/in.	12	12	-
8B SAW 200 KJ/in.	12	12	-
7B FCAW 40 KJ/in.	12	12	-
7A FCAW 40 KJ/in.	12	12	-

TABLE V

Weld Metal Charpy V-Notch Test Results

SMAW (50KJ/in)		FCAW(0.045in. dia) (40KJ/in)		FCAW(0.0625in. dia) (40KJ/in)	
Test Temperature (C)	Energy Absorbed (ft-lb)	Test Temperature (C)	Energy Absorbed (ft-lb)	Test Temperature (C)	Energy Absorbed (ft-lb)
21	119.0	0	104.5	21	80.0
21	89.5	0	131.0	21	100.0
21	106.0	0	100.5	21	136.0
0	96.5	0	112.5	0	94.5
0	89.5	0	102.5	0	104.0
0	104.0	-29	83.0	0	80.0
0	100.0	-29	76.5	0	100.5
0	94.5	-29	78.5	0	88.0
-18	90.5	-40	52.0	-29	49.0
-18	85.0	-40	31.0	-29	30.0
-35	78.5	-40	41.0	-29	31.5
-35	70.0	-51	15.5	-51	22.5
-51	61.5	-51	25.5	-51	16.0
-51	60.0	-51	23.5	-51	16.0
		-62	12.0	-62	10.0
		-62	12.5	-62	10.0
97.0 ft-lbs Avg.@0°C		106.3 ft-lbs Avg.@0°C		94.3 ft-lbs Avg.@0°C	

SAW (50KJ/in)		SAW (100KJ/in)		SAW (200KJ/in)	
Test Temperature (C)	Energy Absorbed (ft-lb)	Test Temperature (C)	Energy Absorbed (ft-lb)	Test Temperature (C)	Energy Absorbed (ft-lb)
0	112.5	0	84.5	21	100.0
0	110.0	0	70.0	21	93.0
0	68.5	0	88.5	21	85.0
0	72.0	0	84.5	0	30.0
0	73.0	0	27.5	0	55.0
-40	45.0	-29	55.0	0	68.0
-40	33.0	-29	43.0	0	75.0
-40	80.0	-29	32.0	0	86.0
		-40	19.0	-29	48.0
		-40	22.0	-29	11.0
		-40	43.0	-29	18.0
		-51	40.0	-40	22.0
		-51	31.0	-40	11.0
		-62	9.0	-40	33.0
		-62	12.0	-51	20.0
		-62	17.5	-51	23.0
85.0 ft-lbs Avg.@0°C		85.8 ft-lbs Avg.@0°C		66.2 ft-lbs Avg.@0°C	

TABLE VI
BASE METAL CHARPY V-NOTCH TEST RESULTS
(Heat 89322-9041)

1/6W-Surface		1/6W-1/4Thickness		1/6W-1/2Thickness		1/6W-3/4Thickness	
Test Temperature (C)	Energy Absorbed (ft-lbs)	Test Temperature (C)	Energy Absorbed (ft-lbs)	Test Temperature (C)	Energy Absorbed (ft-lbs)	Test Temperature (C)	Energy Absorbed (ft-lbs)
Position 1							
0	82	0	183.0	0	219.0	24	199.5
0	118.0	0	151.0	0	220.0	24	233.0
0	95.0	0	107.0	0	238.0	24	237.0
-40	113.5	-40	141.0	-20	192.0	0	167.0
-40	51.5	-40	48.0	-20	191.0	0	187.0
-40	63.5	-40	109.0	-20	203.0	0	96.0
-60	83.0	-60	113.0	-40	97.0	-20	73.0
-60	26.5	-60	7.0	-40	98.0	-20	64.5
-60	25.5	-60	4.5	-40	63.5	-20	83.5
-93	11.0	-80	5.0	-60	13.5	-40	20.0
-93	12.0	-80	12.0	-60	32.0	-40	10.0
-93	13.5	-80	6.0	-60	7.5	-40	18.0
Position 2							
0	132.5	0	97.5	0	107.0	24	182.0
0	116.5	0	191.5	0	176.0	24	186.0
0	122.0	0	198.5	0	196.0	24	188.0
-40	81.5	-40	17.0	-20	176.0	0	232.0
-40	106.5	-40	86.0	-20	115.0	0	78.0
-40	97.0	-40	187.0	-40	112.0	0	125.0
-60	82.5	-60	8.0	-40	69.0	-20	82.0
-60	102.0	-60	131.0	-40	130.0	-20	76.0
-80	18.0	-60	33.5	-60	9.0	-20	78.5
-80	36.5	-80	7.0	-60	4.5	-40	11.5
-90	30.0	-80	7.5	-80	3.0	-40	15.0
-90	20.5	-80	21.0	-80	6.0	-40	8.0

TABLE VI (cont'd)

1/4W-Surface		1/4W-1/4Thickness		1/4W-1/2Thickness		1/4W-3/4Thickness	
Test Temperature (C)	Energy Absorbed (ft-lbs)	Test Temperature (C)	Energy Absorbed (ft-lbs)	Test Temperature (C)	Energy Absorbed (ft-lbs)	Test Temperature (C)	Energy Absorbed (ft-lbs)
Position 1							
0	191.0	0	235	24	239.0	24	239.0
0	223.5	0	237.0	24	238.0	24	236.0
0	240.0	0	239.0	0	81.0	24	203.0
-40	111.0	-20	206.0	0	55.0	0	239.0
-40	146.5	-20	239.0	0	119.0	0	183.0
-40	237.0	-40	166.0	-20	11.0	0	139.5
-60	92.5	-40	84.0	-20	83.0	-20	35.0
-60	114.5	-40	15.5	-40	17.0	-20	100.0
-80	41.0	-50	12.0	-40	5.5	-20	83.5
-80	121.0	-50	26.5	-40	11.0	-40	8.5
-96	44.5	-60	6.5	-50	8.0	-40	19.0
-96	42.0	-60	9.0	-50	9.0	-40	9.5
Position 2							
0	183.0	0	238.5	24	192.0	24	235.0
0	181.0	0	183.0	24	231.0	24	235.0
0	138.0	0	131.0	0	132.5	24	238.0
-40	129.0	-20	156.0	0	222.5	0	195.0
-40	124.5	-20	112.0	0	122.5	0	79.0
-40	138.0	-40	48.0	-20	7.5	0	83.5
-60	65.0	-40	12.0	-20	12.0	-20	52.0
-60	100.0	-40	15.5	-40	42.0	-20	40.5
-80	47.0	-50	16.0	-40	10.0	-20	18.5
-80	43.5	-50	105.0	-40	9.5	-40	10.0
-96	3.0	-60	13.0	-50	26.0	-40	5.5
-96	5.0	-60	7.0	-50	3.0	-40	12.0

TABLE VI (cont'd)

1/2W-Surface		1/2W-1/4Thickness		1/2W-1/2Thickness		1/2W-3/4Thickness	
Test Temperature (C)	Energy Absorbed (ft-lbs)	Test Temperature (C)	Energy Absorbed (ft-lbs)	Test Temperature (C)	Energy Absorbed (ft-lbs)	Test Temperature (C)	Energy Absorbed (ft-lbs)
0	186.0	0	239.0	20	228.0	20	192.0
0	237.0	0	238.5	20	223.0	20	123.0
0	239.0	0	239.5	0	106.5	0	29.0
-40	167.0	-40	237.0	0	107.0	0	167.0
-40	226.0	-40	239.0	0	200.0	0	134.0
-40	239.0	-40	236.5	-20	86.5	0	235.0
-80	177.5	-60	39.5	-20	93.0	0	74.5
-80	63.5	-60	39.5	-40	18.5	-11	128.5
-92	134.5	-80	9.5	-40	45.5	-11	96.5
-92	128.0	-80	12.5	-40	35.0	-11	111.5
-96	8.0	-96	4.5	-60	3.5	-20	5.0
-96	128.5	-96	5.5	-60	10.0	-20	7.0

TABLE VII

BASE METAL CHARPY V-NOTCH TEST RESULTS
(Heat 89322-9009)

1/6W-Surface		1/6W-1/4Thickness		1/6W-1/2Thickness		1/6W-3/4Thickness	
Test Temperature (C)	Energy Absorbed (ft-lbs)	Test Temperature (C)	Energy Absorbed (ft-lbs)	Test Temperature (C)	Energy Absorbed (ft-lbs)	Test Temperature (C)	Energy Absorbed (ft-lbs)
Position 1							
0	171.0	0	151.0	0	12.5	25	190.0
0	144.0	0	123.0	0	240.0	25	154.5
0	185.0	0	235.0	0	240.5	0	114.0
-20	118.0	-20	149.0	-20	186.0	0	135.0
-20	114.0	-20	153.0	-20	188.5	0	79.0
-40	124.0	-20	238.5	-40	7.0	-20	84.0
-40	130.0	-40	97.5	-40	136.0	-20	113.0
-40	63.0	-40	12.0	-40	95.0	-40	34.0
-60	101.0	-40	42.5	-60	6.0	-40	27.0
-60	114.0	-60	5.5	-60	5.5	-40	33.0
-93	17.0	-60	8.0	-60	20.5	-60	5.5
-93	32.5	-60	28.0	-60	7.5	-60	4.0
Position 2							
0	154.0	0	151.5	24	182.5	24	130.0
0	163.5	0	145.0	24	169.0	24	136.0
0	141.5	0	130.0	0	119.0	0	150.5
-40	111.5	-20	135.0	0	111.0	0	82.0
-40	123.0	-20	140.0	0	104.5	0	53.5
-40	120.5	-40	98.0	-20	49.0	-20	63.5
-80	14.5	-40	76.0	-20	124.0	-20	104.0
-80	90.0	-40	116.0	-40	44.0	-40	39.5
-80	53.0	-60	74.5	-40	76.5	-40	7.5
-93	51.0	-60	39.0	-40	32.0	-40	41.5
-93	5.0	-80	16.0	-60	6.0	-60	15.5
-93	40.0	-80	9.0	-60	5.5	-60	5.0

TABLE VII (cont'd)

1/4W-Surface		1/4W-1/4Thickness		1/4W-1/2Thickness		1/4W-3/4Thickness	
Test Temperature (C)	Energy Absorbed (ft-lbs)	Test Temperature (C)	Energy Absorbed (ft-lbs)	Test Temperature (C)	Energy Absorbed (ft-lbs)	Test Temperature (C)	Energy Absorbed (ft-lbs)
Position 1							
0	140.0	0	191.0	24	194.5	24	169.0
0	115.5	0	158.5	24	238.0	24	176.5
0	106.5	-20	160.0	0	75.5	24	179.0
-40	115.0	-20	18.5	0	184.0	0	126.5
-40	83.0	-40	9.0	0	139.0	0	114.5
-40	69.5	-40	101.0	-20	85.5	0	116.5
-60	103.5	-40	100.0	-20	194.0	-20	49.5
-60	94.0	-50	11.5	-40	7.0	-20	111.0
-80	70.0	-50	77.0	-40	77.0	-20	53.5
-80	15.0	-50	43.5	-40	19.5	-40	41.0
-96	7.0	-60	9.0	-60	7.0	-40	12.5
96	35.0	-60	16.0	-60	17.0	-40	7.5
Position 2							
0	145.5	0	159.0	24	128.0	24	177.0
0	170.5	0	223.0	24	238.0	24	180.0
0	117.5	0	238.0	0	157.0	24	124.0
-40	118.0	-20	155.5	0	169.5	0	99.5
-40	116.0	-20	157.0	0	143.5	0	69.5
-40	74.5	-40	12.5	-20	8.5	0	104.0
-60	111.5	-40	96.0	-20	124.0	-20	105.0
-60	115.0	-40	144.0	-40	39.5	-20	8.5
-80	102.5	-60	40.0	-40	125.5	-20	41.5
-80	24.5	-60	36.5	-40	68.0	-40	27.0
-96	11.0	-80	6.0	-60	11.0	-40	11.0
-96	6.0	-80	5.5	-60	4.0	-40	30.5

TABLE VII (cont'd)

1/2W-Surface		1/2W-1/4Thickness		1/2W-1/2Thickness		1/2W-3/4Thickness	
Test Temperature (C)	Energy Absorbed (ft-lbs)	Test Temperature (C)	Energy Absorbed (ft-lbs)	Test Temperature (C)	Energy Absorbed (ft-lbs)	Test Temperature (C)	Energy Absorbed (ft-lbs)
0	238.0	0	238.0	20	237.0	21	25.0
0	238.0	0	239.0	20	239.0	21	238.0
0	237.0	0	239.0	0	71.0	0	76.0
-40	239.0	-40	238.0	0	128.0	0	39.0
-40	236.0	-40	239.5	0	144.0	0	94.0
-40	-237.0	-40	236.0	-20	175.0	0	69.0
-80	186.0	-60	239.0	-20	177.0	0	33.0
-80	183.0	-60	60.5	-40	73.0	-20	130.0
-93	5.0	-80	4.0	-40	6.5	-20	55.0
-93	163.0	-80	31.0	-40	49.5	20	82.0
-96	26.5	-96	5.0	-60	38.0	-40	18.0
-96	156.0	-96	6.0	-60	16.0	-40	26.0

TABLE VIII

AVERAGE BASE METAL CHARPY V-NOTCH TEST RESULTS @ 0 C
(Heat 89322-9009)

Pos.1 Pos.2	1/6W	1/4W	1/2W
Surface	167 ft-lbs 153 ft-lbs	121 145	238
1/4T	170 142	175 207	238
1/2T	164 112	134 157	114
3/4T	109 95	119 91	62*

* AISC Supp. 2

(Heat 89322-9041)

Pos.1 Pos.2	1/6W	1/4W	1/2W
Surface	98 ft-lbs 124 ft-lbs	218 167	221
1/4T	147 163	237 184	239
1/2T	226 160	85 159	138
3/4T	150 145	187 119	125*

* AISC Supp.2

TABLE IX
HAZ CHARPY V-NOTCH TEST RESULTS
(Heat 89322-9041)

	SAW50		SAW100		SAW200	
	Test Temperature (C)	Energy Absorbed (ft-lbs)	Test Temperature (C)	Energy Absorbed (ft-lbs)	Test Temperature (C)	Energy Absorbed (ft-lbs)
Position 1						
1/6W-Surface						
	-40	29.0	-40	77.0	-40	42.0
		59.0		33.0		28.0
		10.5		40.0		32.0
1/6W-1/4Thickness						
	-20	83.0	-40	36.0	-40	30.0
		59.0		34.0		40.0
		38.0		27.5		22.5
1/6W-1/2Thickness						
	-40	75.0	-40	49.5	-40	29.0
		62.5		42.0		25.0
		30.0		26.0		41.0
1/6W-3/4Thickness						
	0	78.0	-20	45.0	-20	56.5
		179.0		86.5		58.0
		102.0		97.0		113.5
Position 2						
1/6W-Surface						
	-40	66.0	-40	27.0	-40	83.0
		49.0		28.0		102.0
		61.0		25.0		107.0
1/6W-1/4Thickness						
	-20	112.0	-40	33.0	-40	28.0
		68.0		61.0		18.5
		84.0		63.0		25.0
1/6W-1/2Thickness						
	-40	70.0	-40	56.0	-40	31.0
		40.0		24.0		37.0
		40.0		31.0		72.0
1/6W-3/4Thickness						
	-40	31.0	-20	55.0	-20	88.5
		27.0		74.0		239.0
		24.0		48.0		71.0

TABLE IX (cont'd)

	SAW50		SAW100		SAW200	
	Test Temperature (C)	Energy Absorbed (ft-lbs)	Test Temperature (C)	Energy Absorbed (ft-lbs)	Test Temperature (C)	Energy Absorbed (ft-lbs)
Position 1						
1/4W-Surface	-40	43.0	-40	21.5	-40	80.0
		28.5		20.5		72.0
		15.0		45.0		48.0
1/4W-1/4Thickness	-40	134.0	-40	45.5	-40	13.5
		43.5		39.0		20.0
		33.0		32.0		19.5
1/4W-1/2Thickness	0	37.5	0	81.0	0	52.0
		118.0		89.0		64.5
		113.5		49.0		97.0
1/4W-3/4Thickness	-20	69.0	-20	96.0	0	65.0
		18.0		89.0		73.5
		48.0		78.0		76.5
Position 2						
1/4W-Surface	-40	157.0	-40	25.5	-40	32.0
		187.5		26.0		33.5
		68.5		13.0		49.0
1/4W-1/4Thickness	-20	43.0	-20	75.0	-20	25.0
		67.5		62.0		48.5
		54.0		41.5		71.0
1/4W-1/2Thickness	0	95.0	0	115.0	0	71.0
	0	79.0		97.0		109.5
		62.0		165.0		40.0
1/4W-3/4Thickness	0	123.0	0	108.5	0	54.0
		97.0		145.0		49.0
		76.5		116.0		74.0

TABLE IX (cont'd)

	SAW50		SAW100		SAW200	
	Test Temperature (C)	Energy Absorbed (ft-lbs)	Test Temperature (C)	Energy Absorbed (ft-lbs)	Test Temperature (C)	Energy Absorbed (ft-lbs)
1/2W-Surface						
	-80	21.0	-80	61.0	-80	104.0
		5.0		5.5		6.0
		19.0		5.0		66.5
1/2W-1/4Thickness						
	-60	111.0	-60	125.0	-60	6.0
		120.0		27.0		14.0
		105.0		11.0		13.5
1/2W-1/2Thickness						
	-20	45.0	-20	76.0	-20	15.0
		67.5		56.0		12.5
		43.0		64.0		82.0
1/2W-3/4Thickness						
	0	70.0	0	47.0	0	94.0
		68.0		70.0		109.0
		79.5		55.0		84.0

TABLE IX (cont'd)

	FCAW40 (Heat 89322-9009)		FCAW40	
	Test Temperature (C)	Energy Absorbed (ft-lbs)	Test Temperature (C)	Energy Absorbed (ft-lbs)
Position 1				
1/6W-Surface	-40	26.5	-40	40.5
		57.0		122.5
		51.5		194.0
1/6W-1/4Thickness	-40	59.0	-40	37.5
		73.0		57.0
		118.0		65.0
1/6W-1/2Thickness	-20	105.0	-20	237.0
		205.0		186.0
		55.0		115.0
1/6W-3/4Thickness	0	33.5	0	165.0
		32.5		91.0
		48.0		66.0
Position 2				
1/6W-Surface	-40	38.0	-40	170.0
		31.0		114.0
		20.0		196.0
1/6W-1/4Thickness	-40	238.0	-40	237.0
		85.0		237.0
		239.0		237.5
1/6W-1/2Thickness	-20	65.0	-20	239.0
		127.0		181.5
		188.0		191.0
1/6W-3/4Thickness	0	31.0	0	188.5
		65.5		97.0
		85.0		168.5

TABLE IX (cont'd)

	FCAW40 (Heat 89322-9009)		FCAW40	
	Test Temperature (C)	Energy Absorbed (ft-lbs)	Test Temperature (C)	Energy Absorbed (ft-lbs)
Position 1				
1/4W-Surface				
	-40	72.0	-40	24.5
		84.5		46.5
		100.0		90.0
1/4W-1/4Thickness				
	-40	47.0	-40	45.0
		239.0		103.5
		104.0		28.0
1/4W-1/2Thickness				
	-20	136.5	-20	26.5
		46.5		70.5
		38.5		102.5
1/4W-3/4Thickness				
	0	66.0	0	85.0
		104.0		66.0
		86.5		51.0
Position 2				
1/4W-Surface				
	-40	74.0	-40	151.5
		95.0		134.5
		73.0		135.0
1/4W-1/4Thickness				
	-40	228.5	-40	239.0
		237.0		165.5
		150.5		238.0
1/4W-1/2Thickness				
	-20	138.0	-20	238.0
		44.5		205.0
		170.0		212.0
1/4W-3/4Thickness				
	0	32.5	0	239.0
		28.0		205.0
		86.0		204.0

TABLE IX (cont'd)

	FCAW40 (Heat 89322-9009)		FCAW40	
	Test Temperature (C)	Energy Absorbed (ft-lbs)	Test Temperature (C)	Energy Absorbed (ft-lbs)
1/2W-Surface				
	-80	10.5	-80	22.0
		11.0		136.0
		11.5		35.0
1/2W-1/4Thickness				
	-60	65.0	-60	62.0
		135.0		236.5
		7.0		71.0
1/2W-1/2Thickness				
	-20	69.0	-20	114.0
		50.0		73.0
		118.0		84.0
1/2W-3/4Thickness				
	-60	52.0	-60	87.0
		82.0		92.5
		92.0		103.0

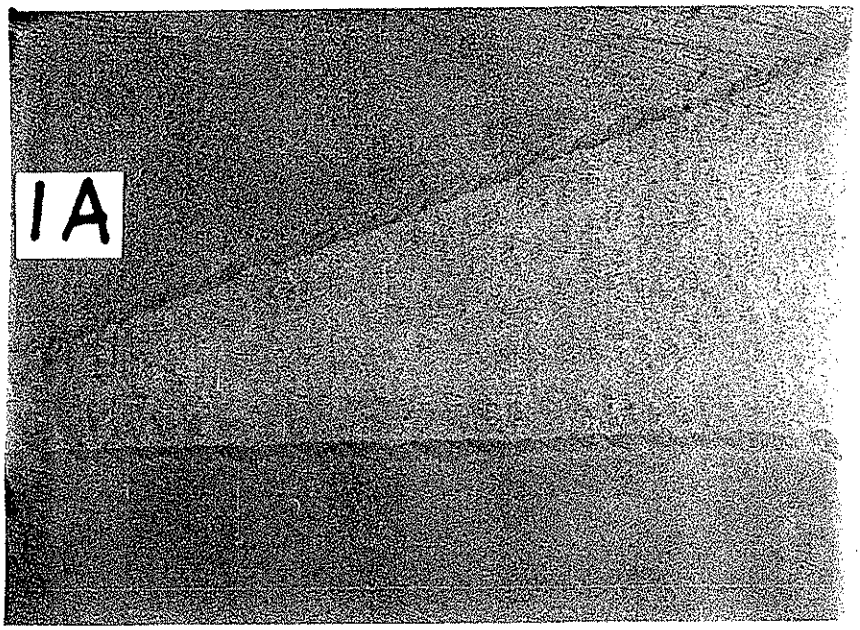

Fig. 1 Etched Cross-Section of Flange Splice 1A[photo: 5/91/2-11]
(SMAW, 50 KJ/in.)

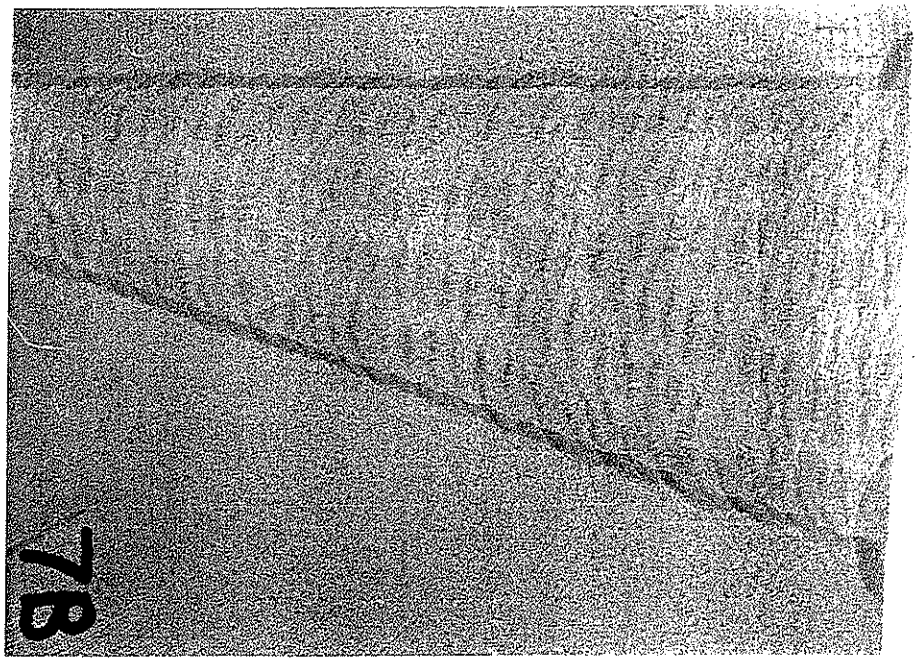

Fig. 2 Etched Cross-Section of Flange Splice 7B[photo: 5/91/3-4]
(FCAW 42KJ/in, 1/16 in. diameter)

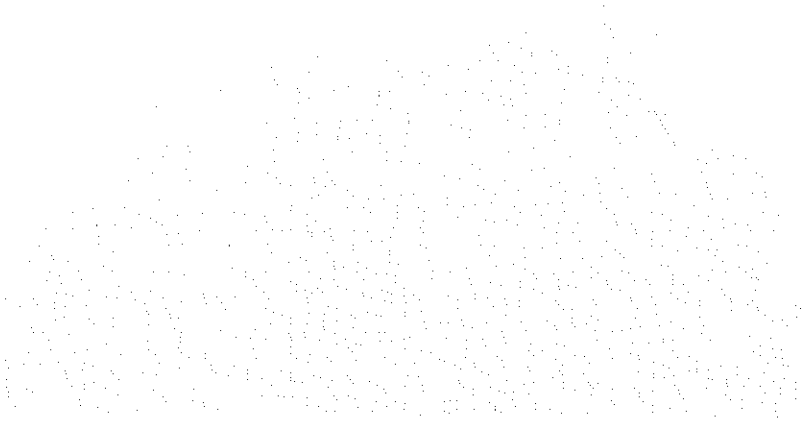

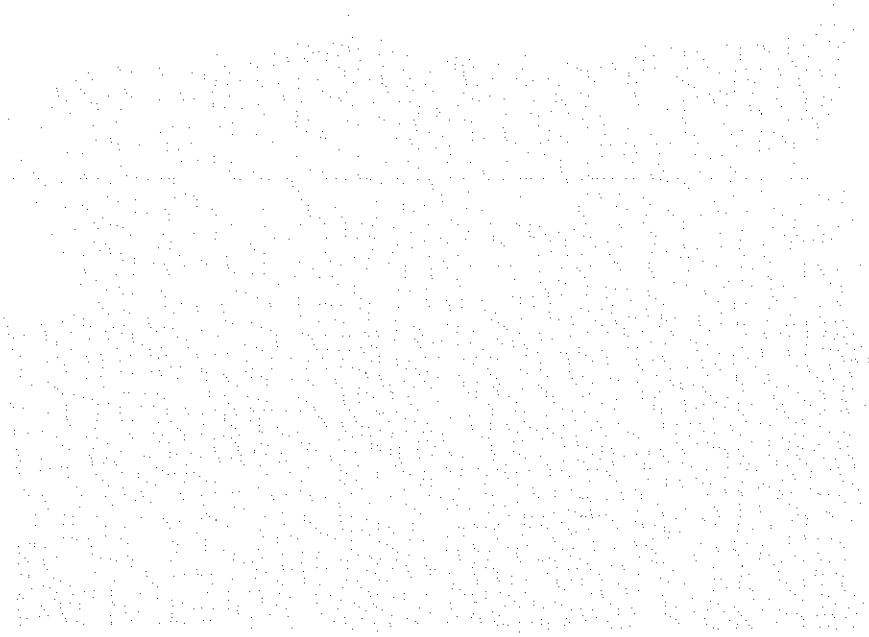

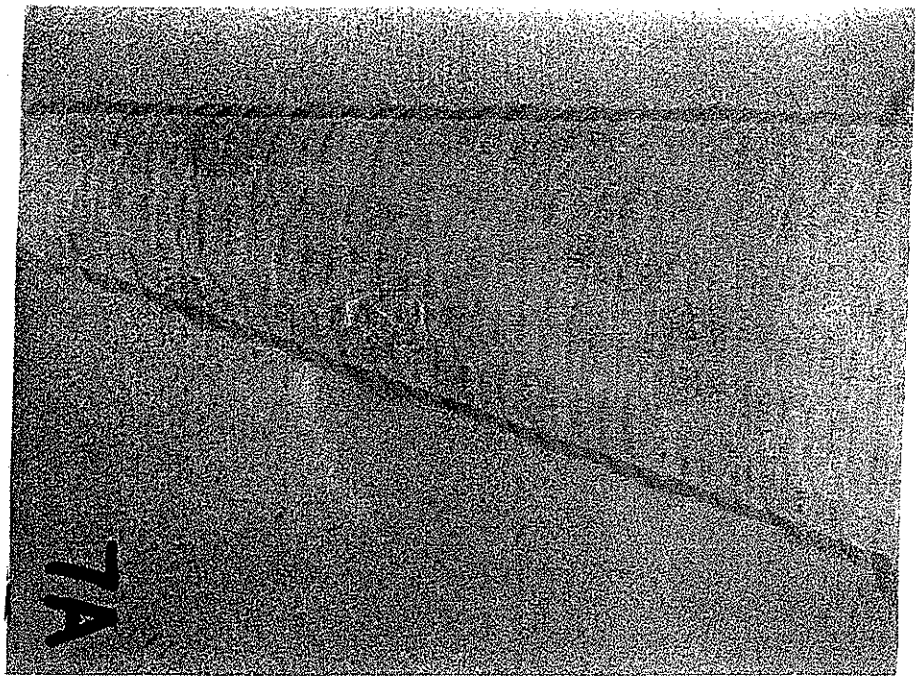

Fig. 3 Etched Cross-Section of Flange Splice 7A[photo:5/91/3-2]
(FCAW, 38 KJ/in., 0.045 in. diameter)

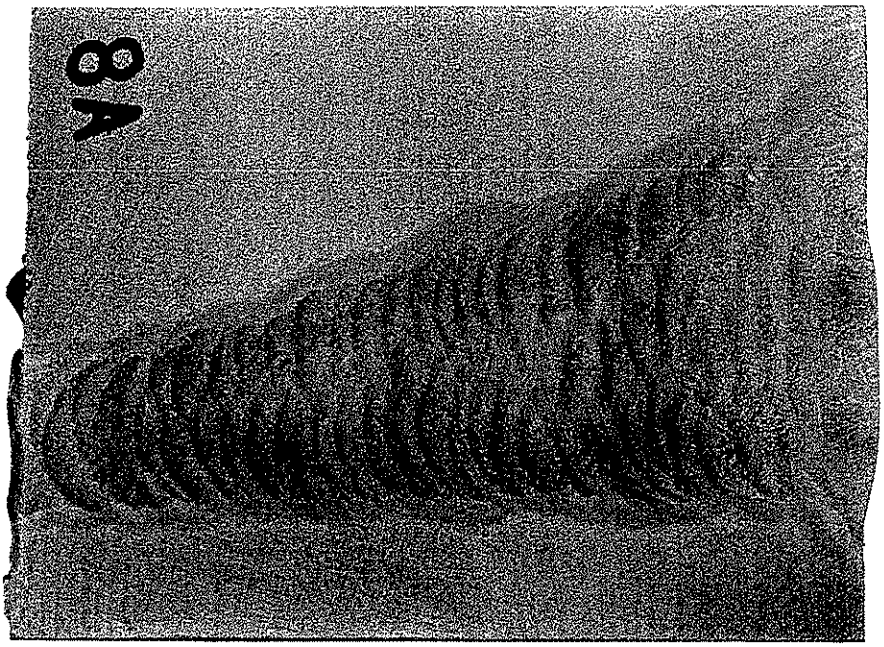

Fig. 4 Etched Cross-Section of Flange Splice 8A[photo:5/91/3-8]
(SAW, 100 KJ/in.)

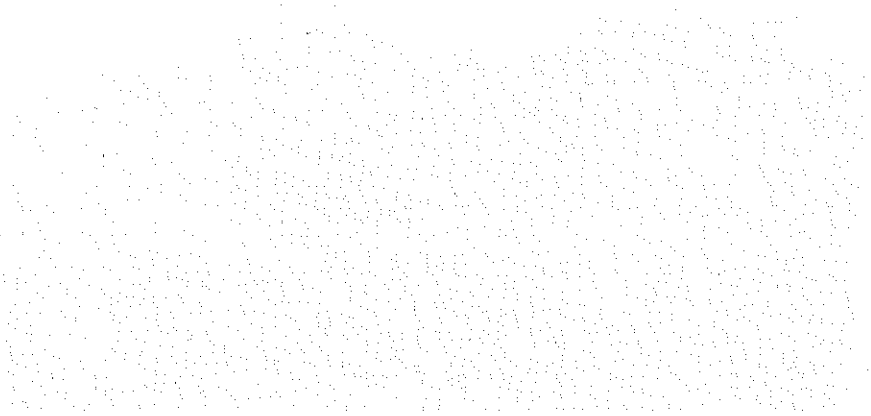

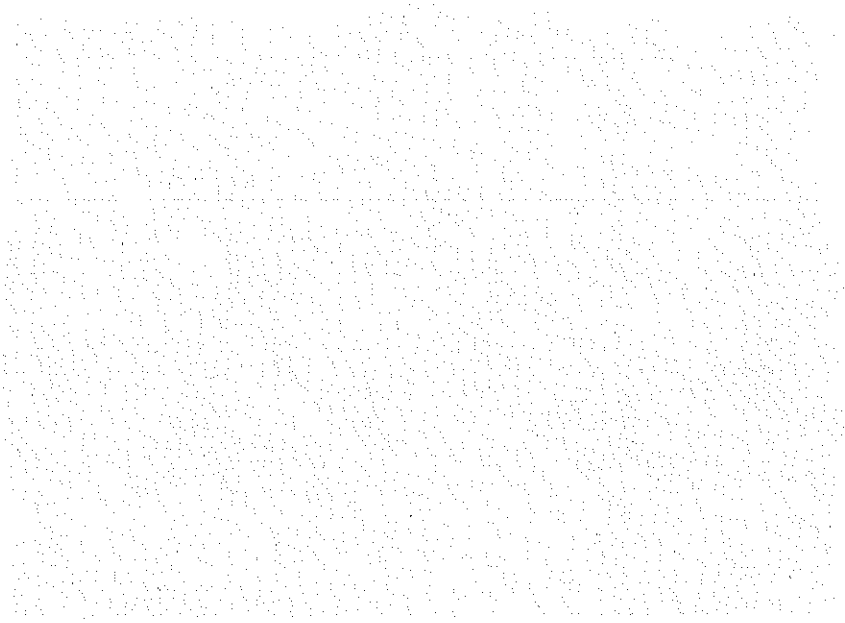

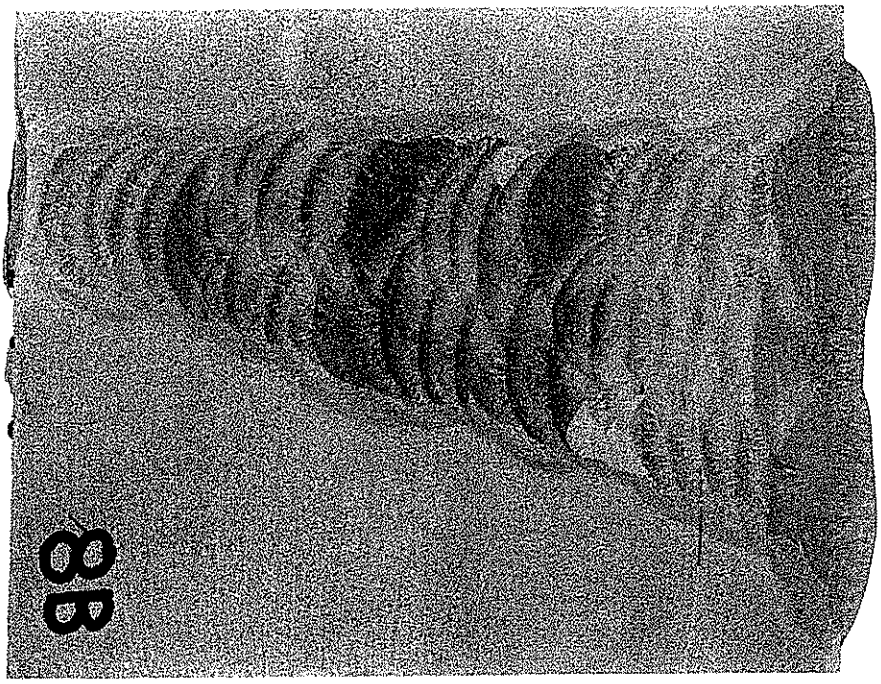

Fig. 5 Etched Cross-Section of Flange Splice 8B[photo:5/91/3-10]
(SAW, 200 KJ/in.)

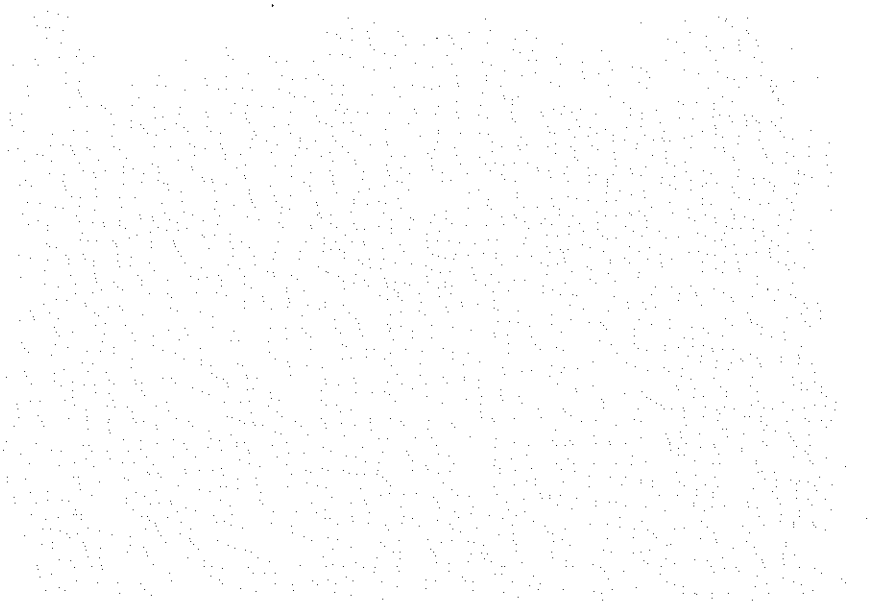

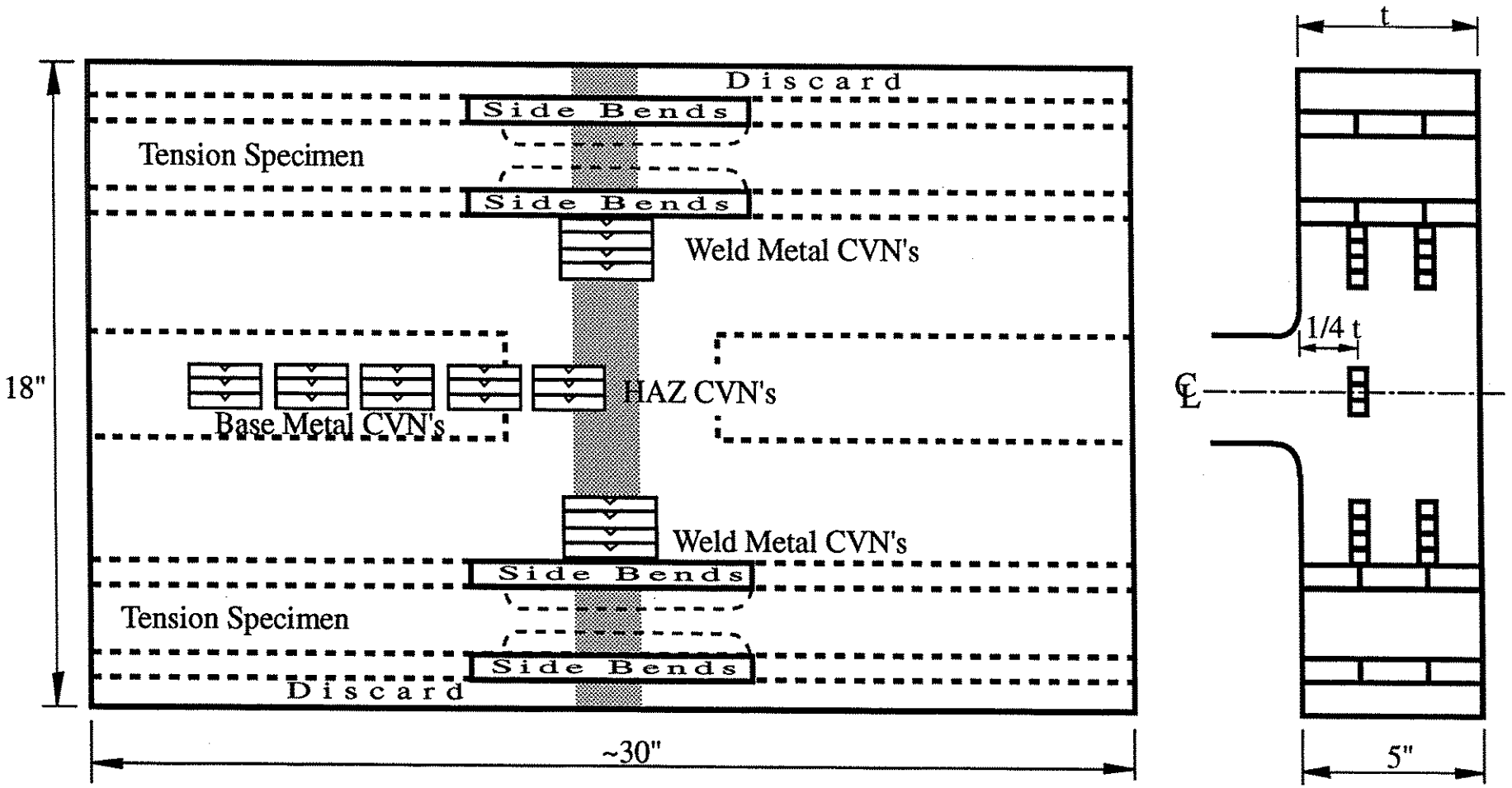

Fig. 6: W14 x 730 Flange Splice Test Specimen Layout

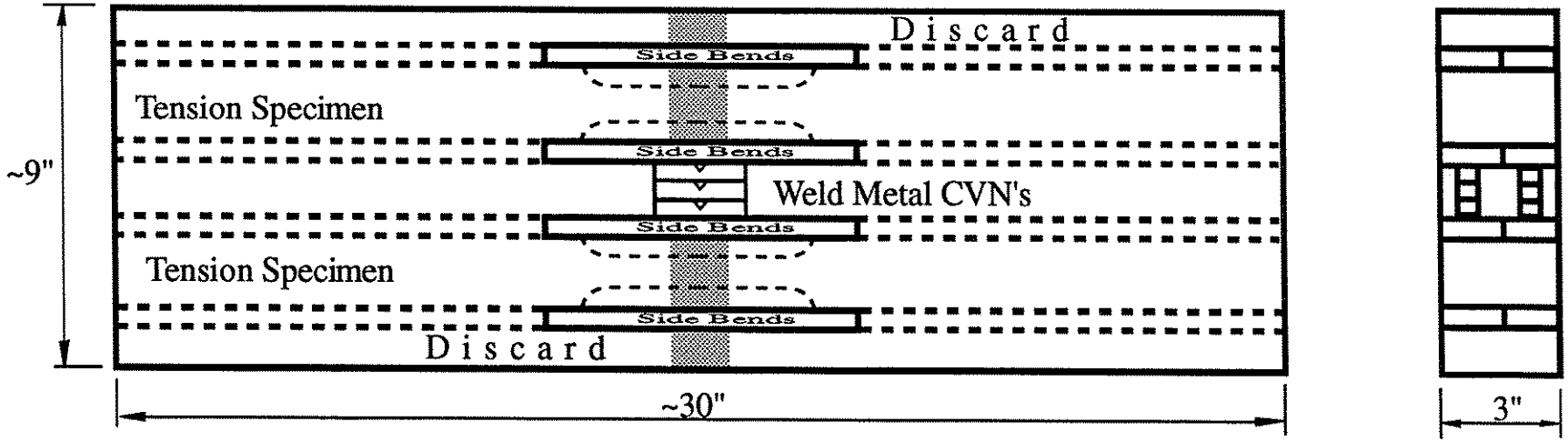

Fig. 7: W14 x 730 Web Splice Te st Specimen Layout

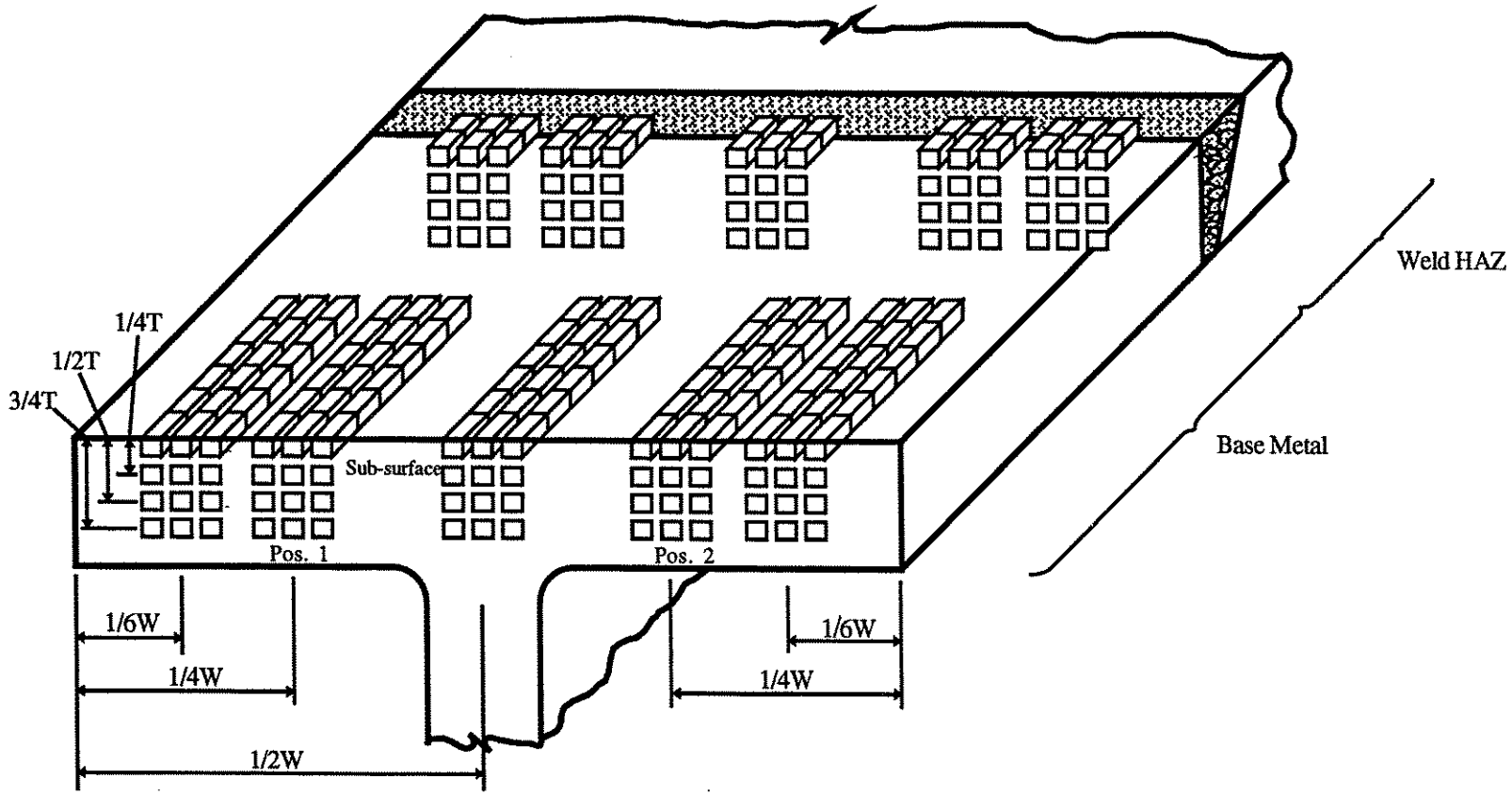

Fig. 8 Charpy V-Notch Test Specimen Layout

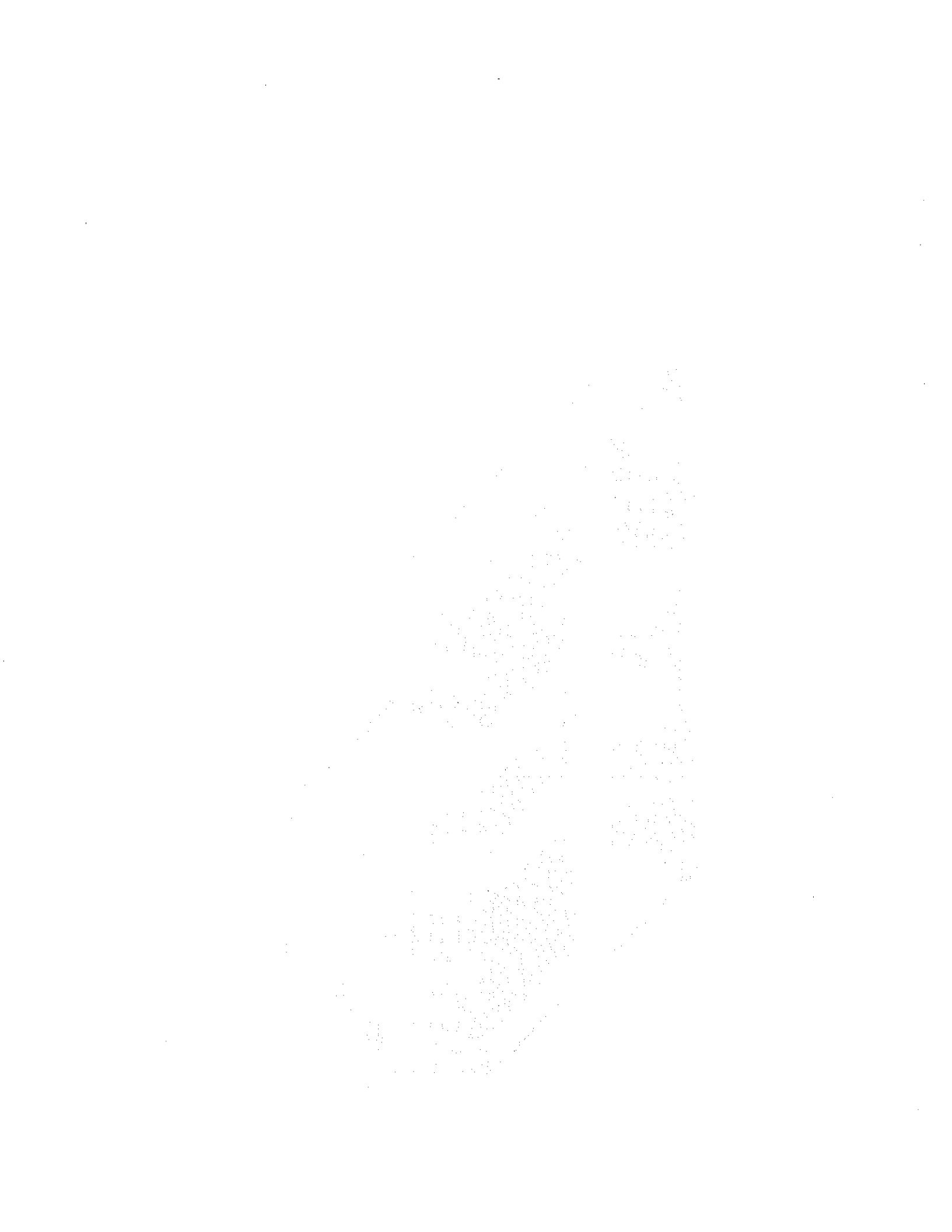

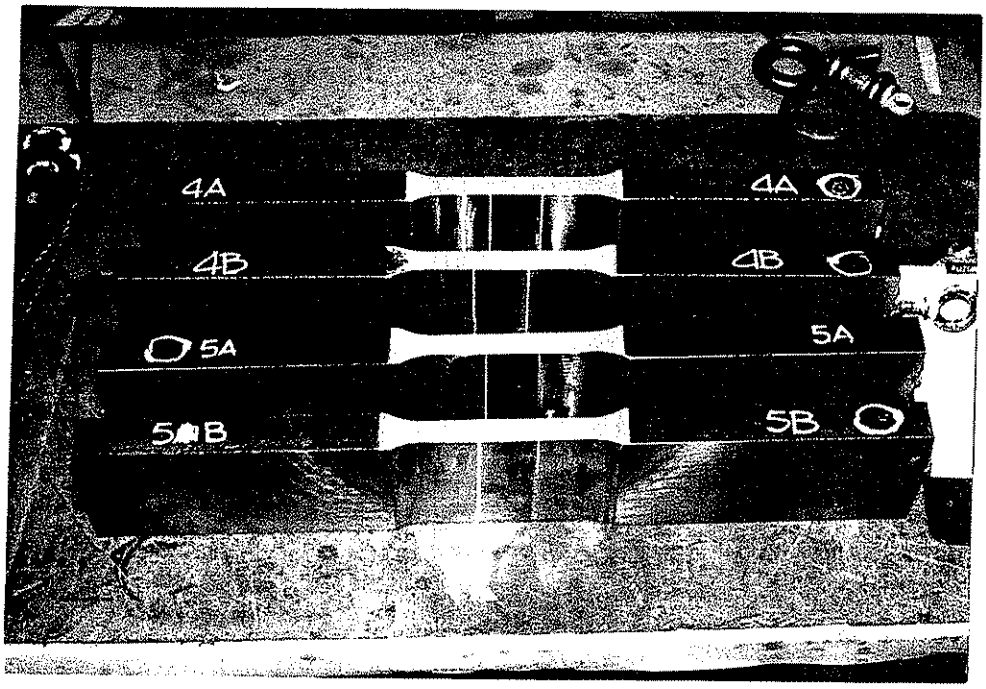

Fig. 9 Full Flange Thickness (5 in.) Tensile Specimens
Fabricated from Flange Splices[photo:3/91/14-7]

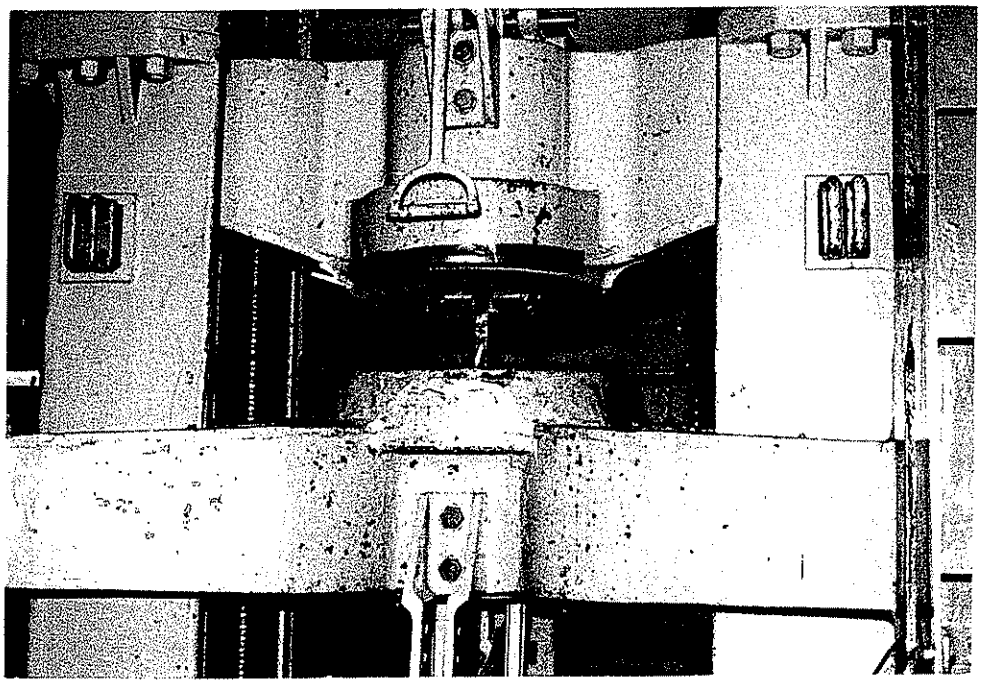

Fig. 10 Flange Splice Tensile Specimen Installed in the Testing Machine
[photo:9/90/5-5]

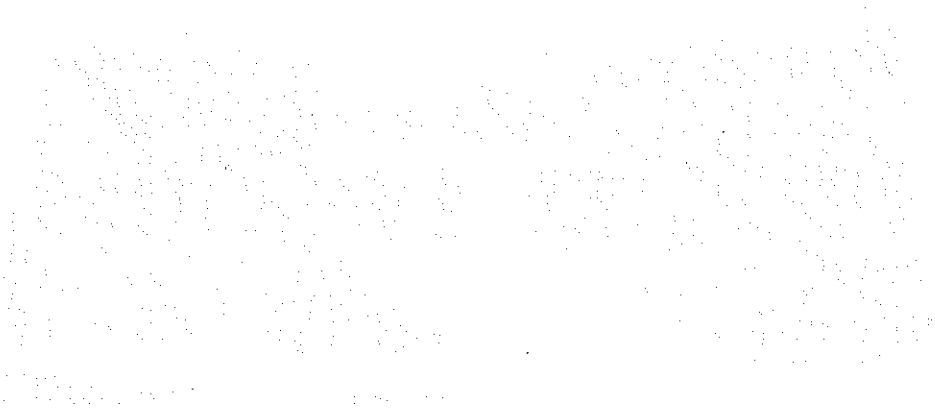

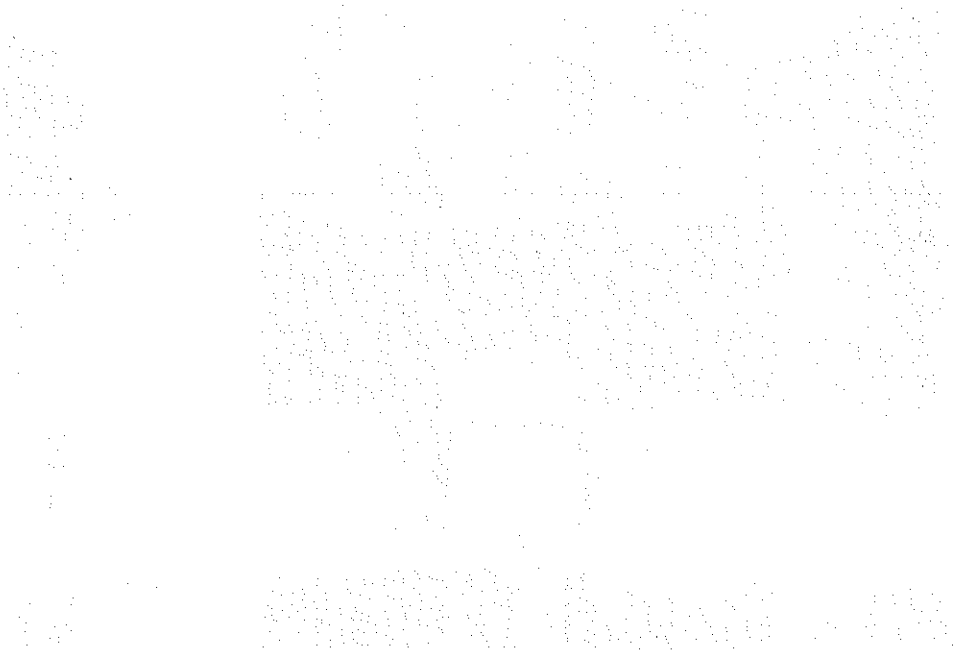

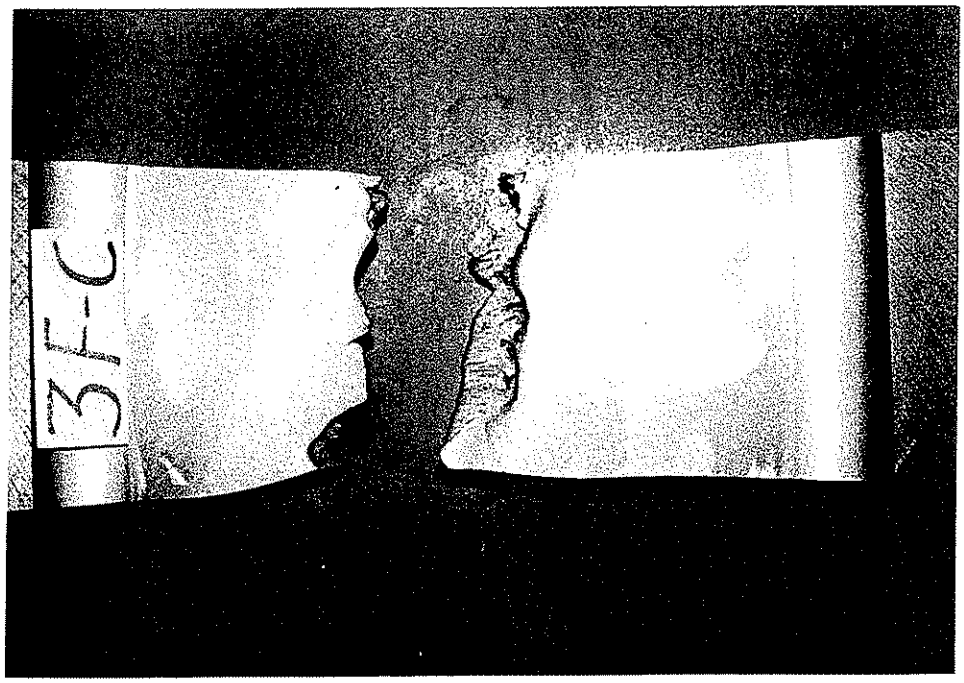

Fig. 11 Fracture Appearance of Tensile Specimen 7A-1.
Ductile Fracture is Within Weld Metal[photo: 1/91/19-4A]

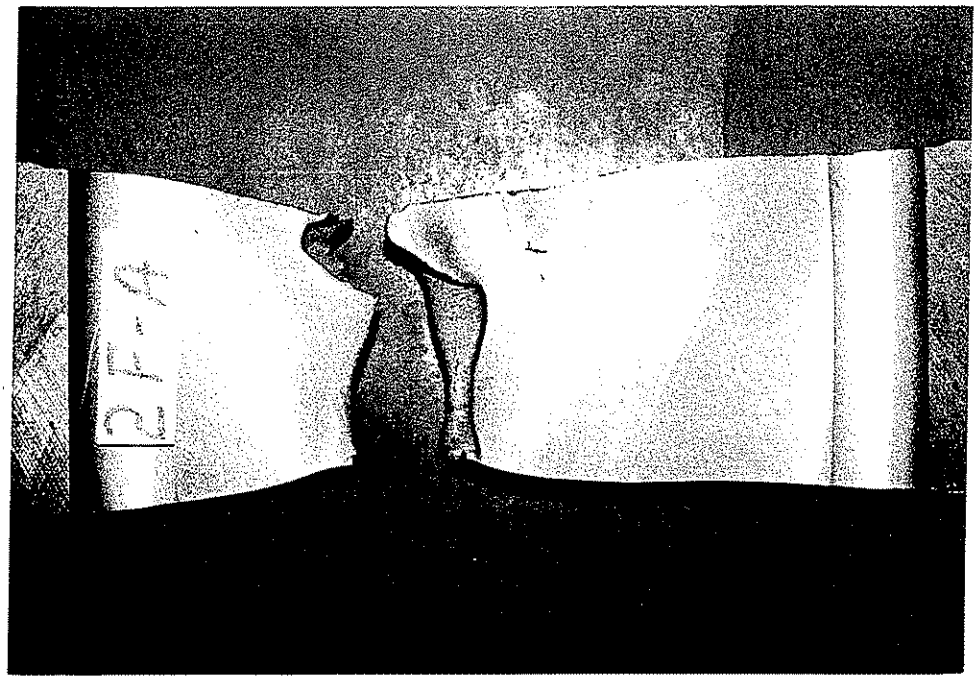

Fig. 12 Fracture Appearance of Tensile Specimen 7B-1.
Ductile fracture is Within Base Metal Adjacent to Weld
[photo: 1/91/19-1A]

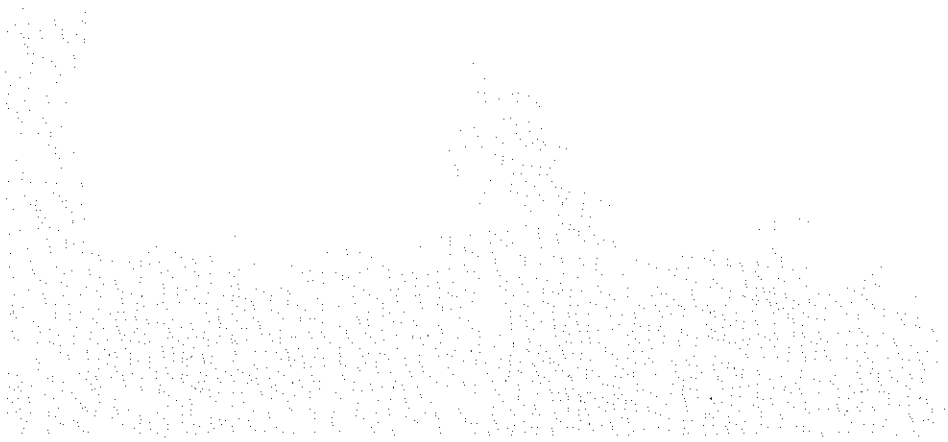

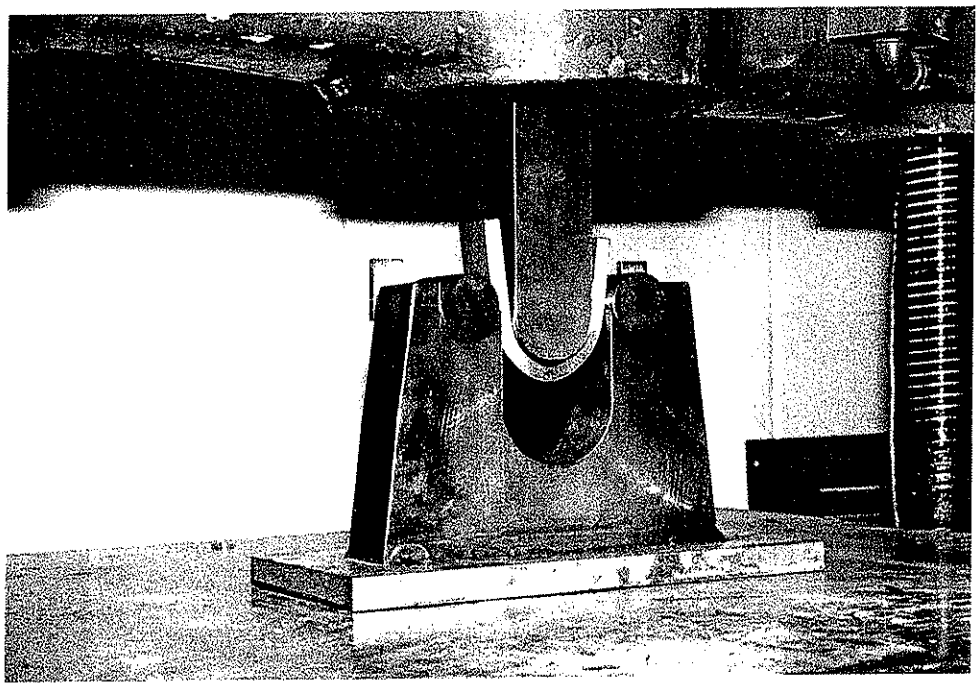

Fig.13 Side Bend Test Setup[photo: 5/92/26-8]

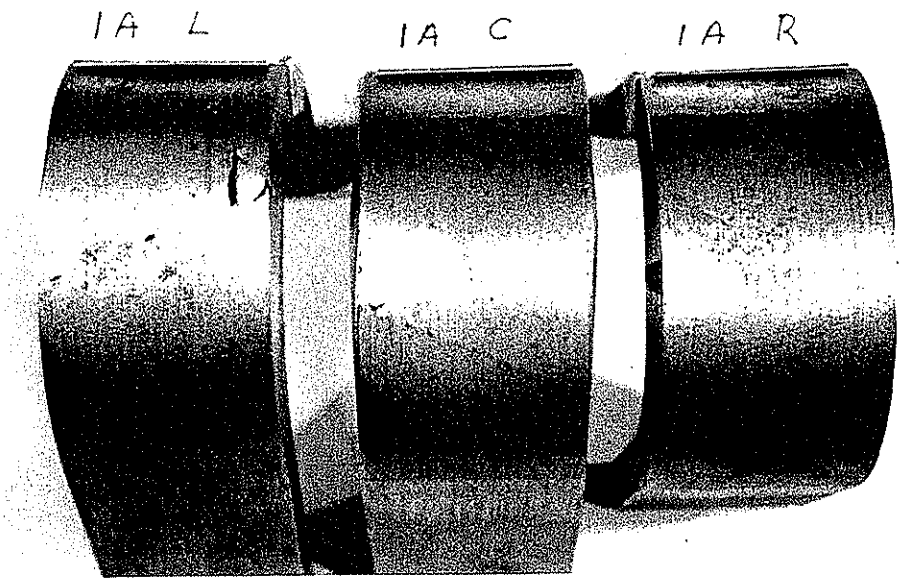

Fig. 14 Side Bend Test Specimens from Flange Splice 1A.
Note Slag Inclusions in Weld Root Area.[Photo:5/91/11-10]

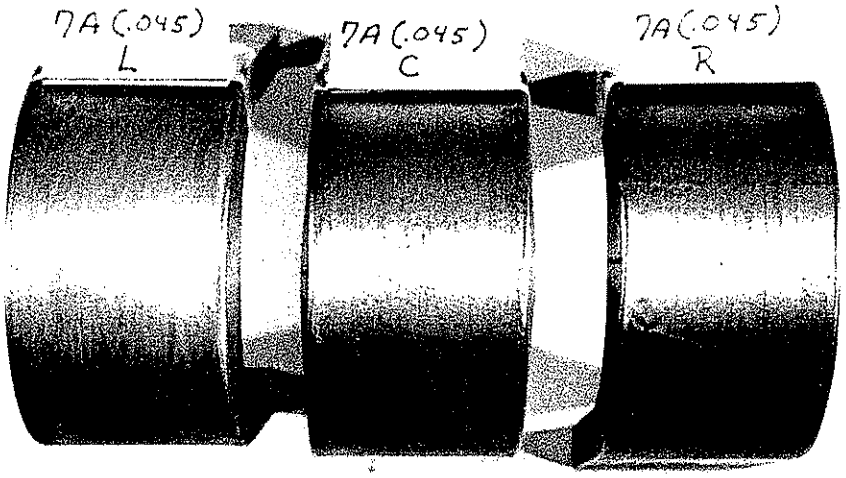

Fig. 15 Side Bend Test Specimens from Flange Splice 7A
[photo: 5/91/11-8]

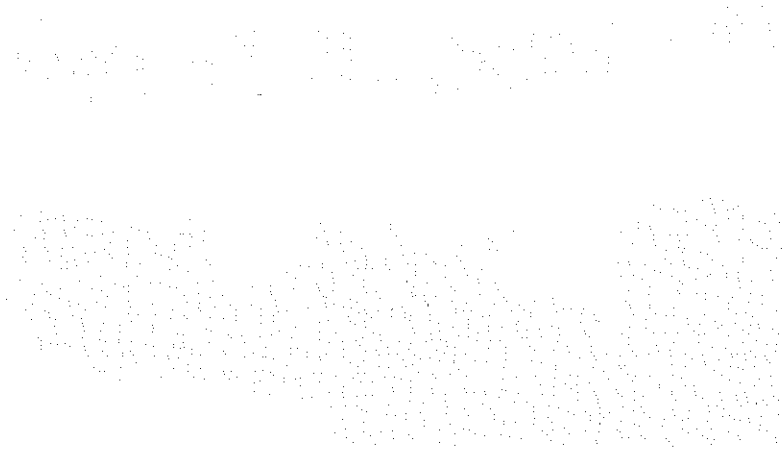

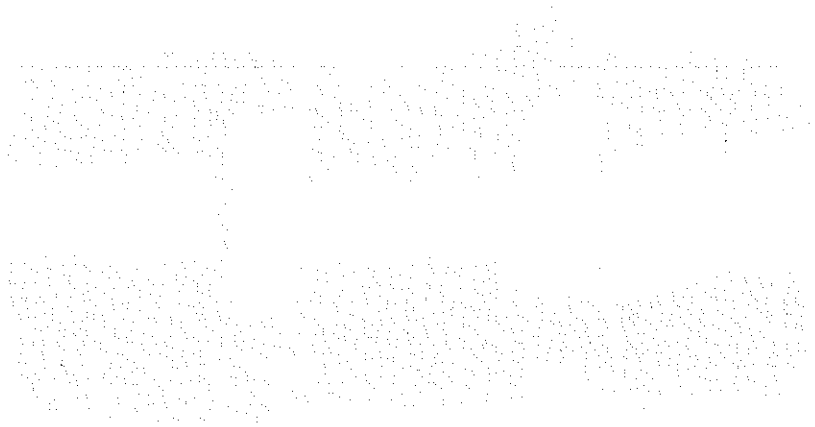

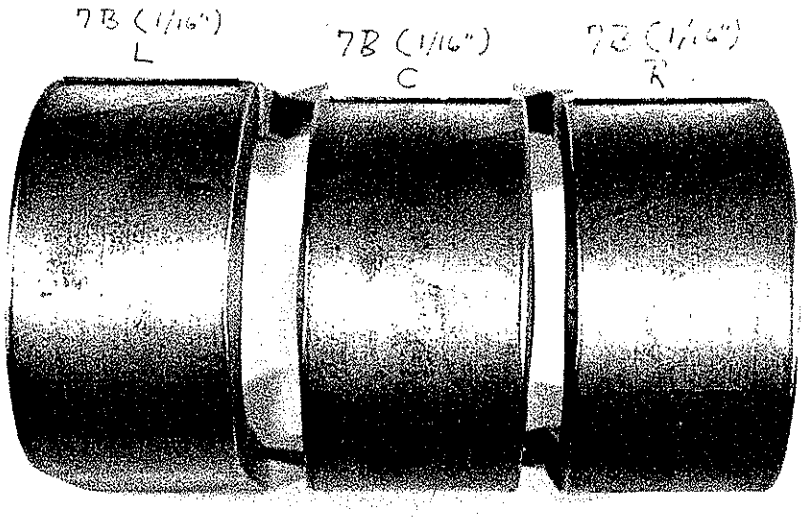

Fig. 16 Side Bend Test Specimens from flange Splice 7B[photo: 5/91/11-4]

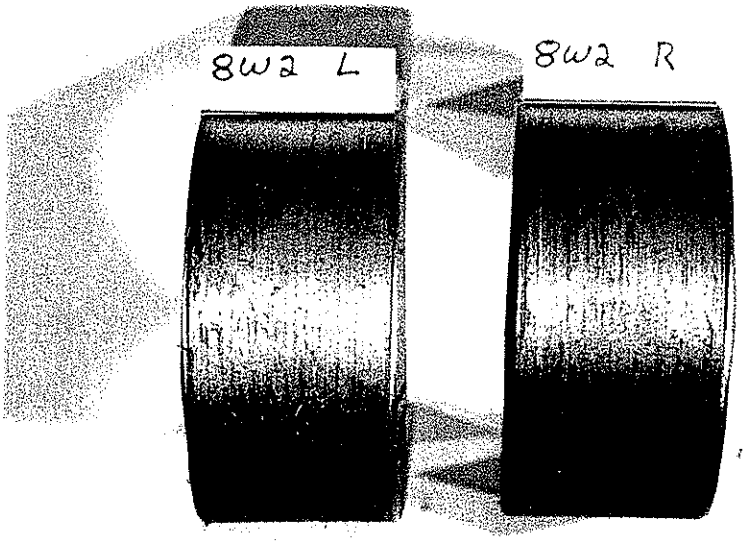

Fig. 17 Side Bend Test Specimens from Web Splice 8W[photo: 5/91/11-6]

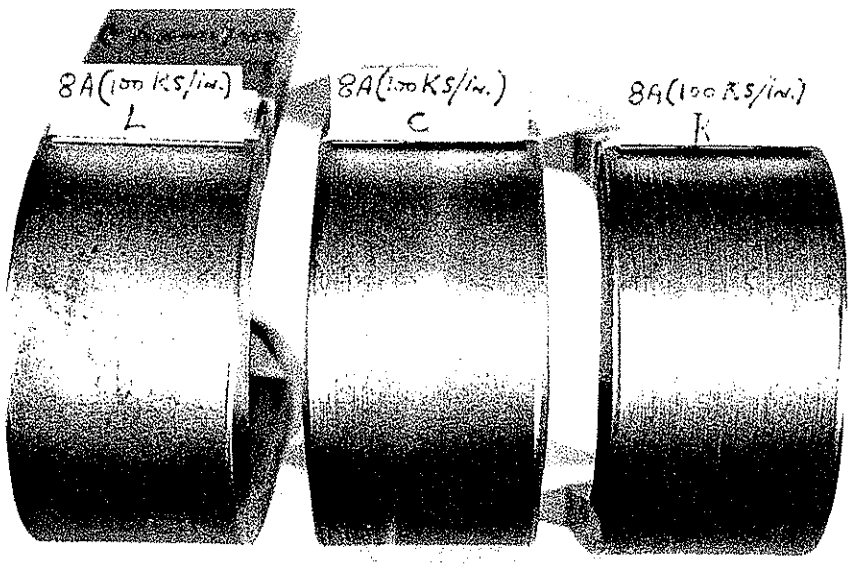

Fig. 18 Side Bend Test Spceimens from Flange Splice 8A[photo: 5/91/11-12]

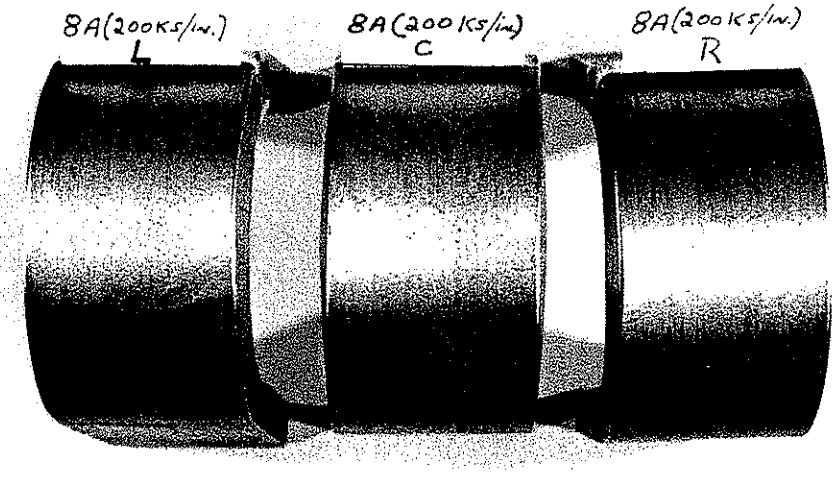

Fig. 19 side Bend Test Specimens from Flange Splice 8B[photo:5/91/11-2]

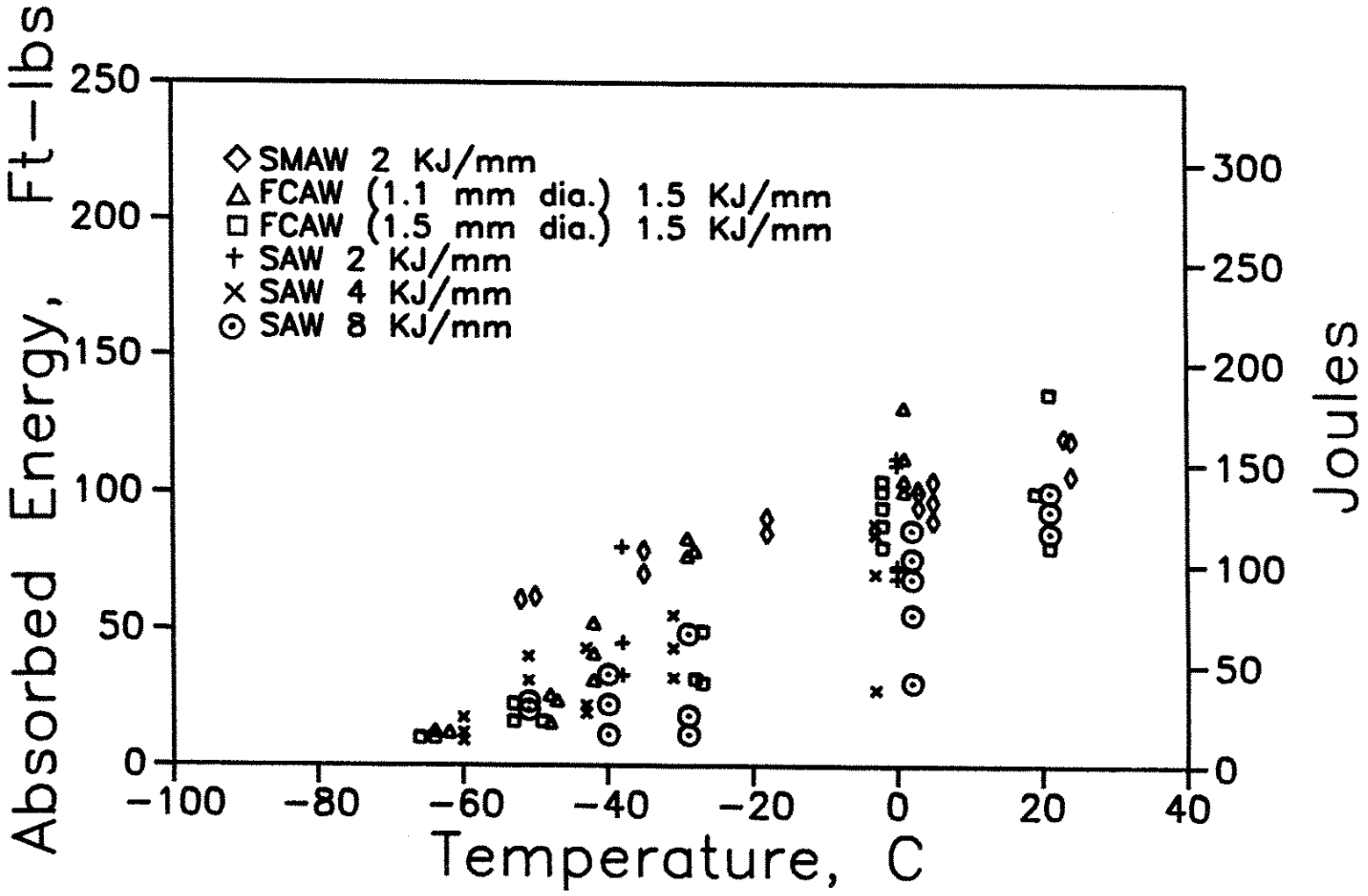

Fig. 20 Weld Metal Charpy V-Notch Test Results

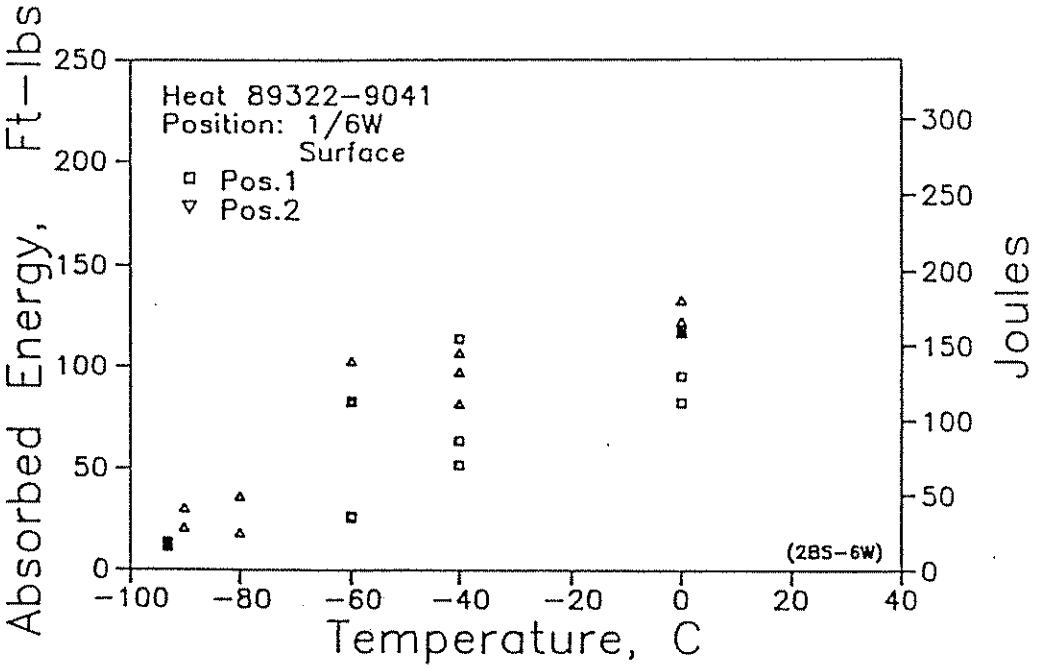

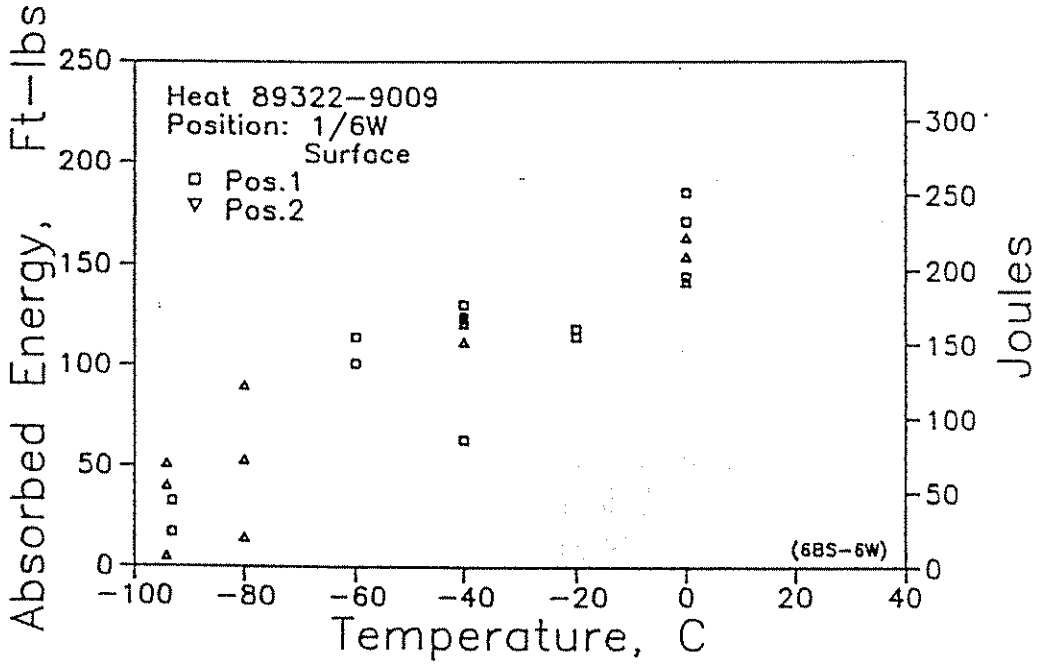

Fig. 21 Base Metal Charpy V-Notch Test Results
at Position 1/6 W - Surface

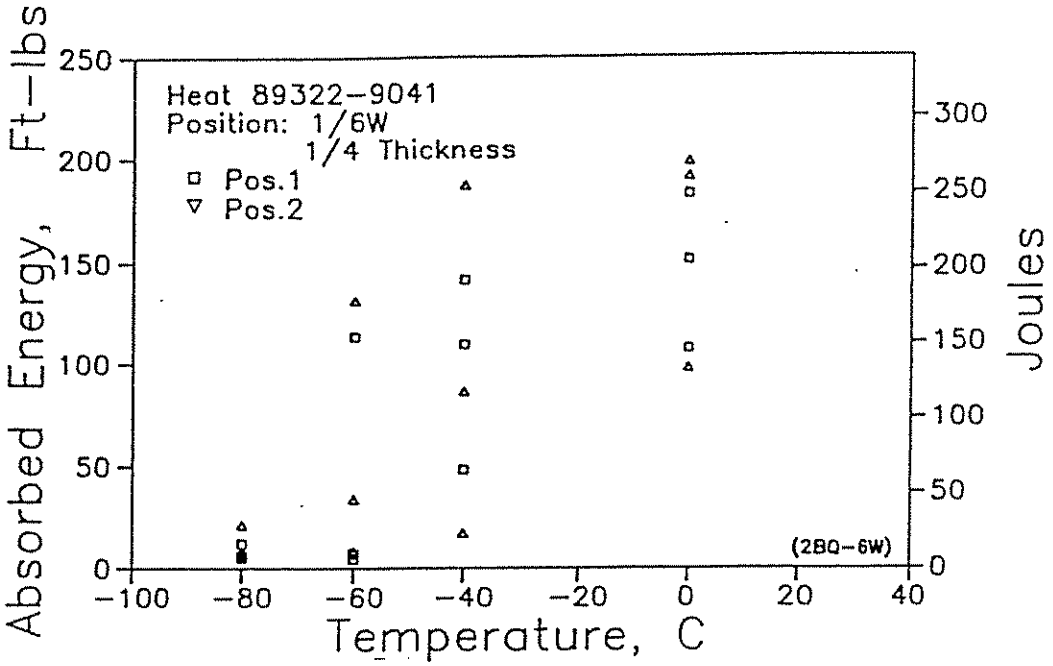

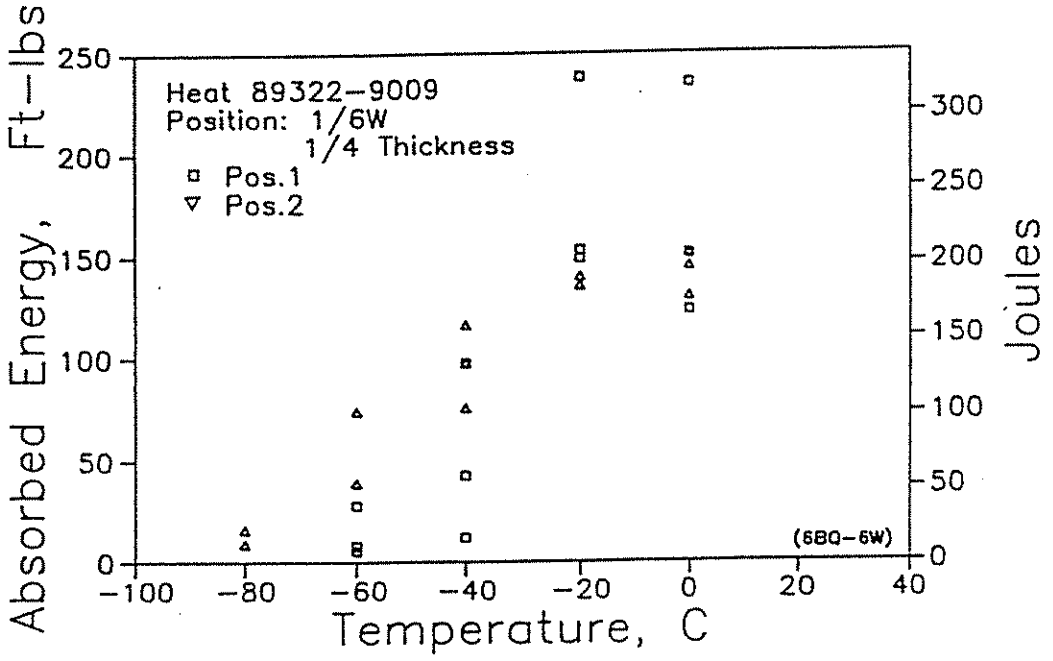

Fig. 22 Base Metal Charpy V-Notch Test Results
at Position 1/6 W - 1/4 Thickness

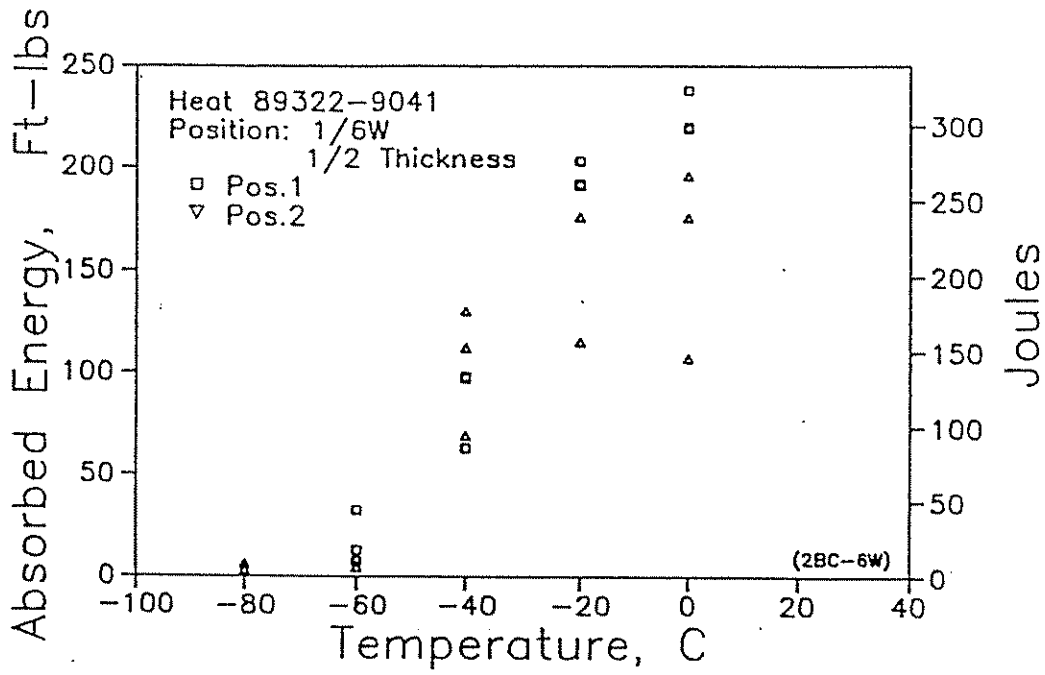

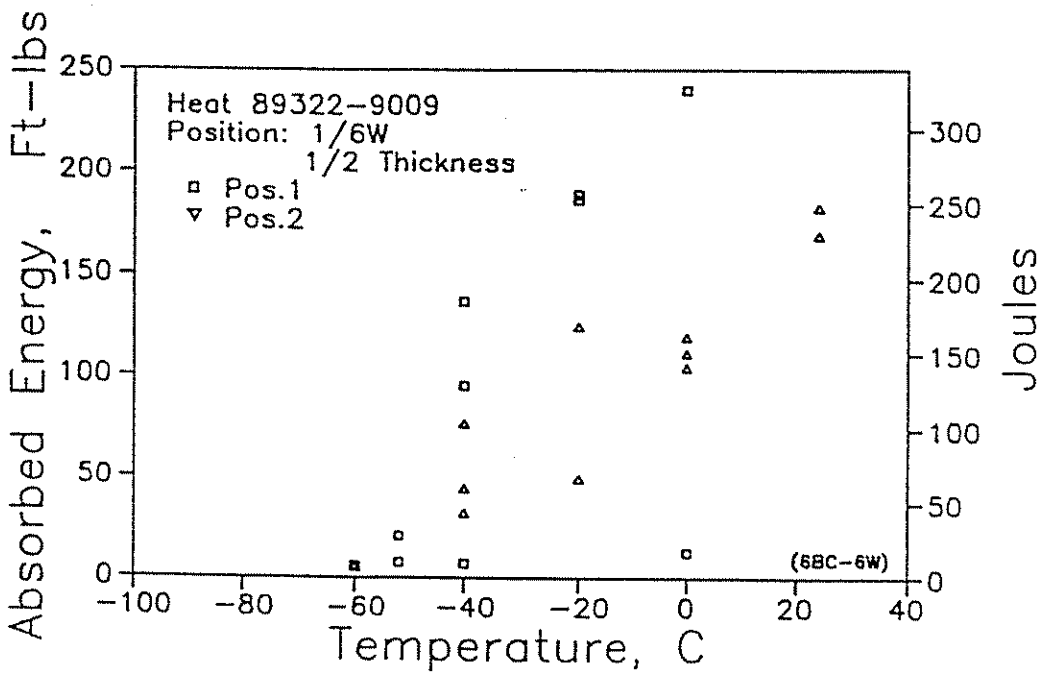

Fig. 23 Base Metal Charpy V-Notch Test Results
at Position 1/6 W - 1/2 Thickness

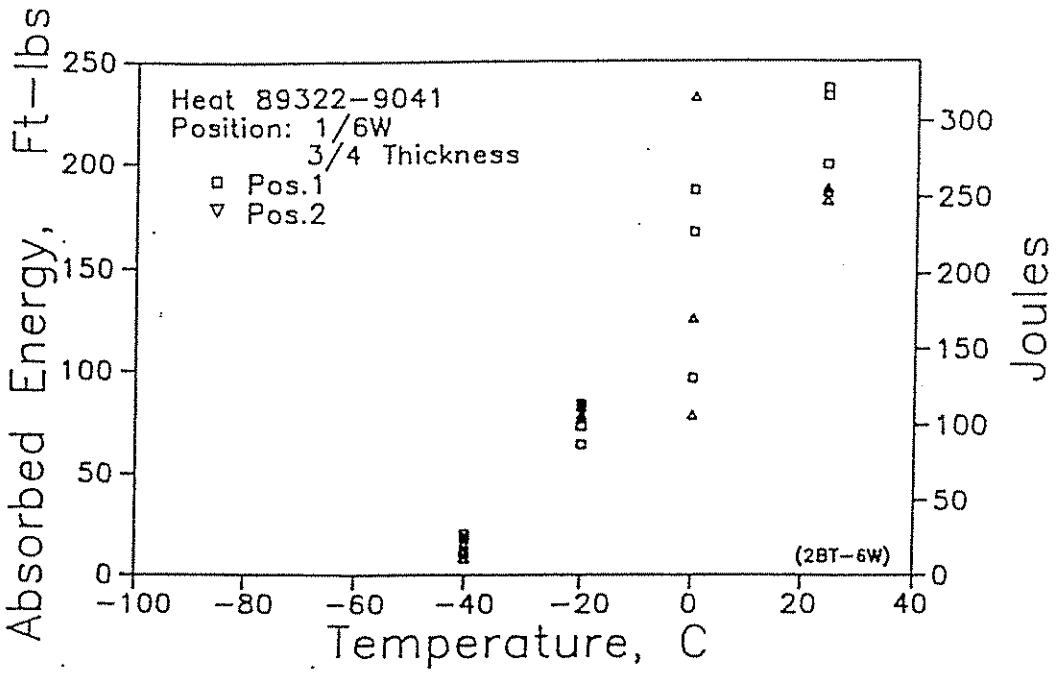

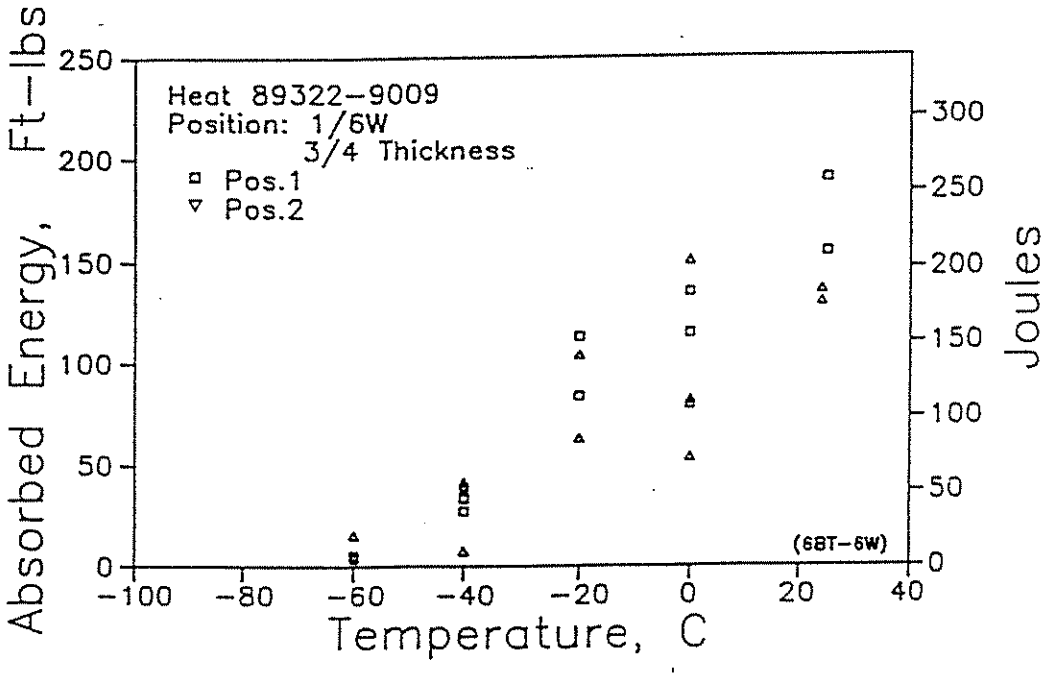

Fig. 24 Base Metal Charpy V-Notch Test Results at Position 1/6 W - 3/4 Thickness

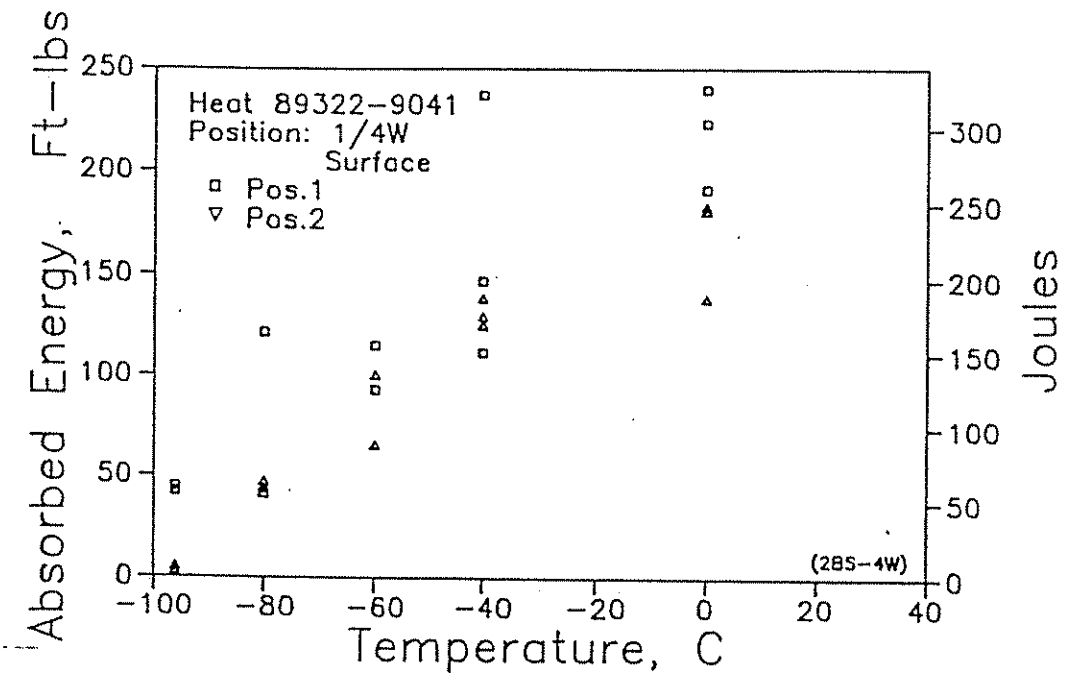

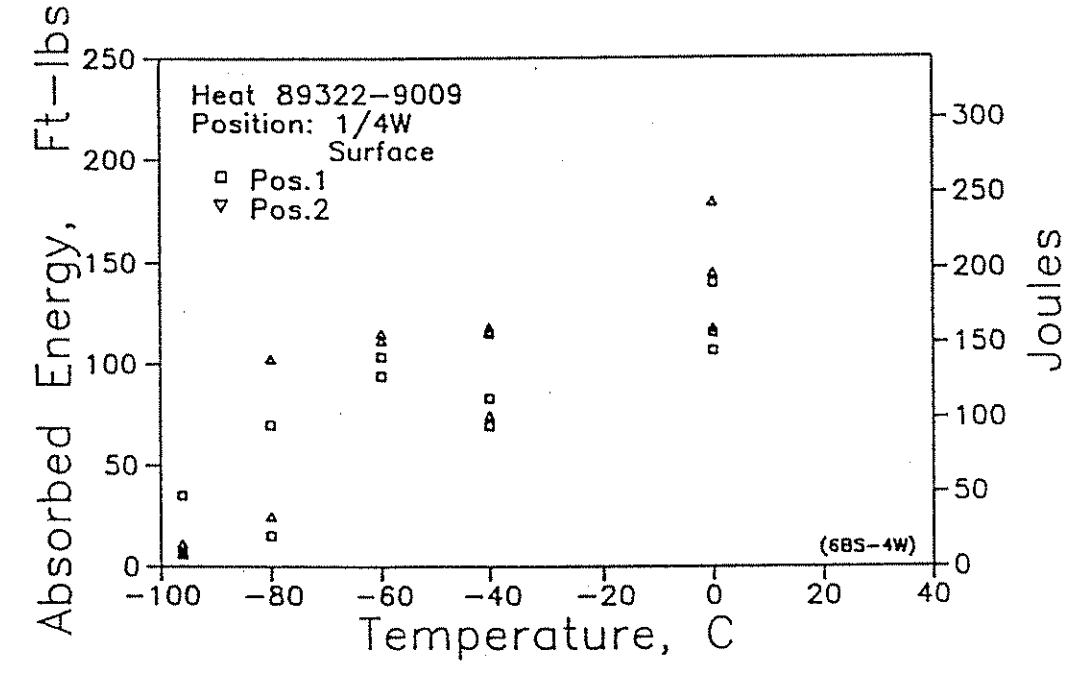

Fig. 25 Base Metal Charpy V-Notch Test Results
at Position 1/4 W - Surface

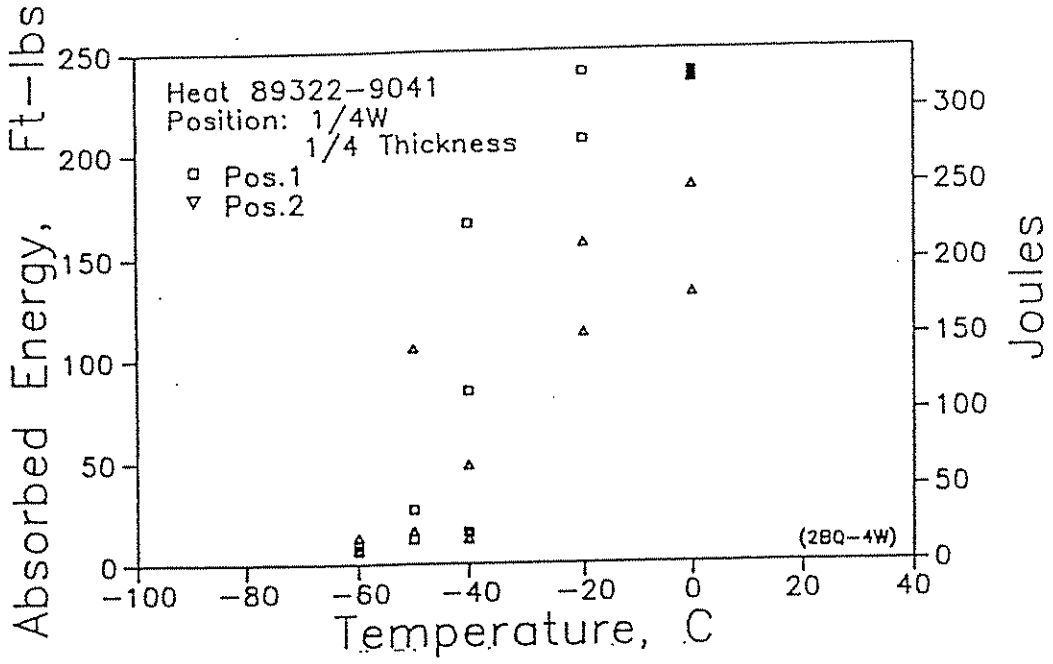

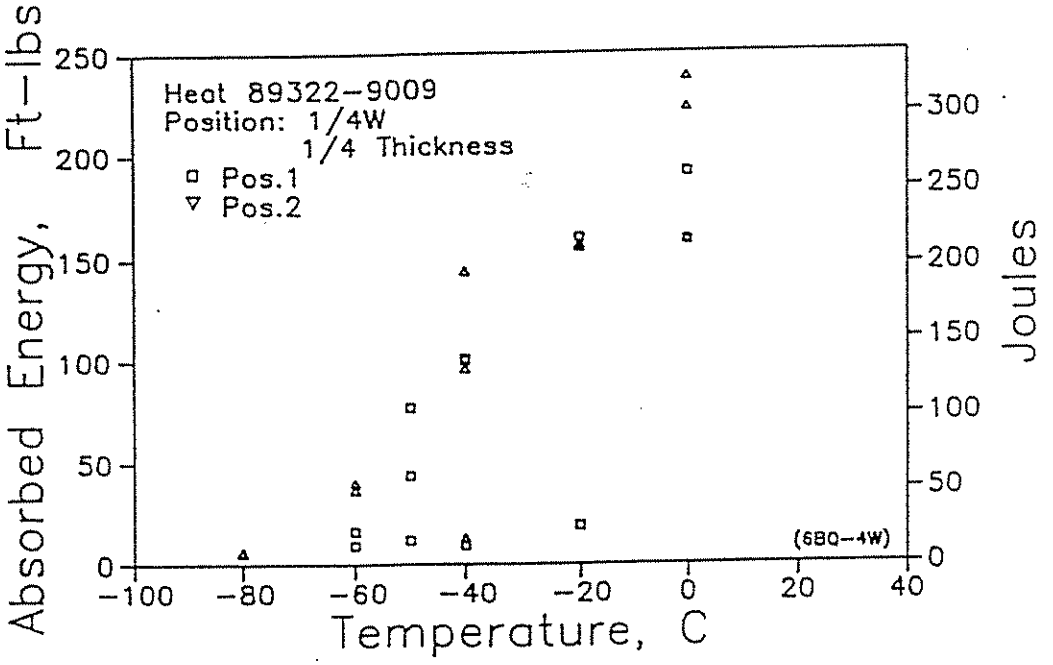

Fig. 26 Base Metal Charpy V-Notch Test Results
at Position 1/4 W - 1/4 Thickness

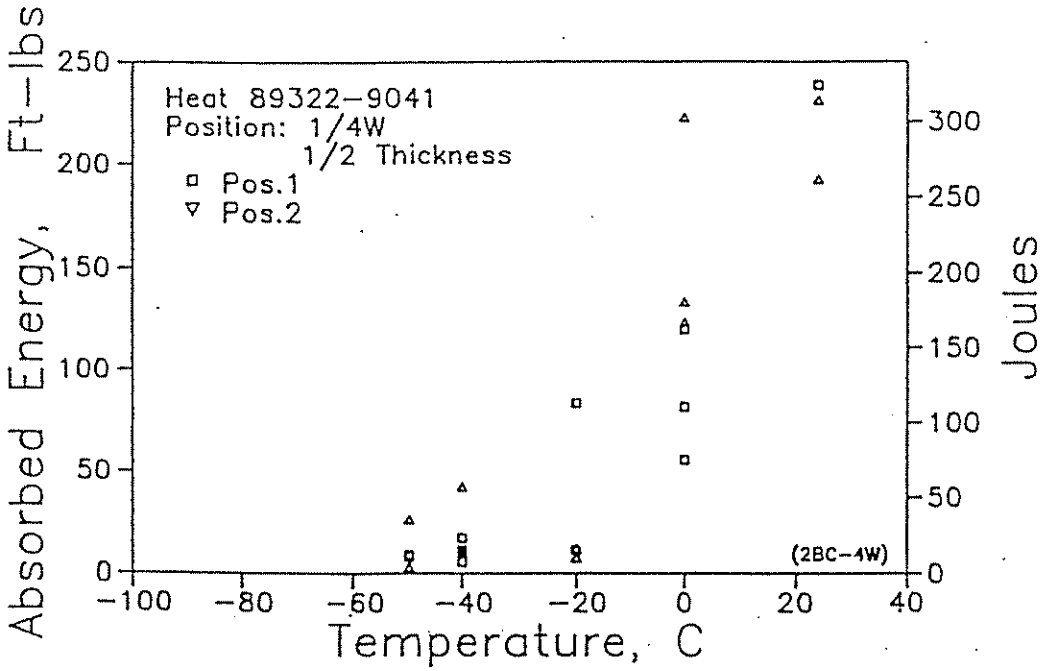

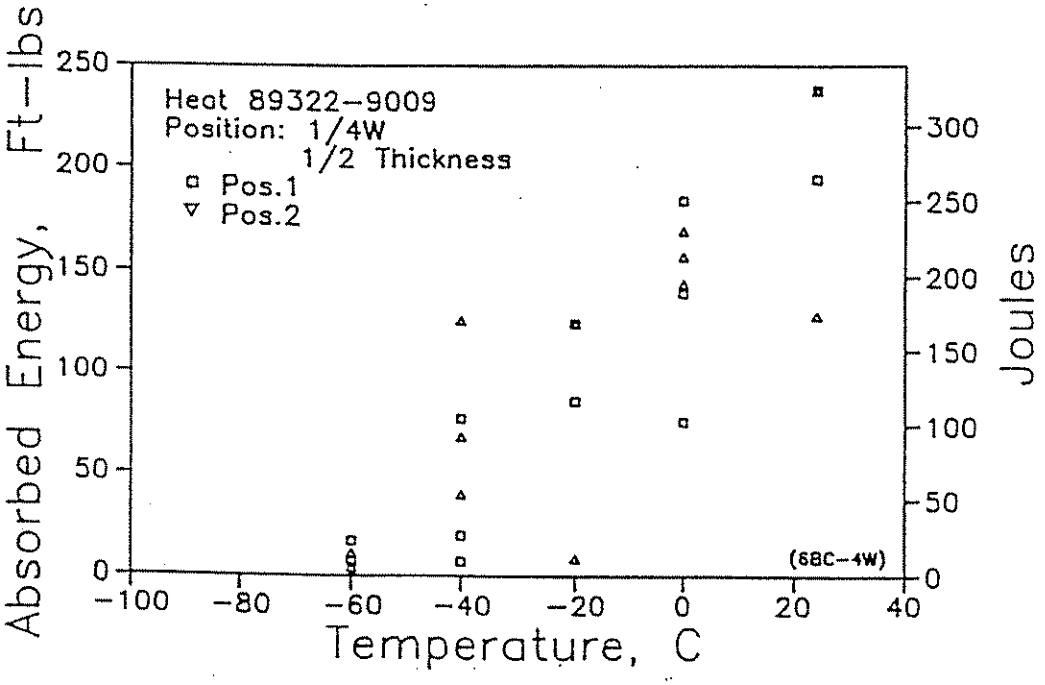

Fig. 27 Base Metal Charpy V-Notch Test Results
at Position 1/4 W - 1/2 Thickness

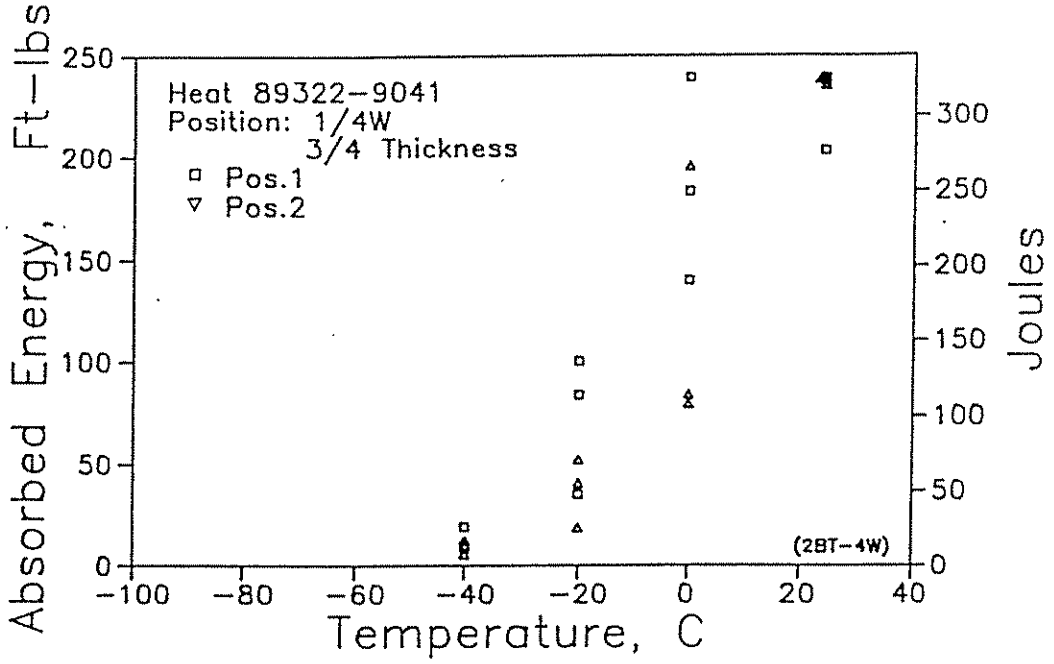

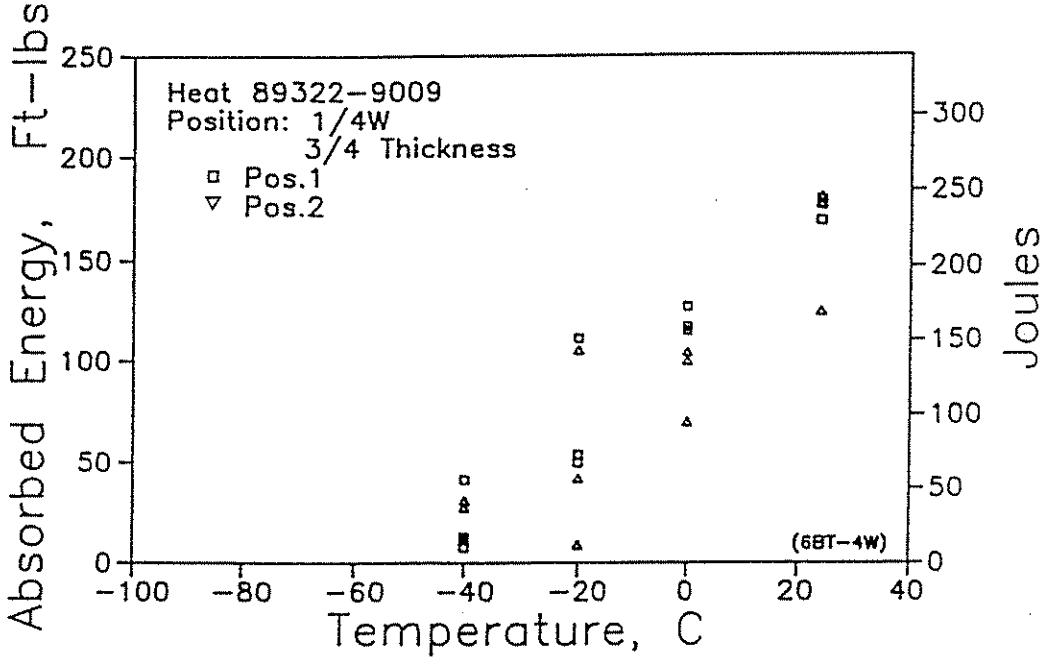

Fig. 28 Base Metal Charpy V-Notch Test Results
at Position 1/4 W - 3/4 Thickness

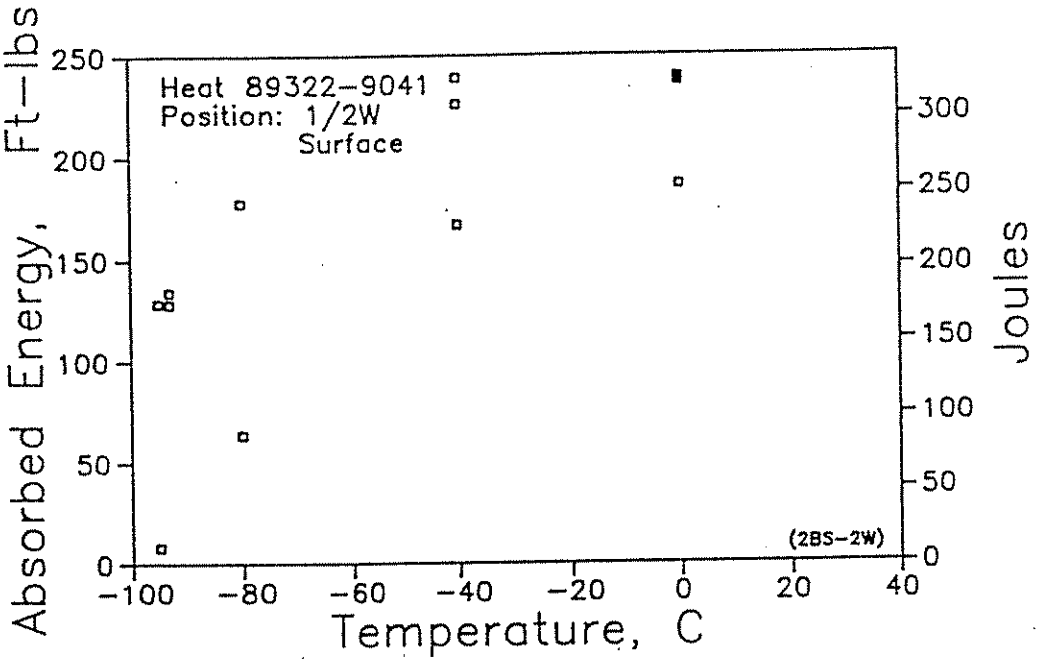

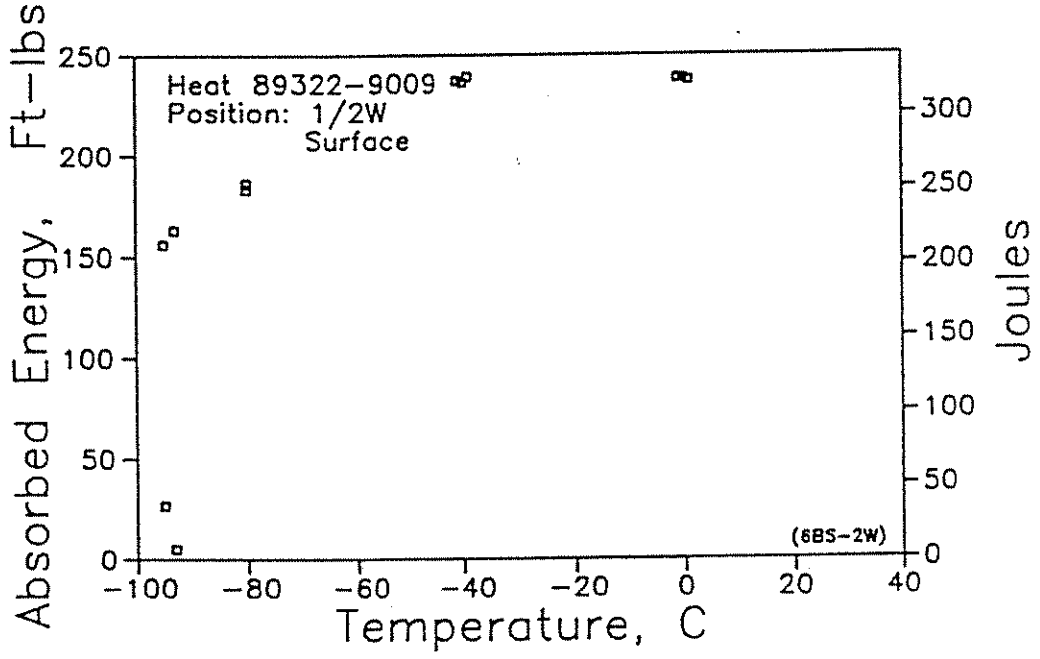

Fig. 29 Base Metal Charpy V-Notch Test Results at Position 1/2 W - Surface

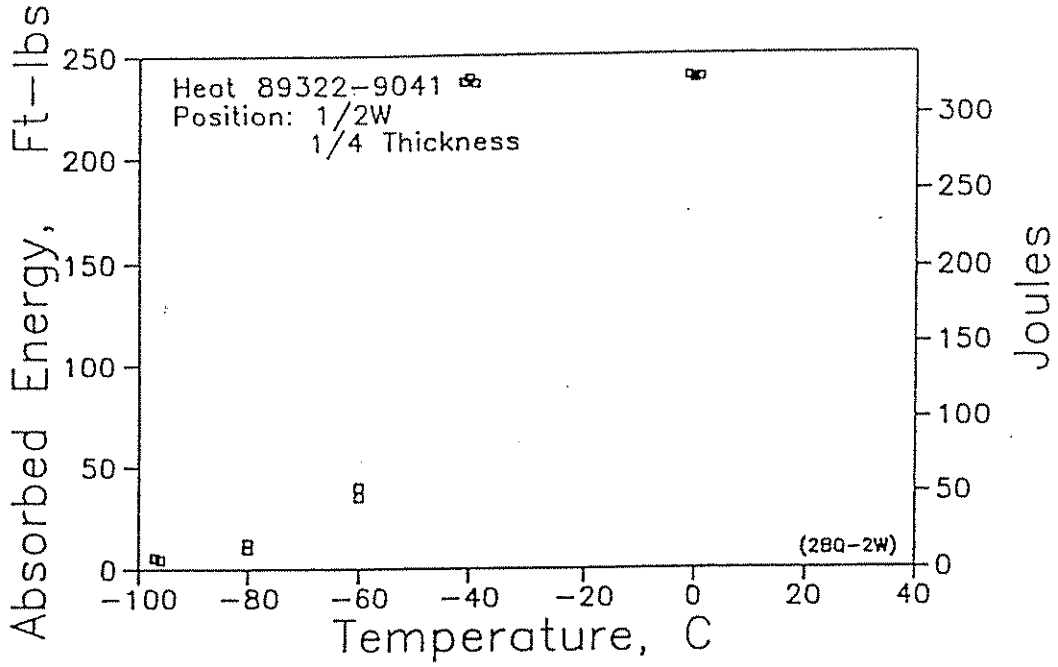

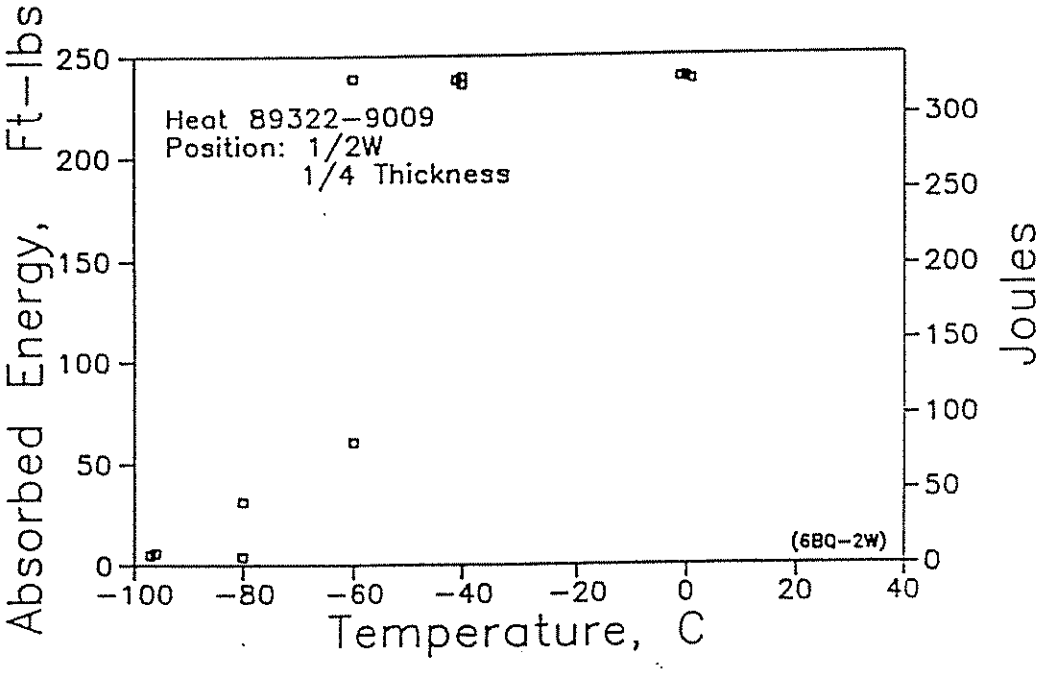

Fig. 30 Base Metal Charpy V-Notch Test Results
at Position 1/2 W - 1/4 Thickness

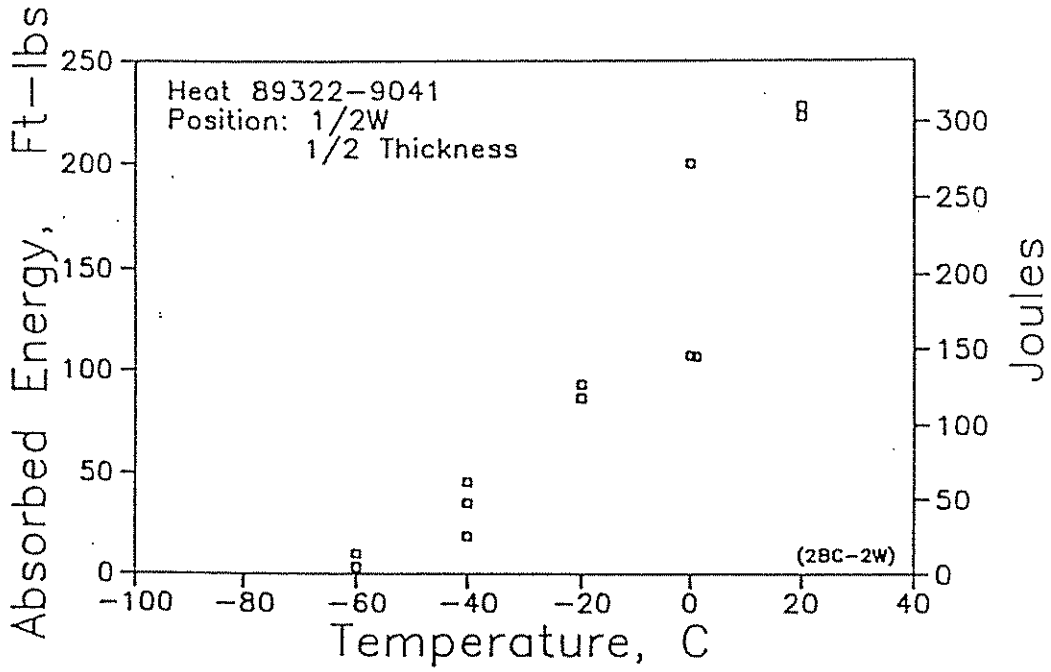

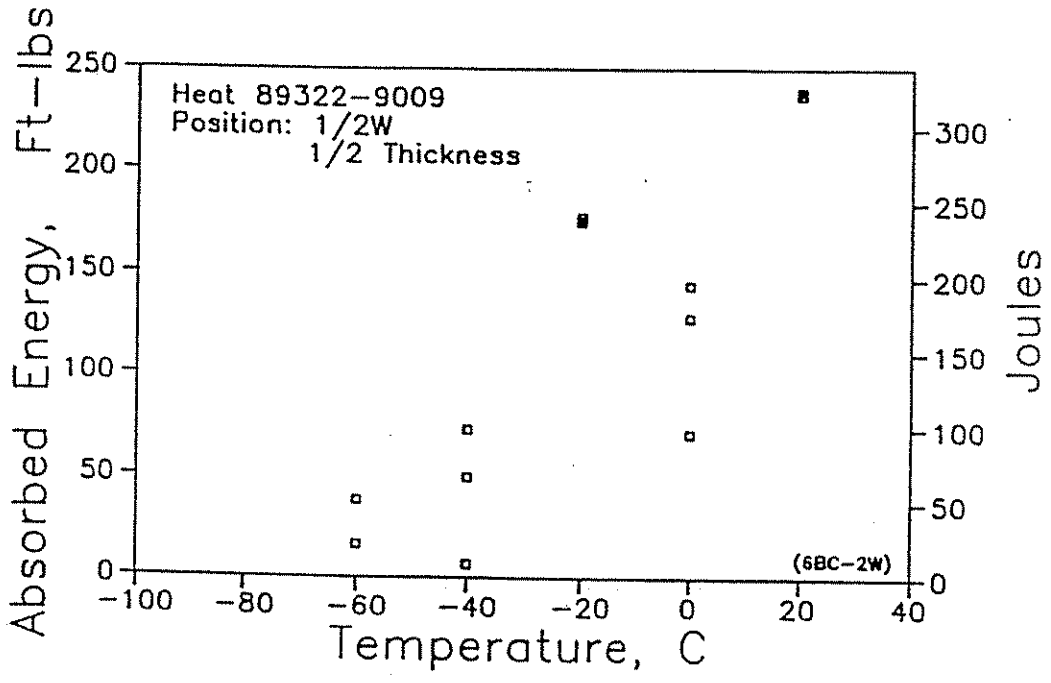

Fig. 31 Base Metal Charpy V-Notch Test Results at Position 1/2 W - 1/2 Thickness

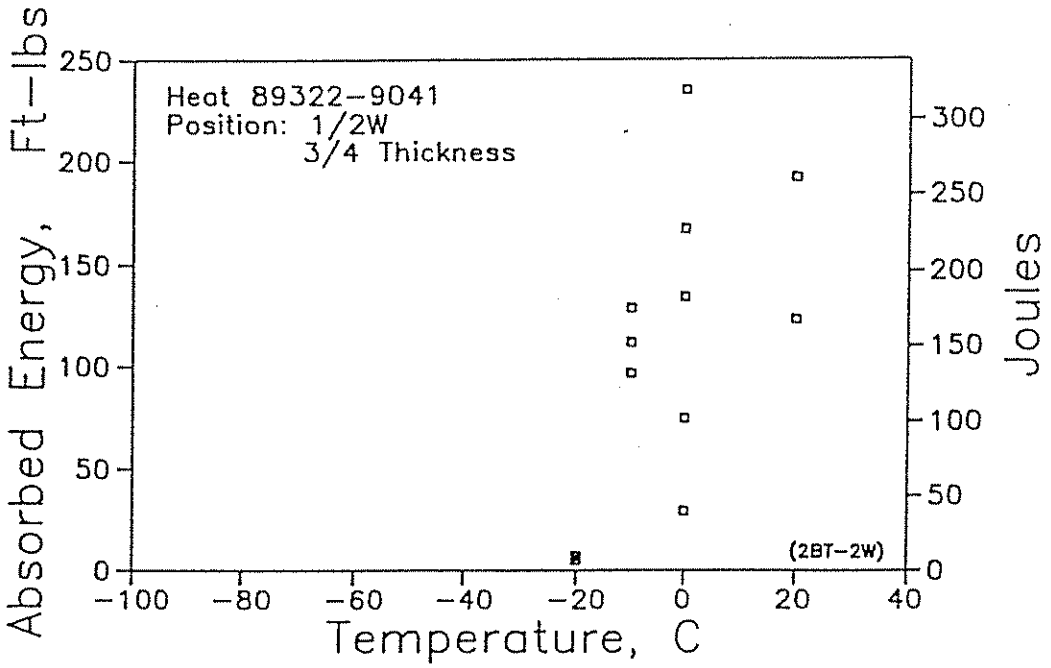

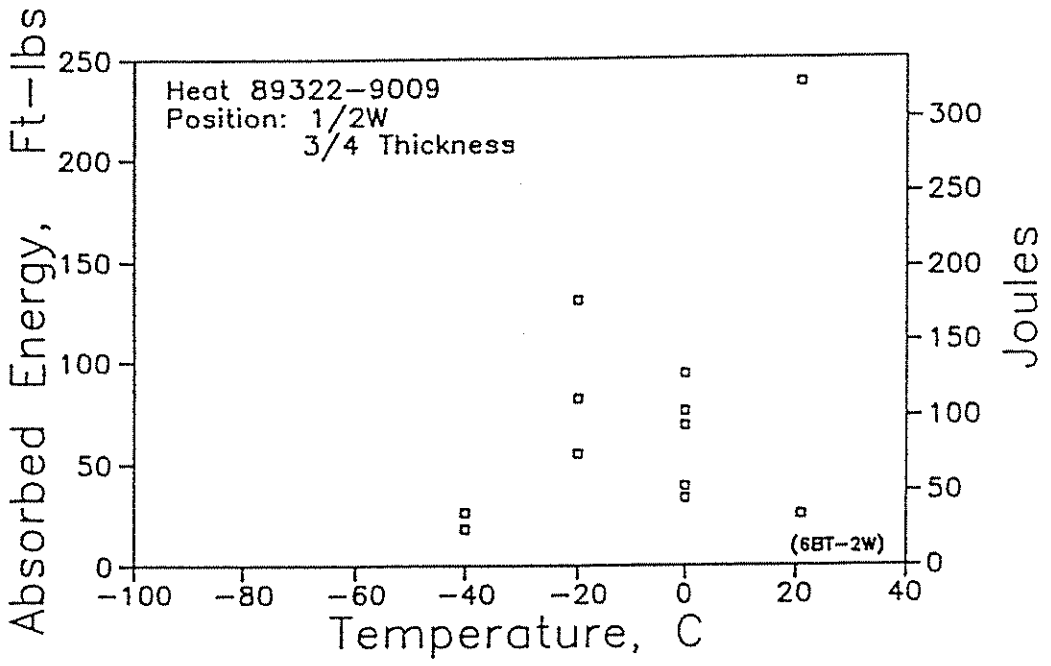

Fig. 32 Base Metal Charpy V-Notch Test Results
at Position 1/2 W - 3/4 Thickness

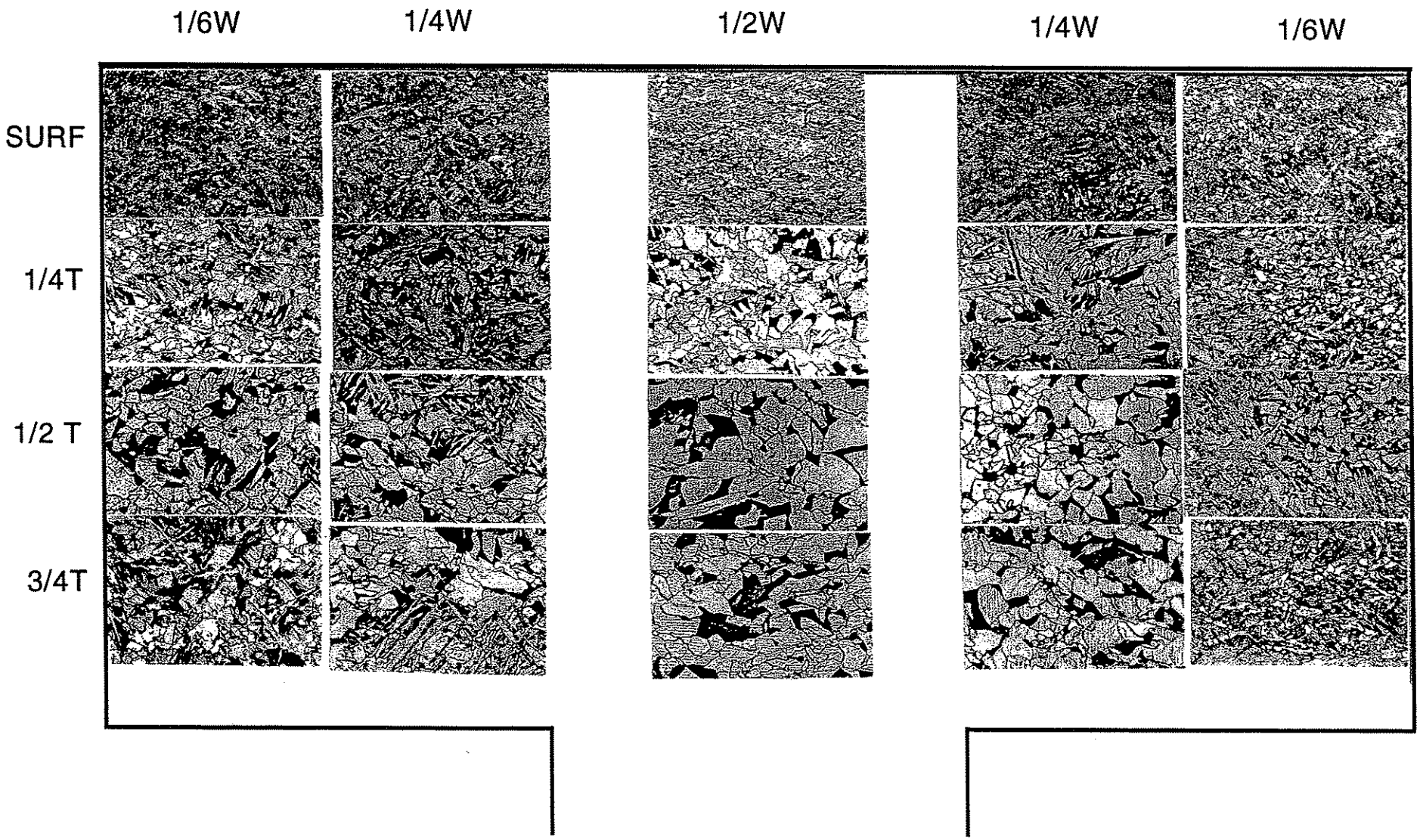

Fig. 33 Flange Microstructure at the Twenty Test Locations (100X)
[Heat 89322-9009]

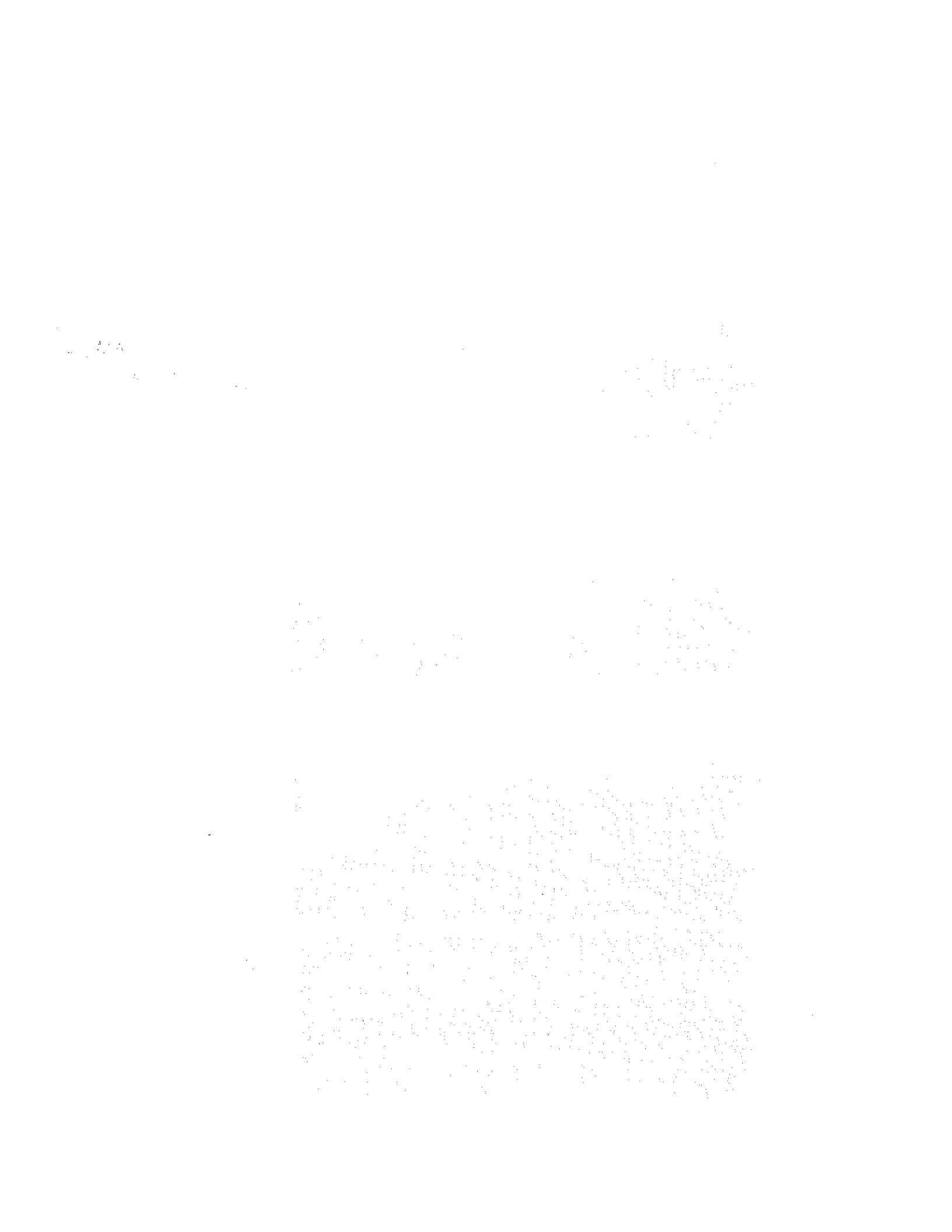

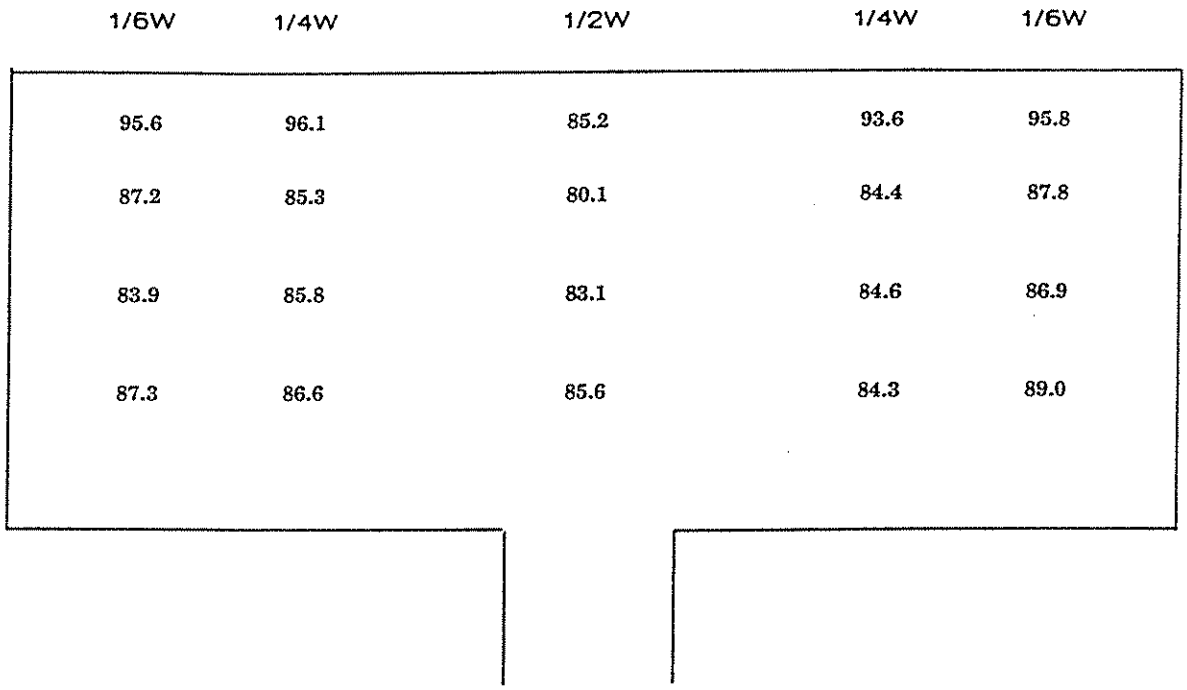

Fig. 34 Rockwell B Hardness at the Flange Test Locations
(Heat 89322-9009)

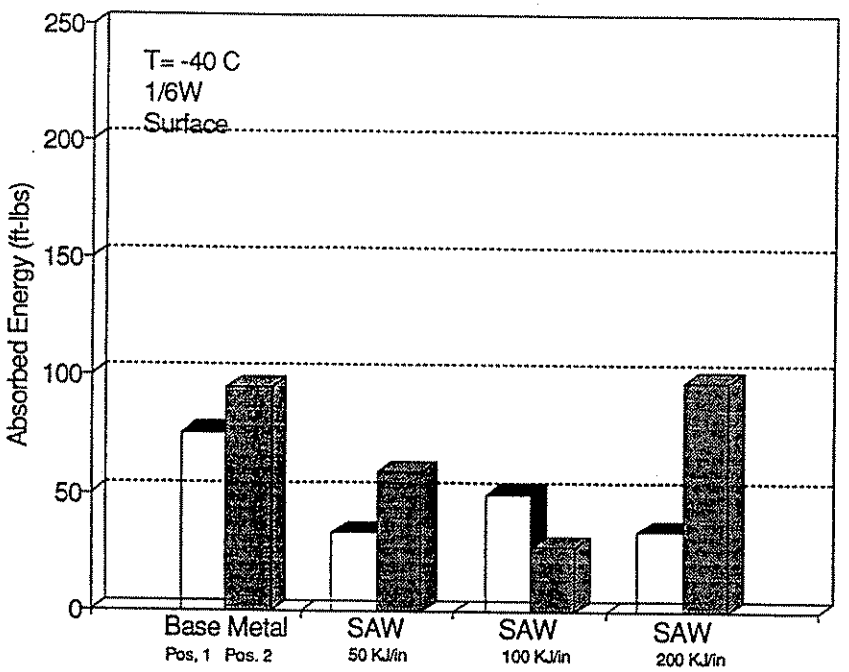

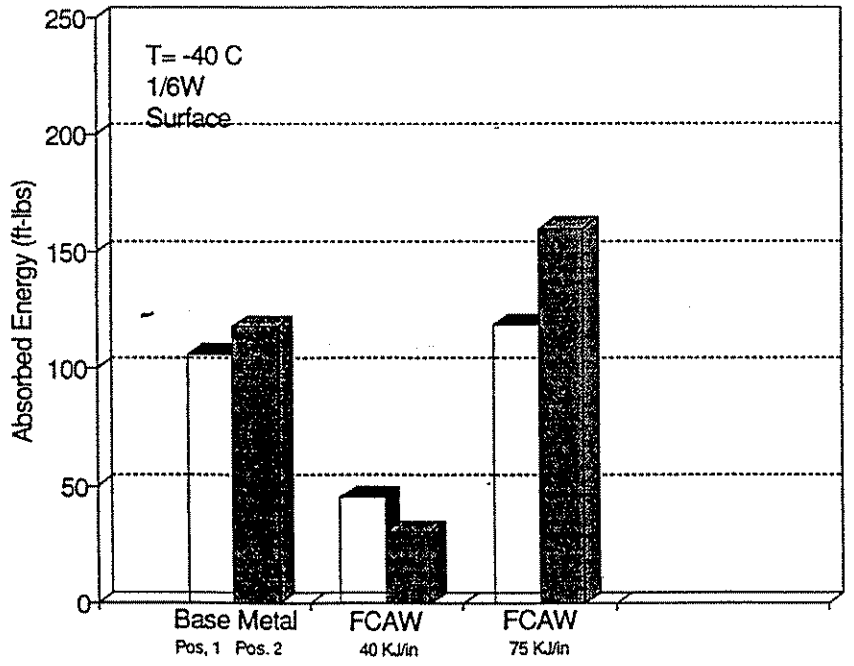

Fig. 35 HAZ Charpy V-Notch Test Results at Position 1/6 W - Surface

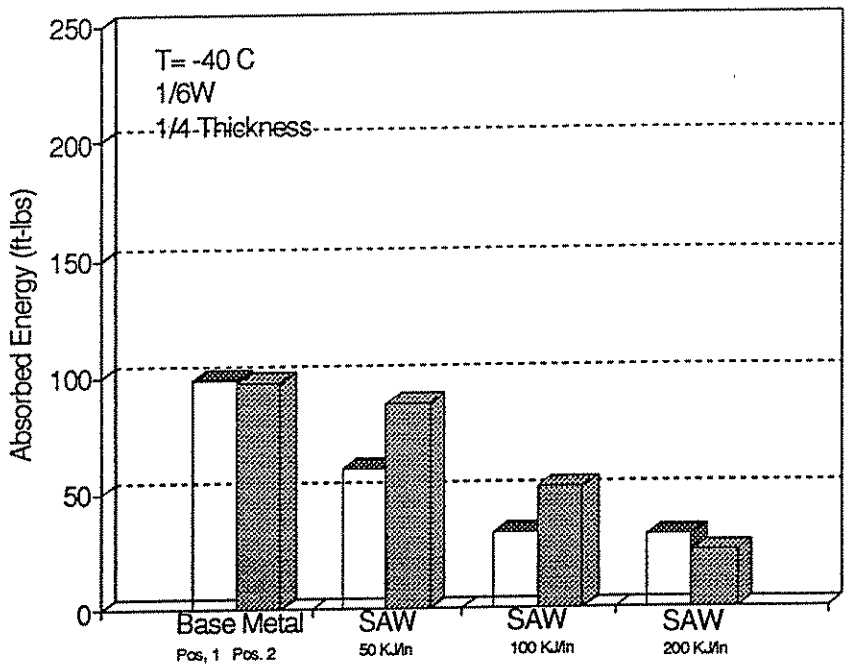

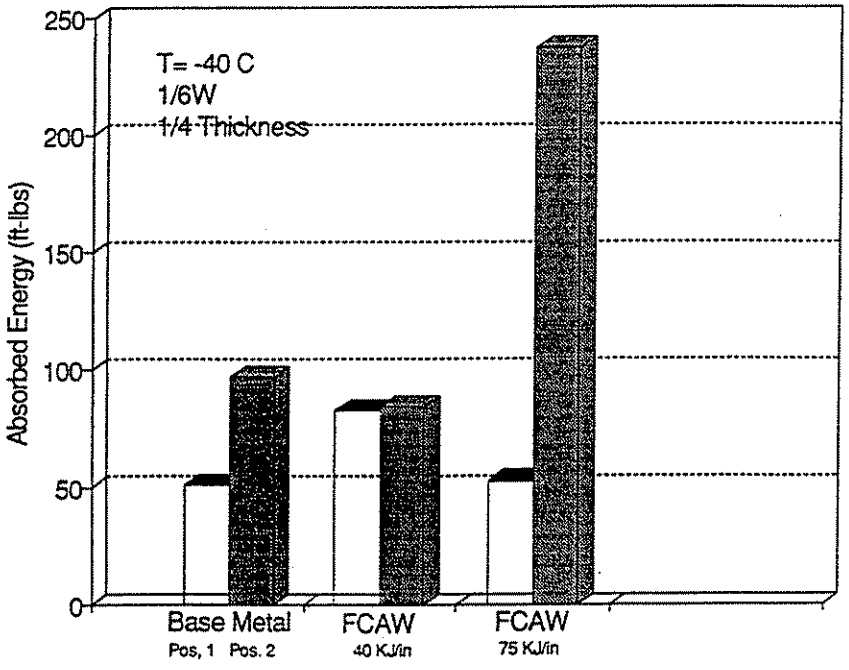

Fig. 36 HAZ Charpy V-Notch Test Results at Position 1/6 W - 1/4 Thickness

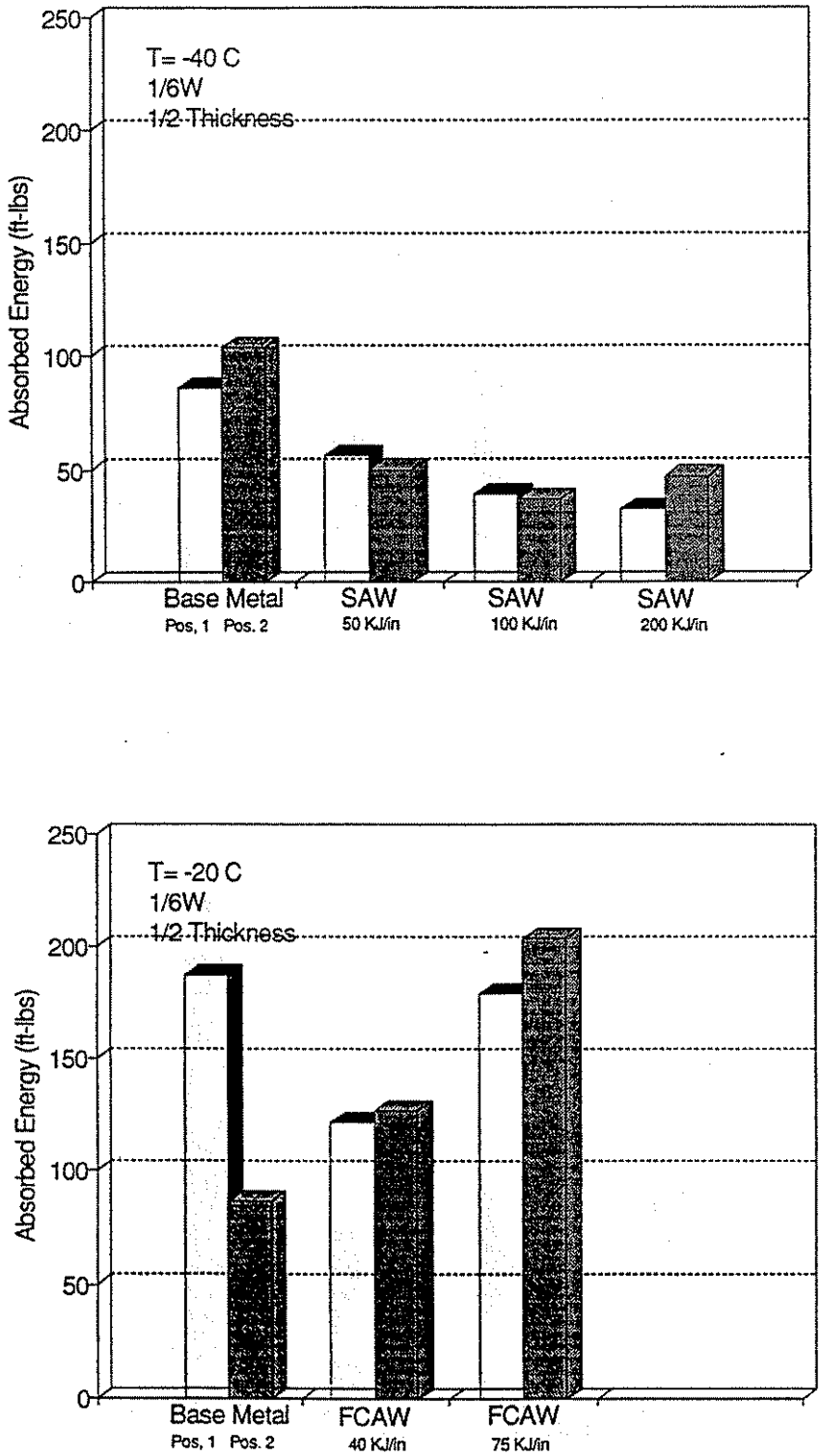

Fig. 37 HAZ Charpy V-Notch Test Results at Position 1/6 W - 1/2 Thickness

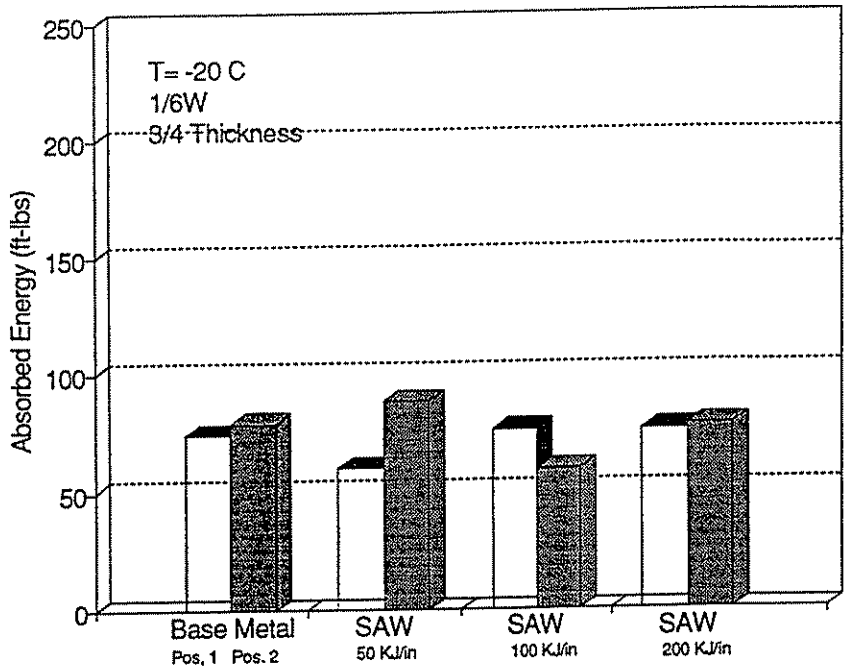

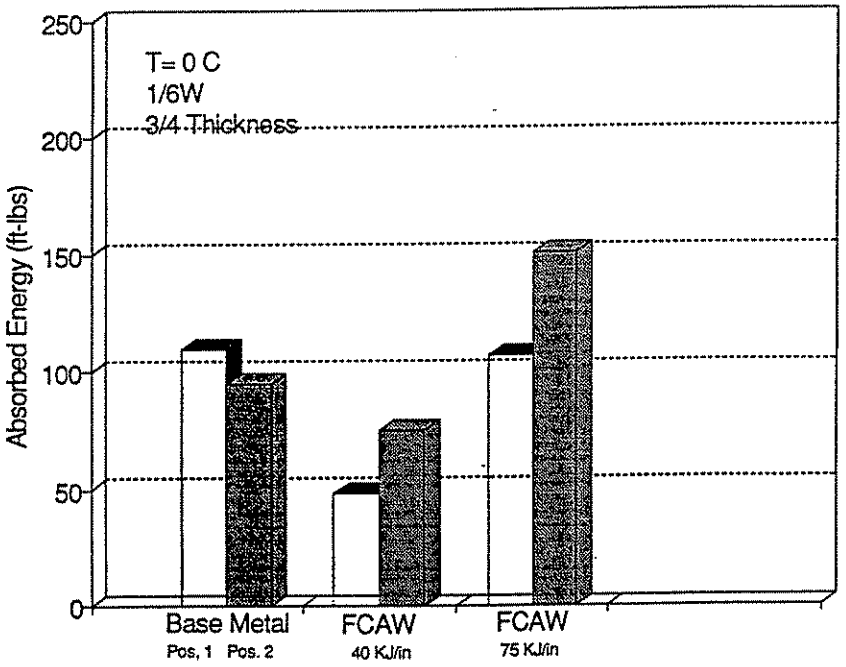

Fig. 38 HAZ Charpy V-Notch Test Results at Position 1/6 W - 3/4 Thickness

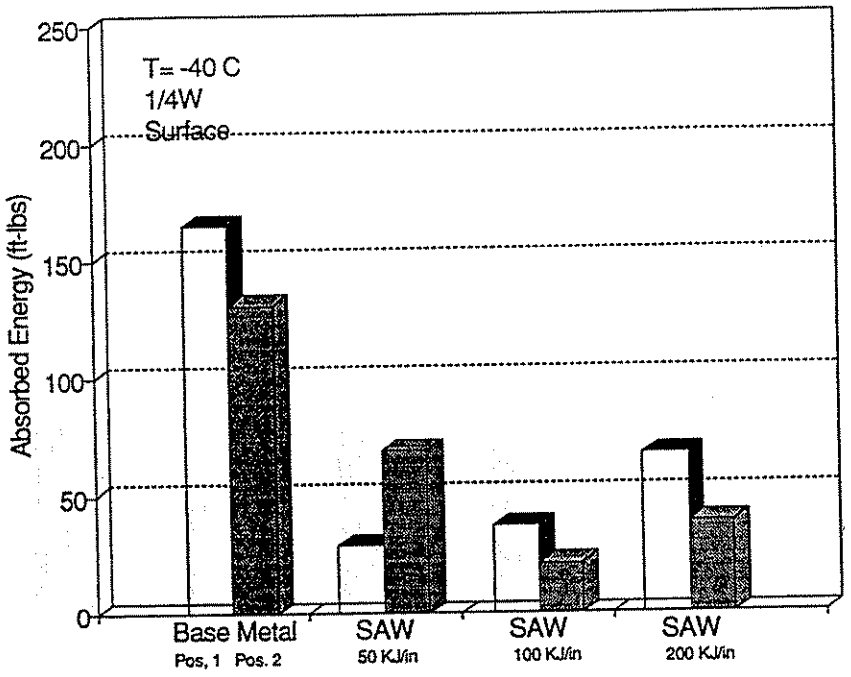

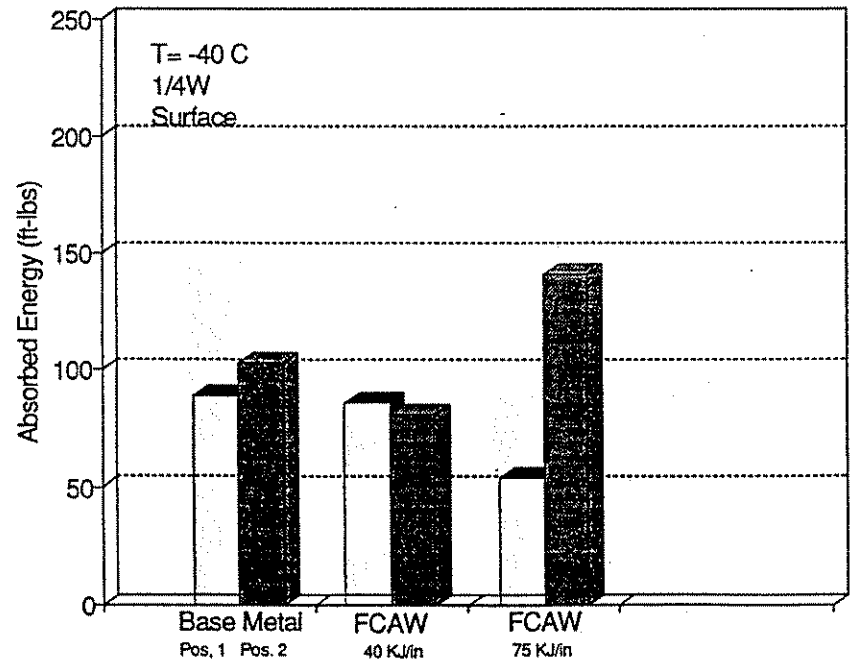

Fig. 39 HAZ Charpy V-Notch Test Results at Position 1/4 W - Surface

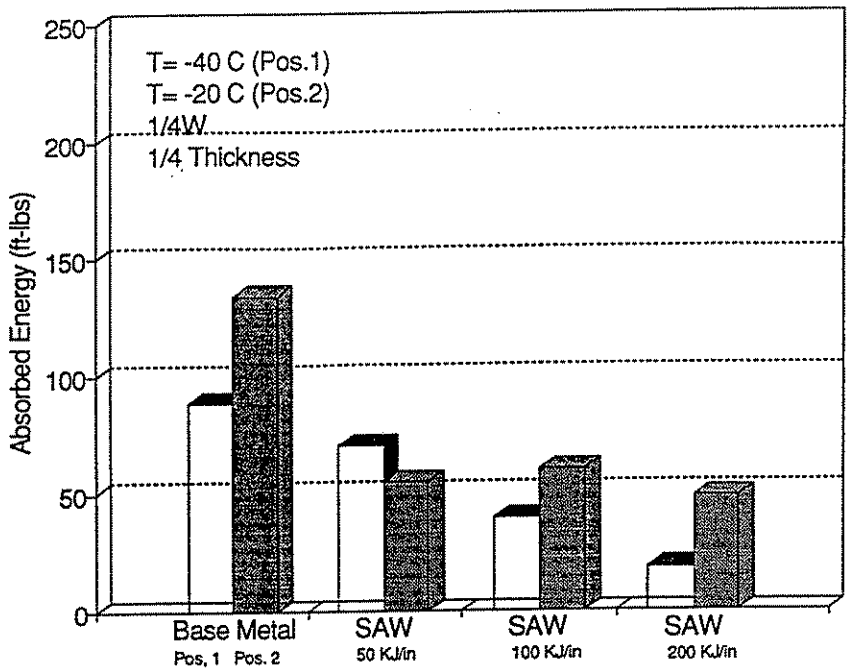

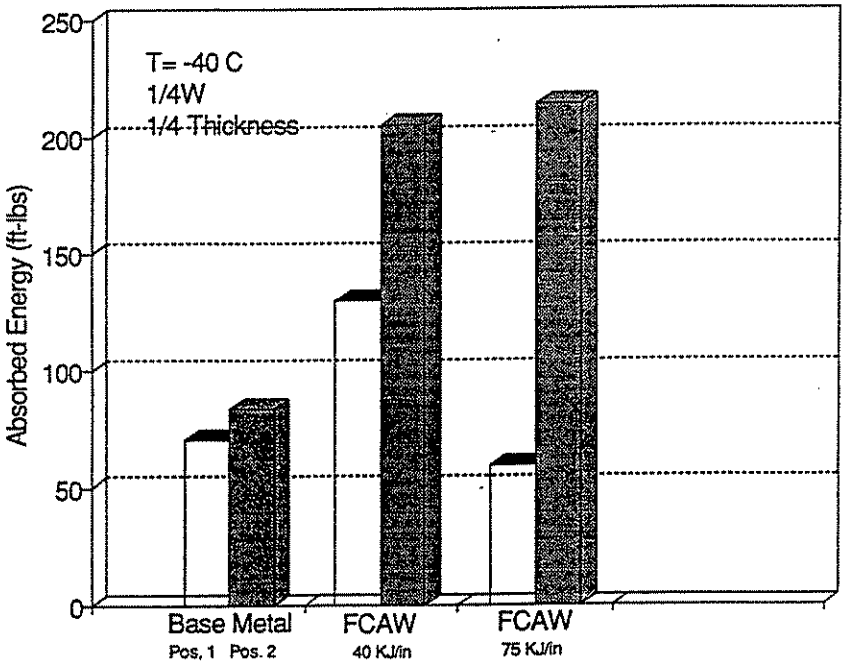

Fig. 40 HAZ Charpy V-Notch Test Results at Position 1/4 W - 1/4 Thickness

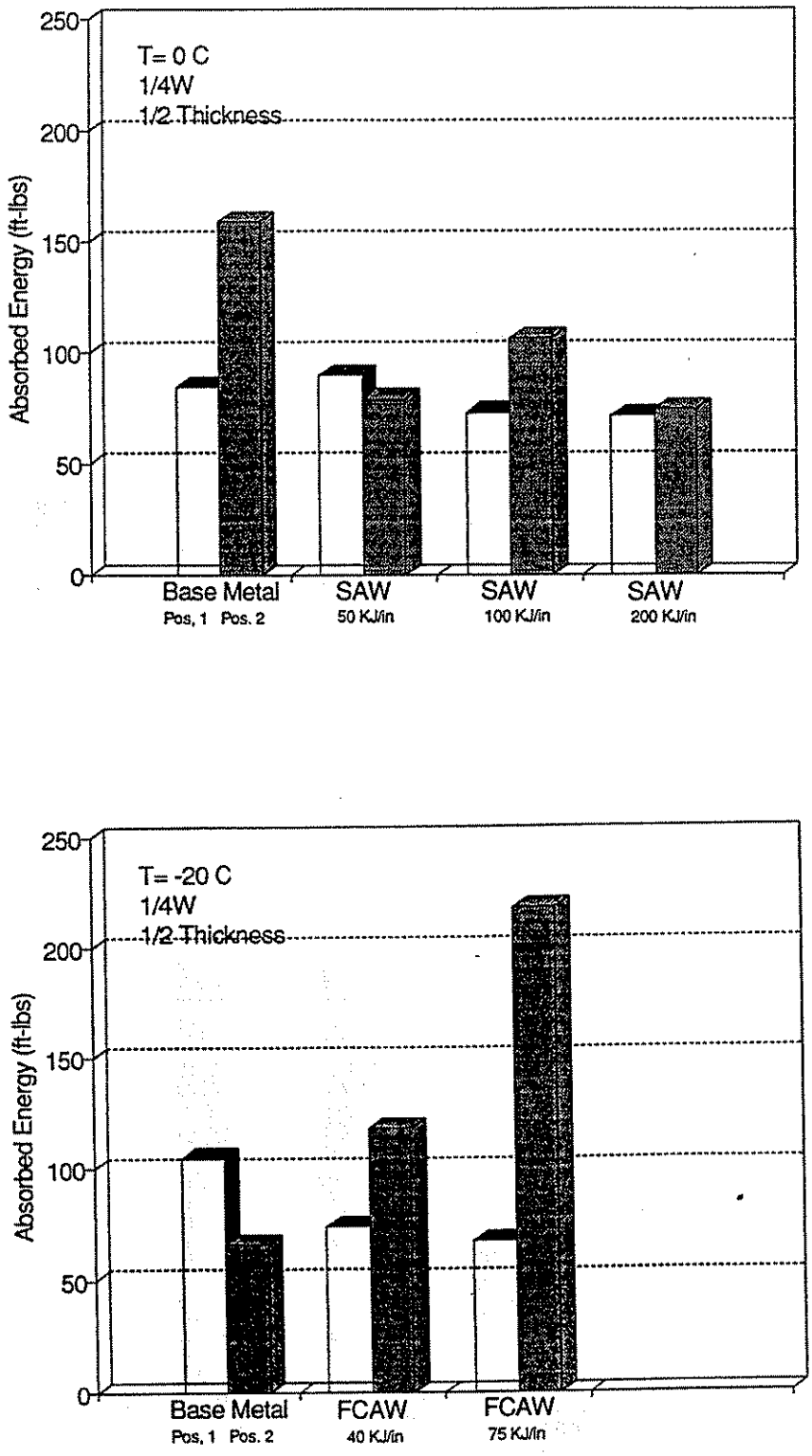

Fig. 41 HAZ Charpy V-Notch Test Results at Position 1/4 W - 1/2 Thickness

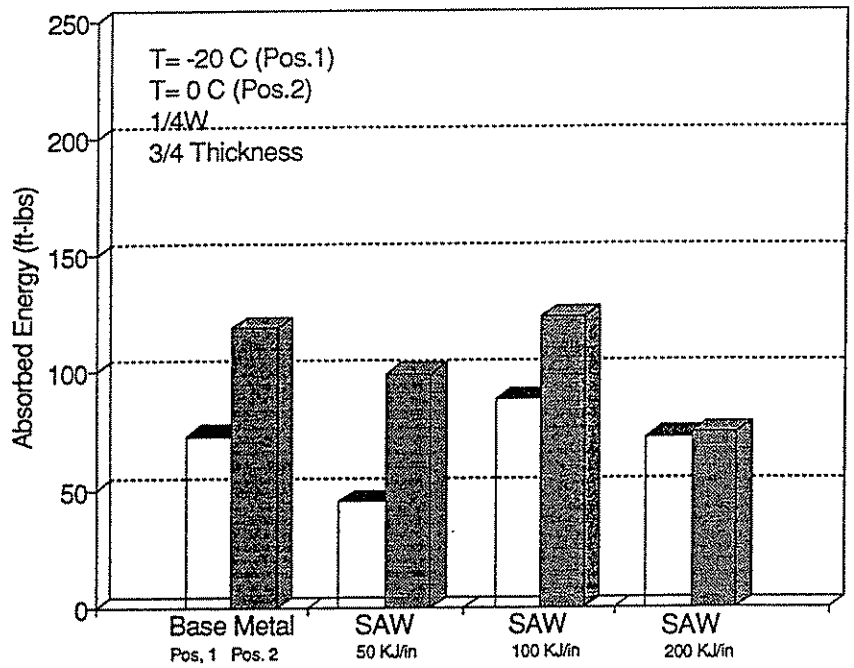

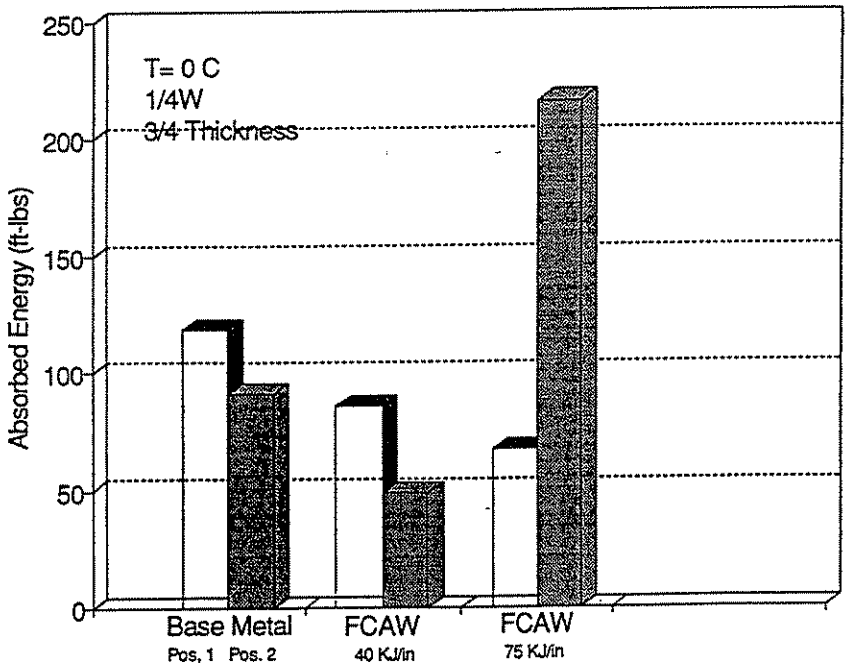

Fig. 42 HAZ Charpy V-Notch Test Results at Position 1/4 W - 3/4 Thickness

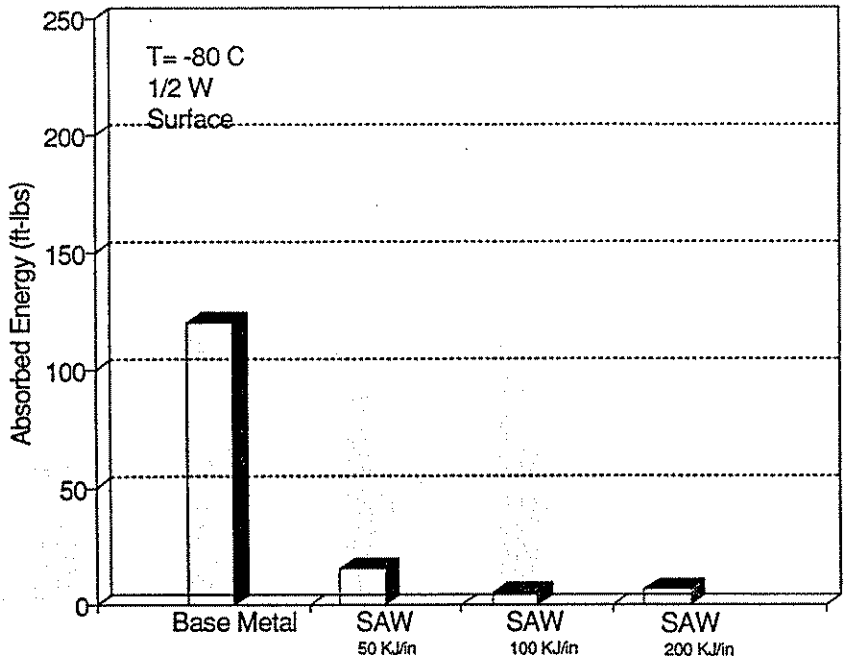

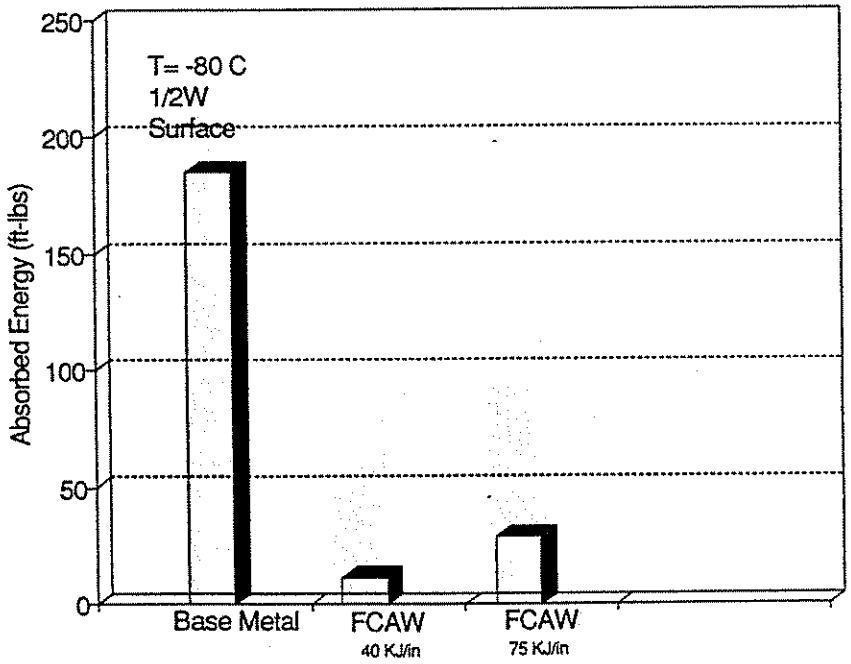

Fig. 43 HAZ Charpy V-Notch Test Results at Position 1/2 W - Surface

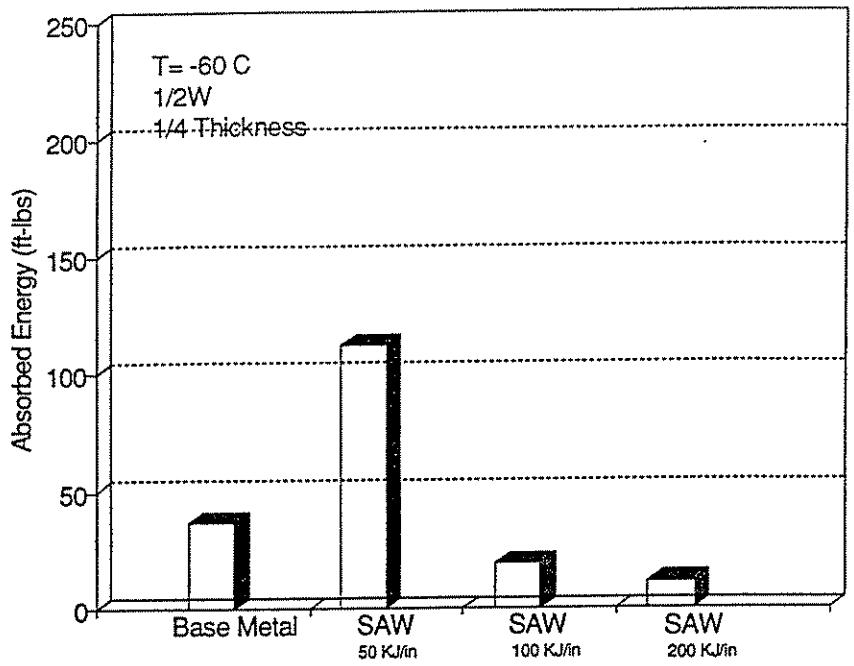

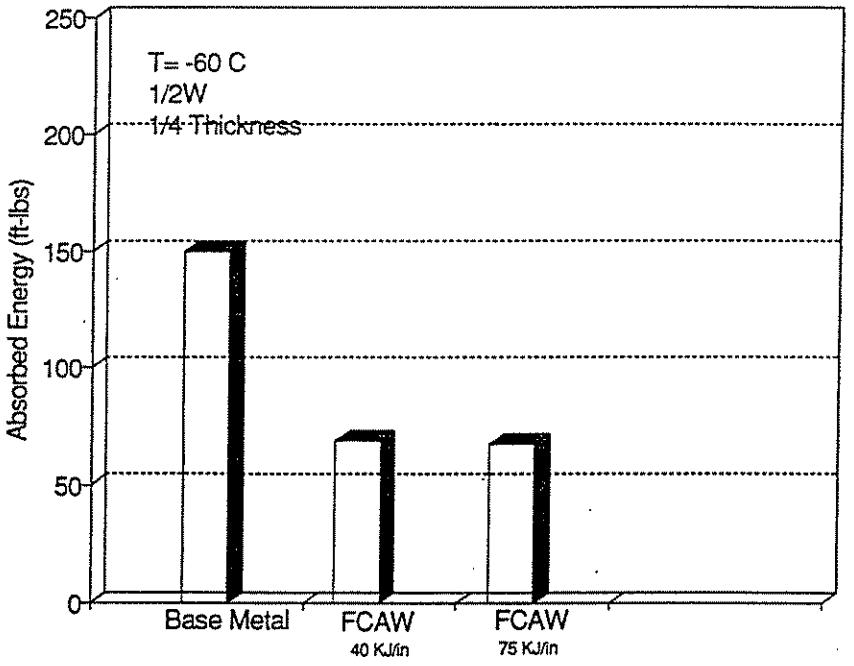

Fig. 44 HAZ Charpy V-Notch Test Results at Position 1/2 W - 1/4 Thickness

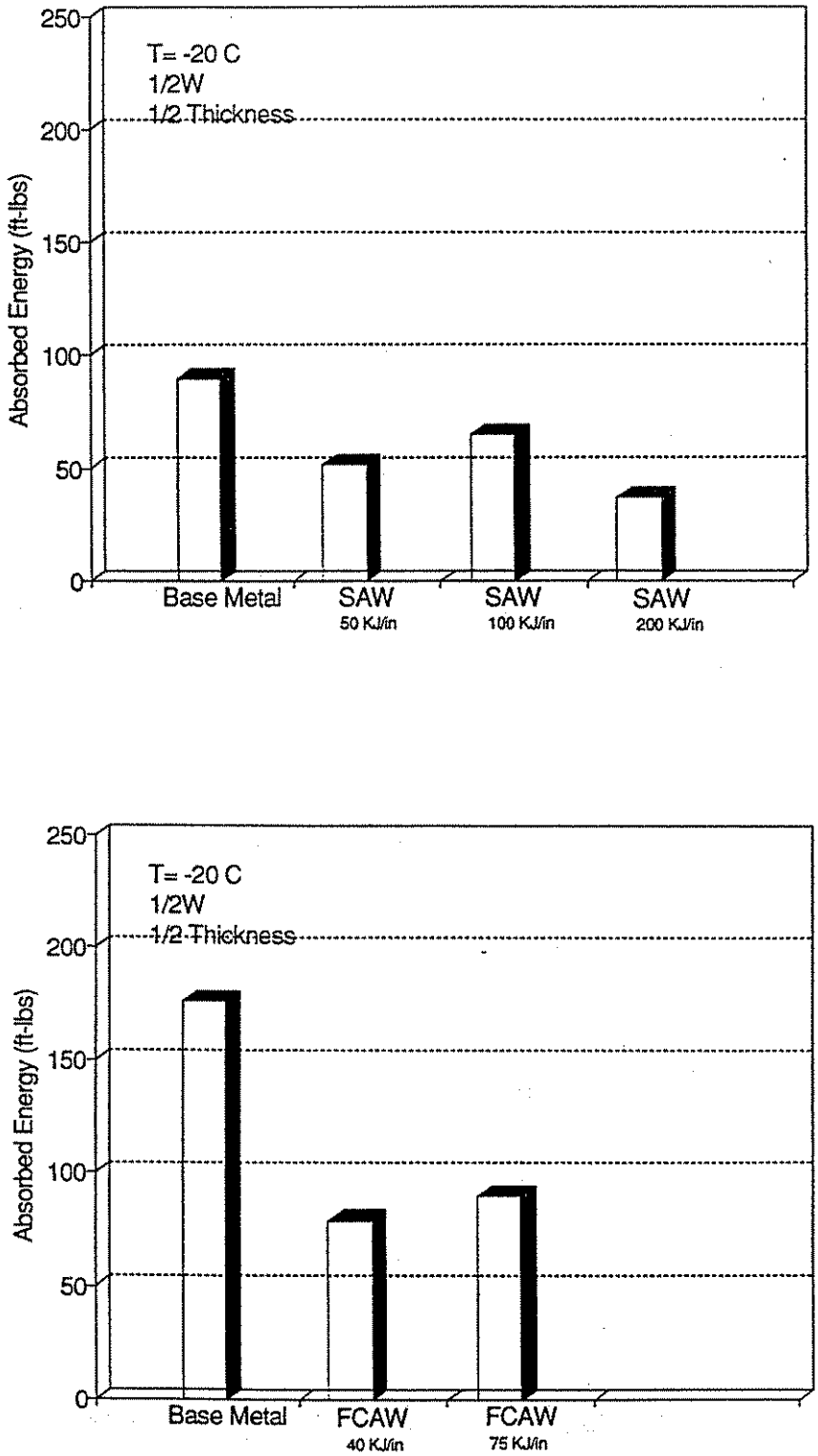

Fig. 45 HAZ Charpy V-Notch Test Results at Position 1/2 W - 1/2 Thickness

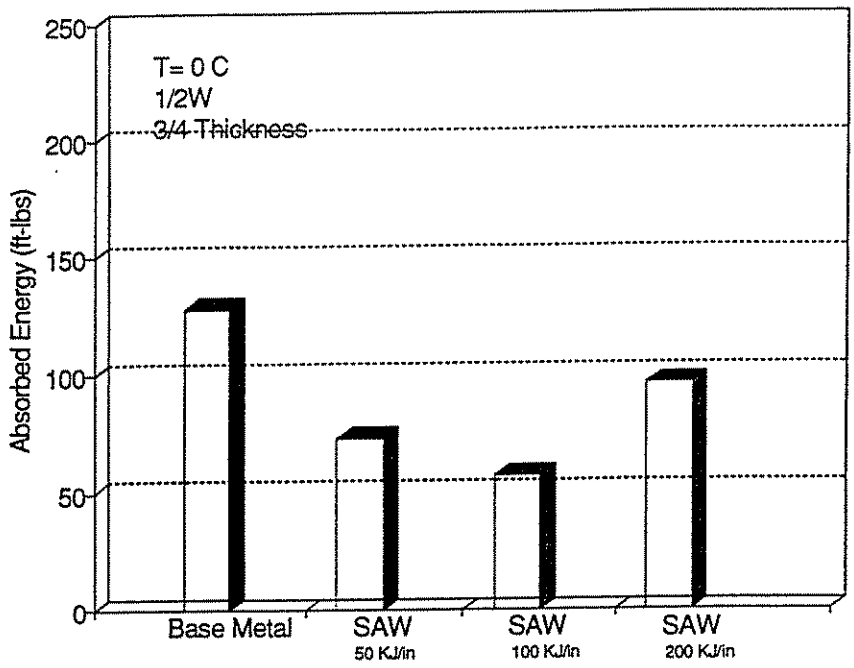

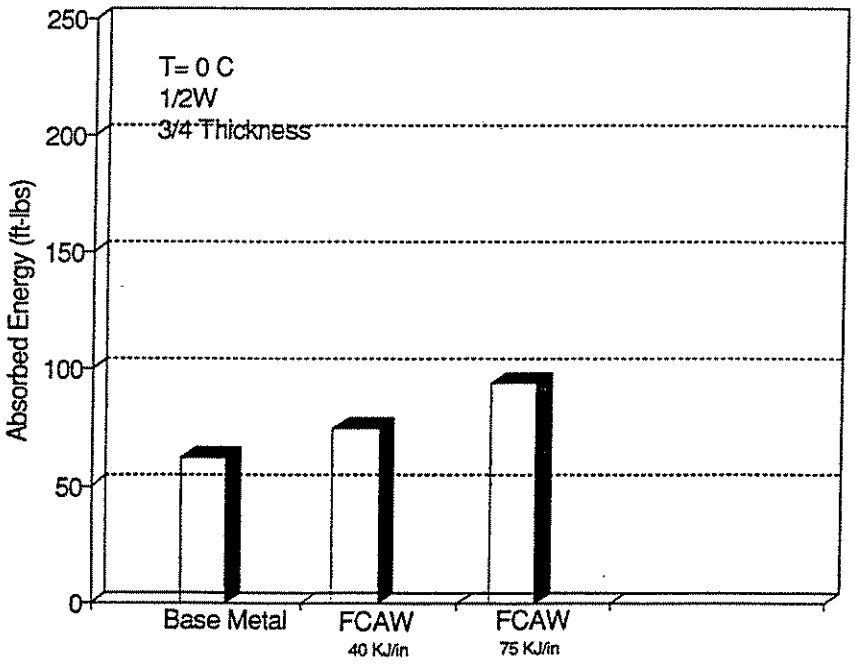

Fig. 46 HAZ Charpy V-Notch Test Results at Position 1/2 W - 3/4 Thickness

APPENDIX A

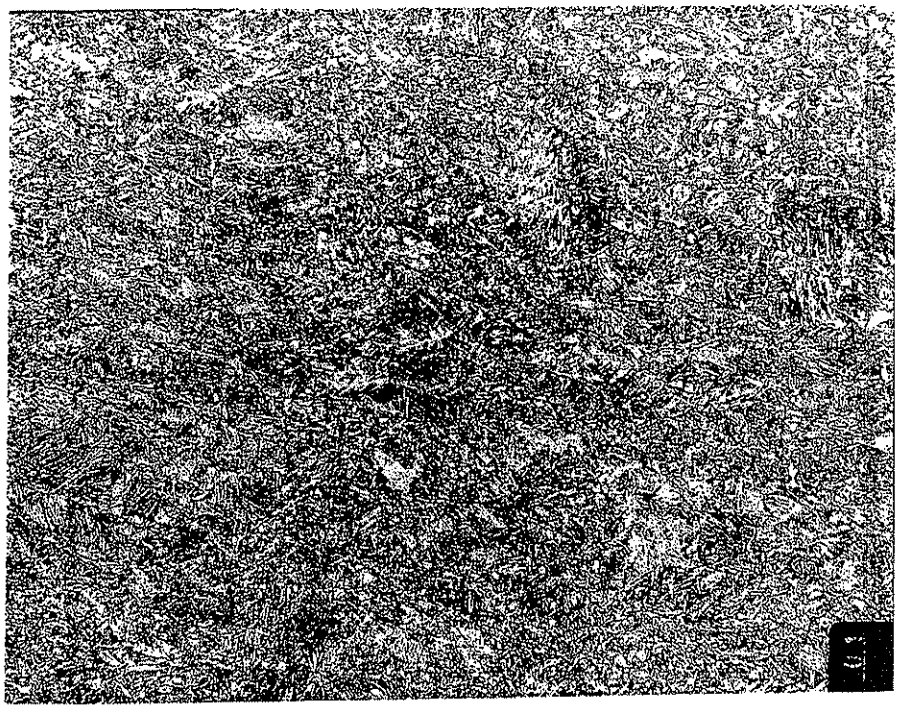

Flange Microstructure at 1/6W-Surface, Pos.1
Heat No. 89322-9009(100X), [Photo 9/91/49]

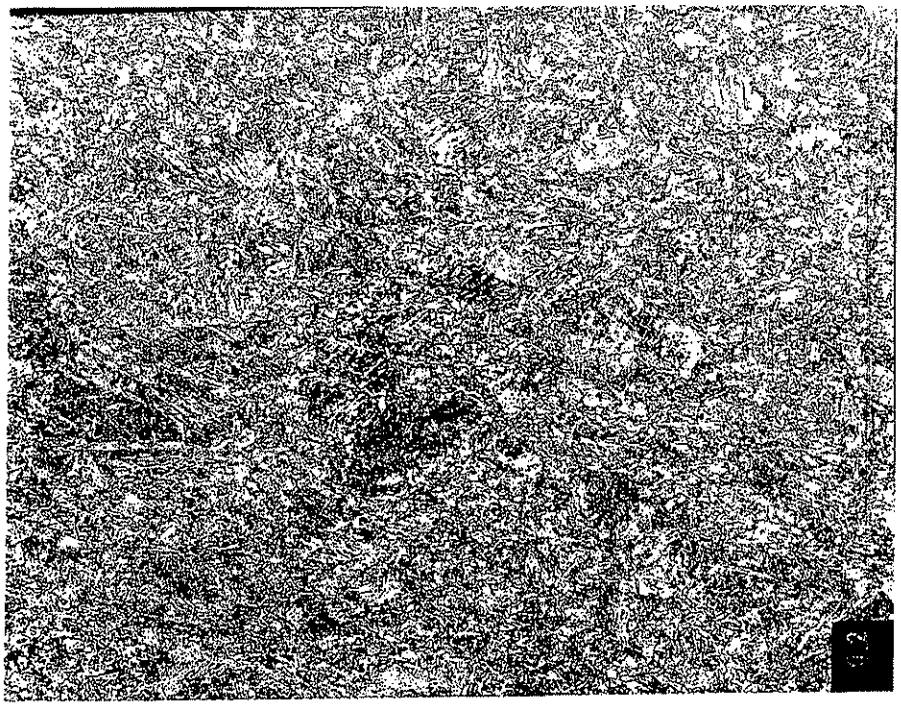

Flange Microstructure at 1/6W-Surface, Pos.2
Heat No. 89322-9009(100X), [Photo 9/91/50]

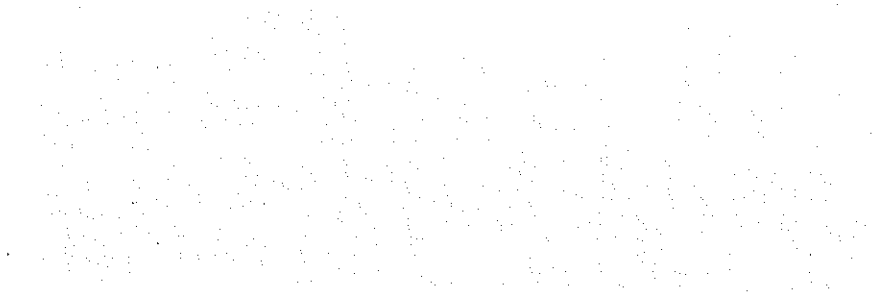

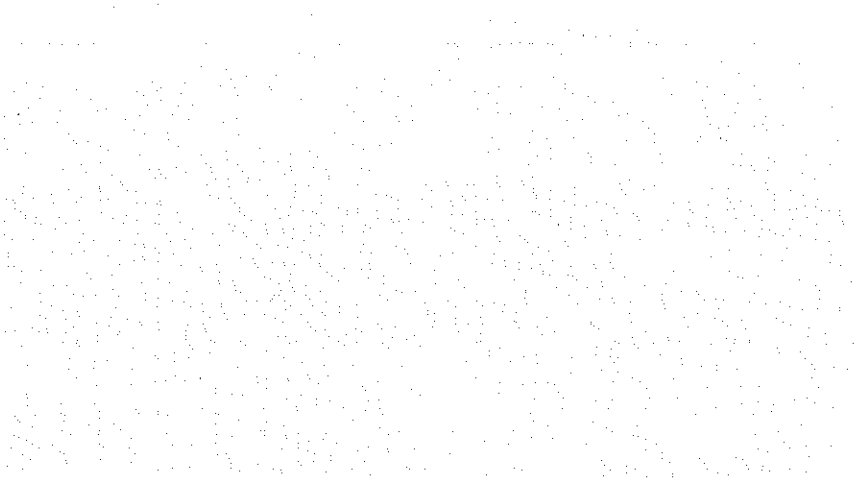

Flange Microstructure at 1/6W-1/4T, Pos.1
Heat No. 89322-9009(100X), [Photo 9/91/51]

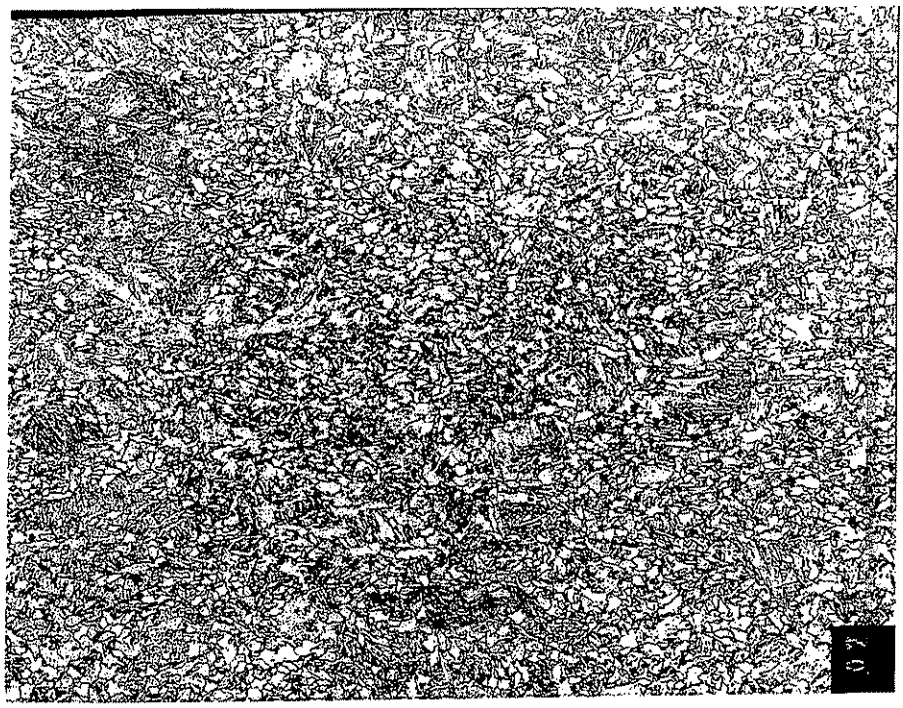

Flange Microstructure at 1/6W-1/4T, Pos.2
Heat No. 89322-9009(100X), [Photo 9/91/52]

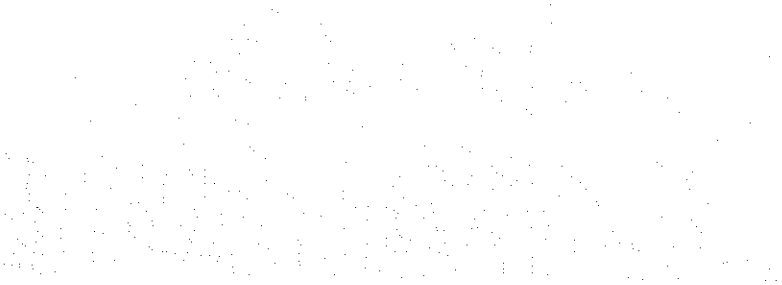

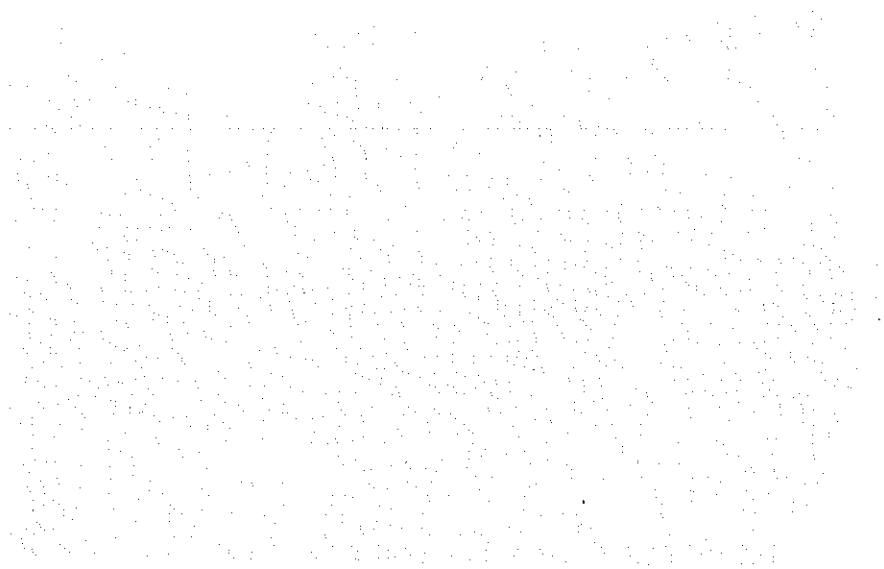

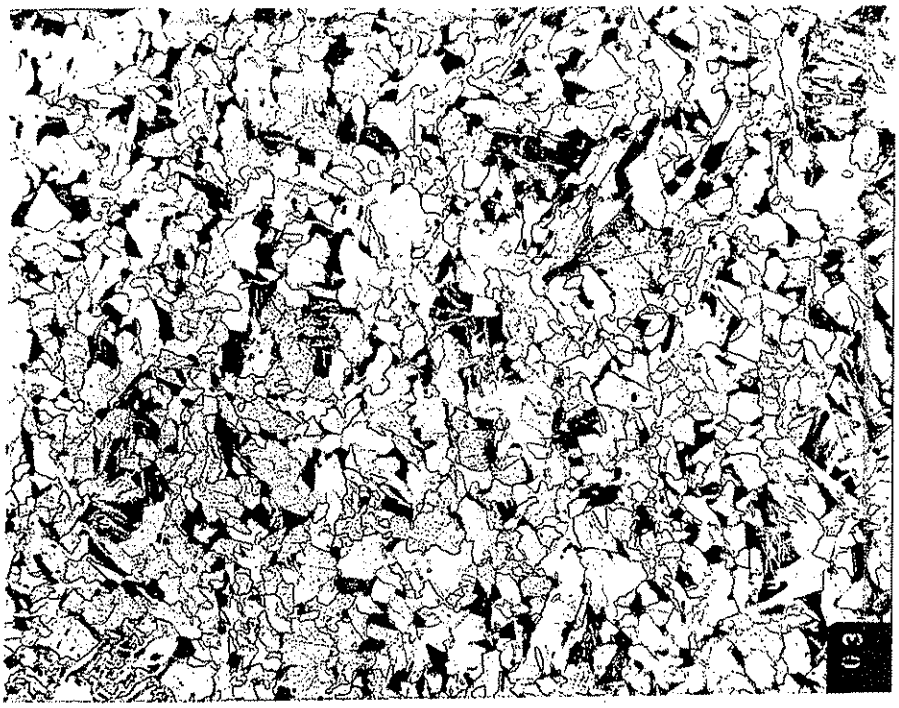

Flange Microstructure at 1/6W-1/2T, Pos.1
Heat No. 89322-9009(100X), [Photo 9/91/54]

Flange Microstructure at 1/6W-1/2T, Pos.2
Heat No. 89322-9009(100X), [Photo 9/91/53]

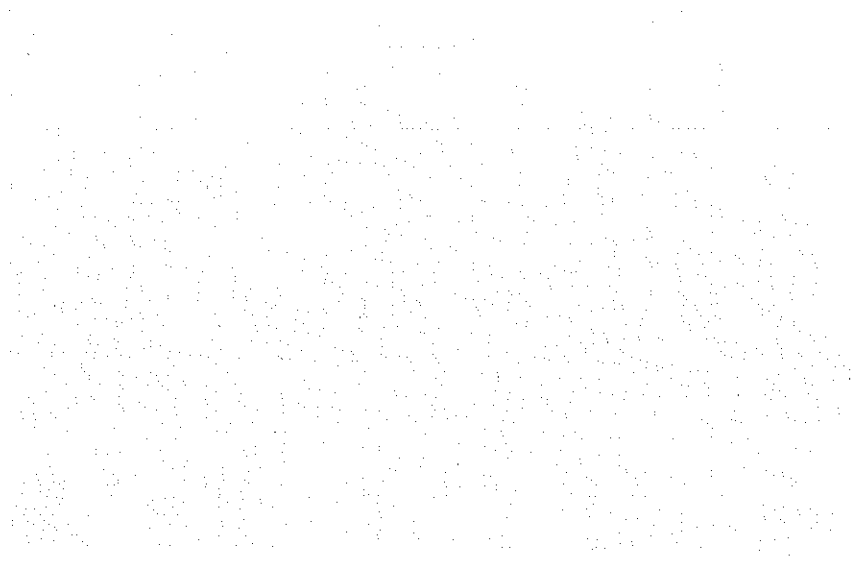

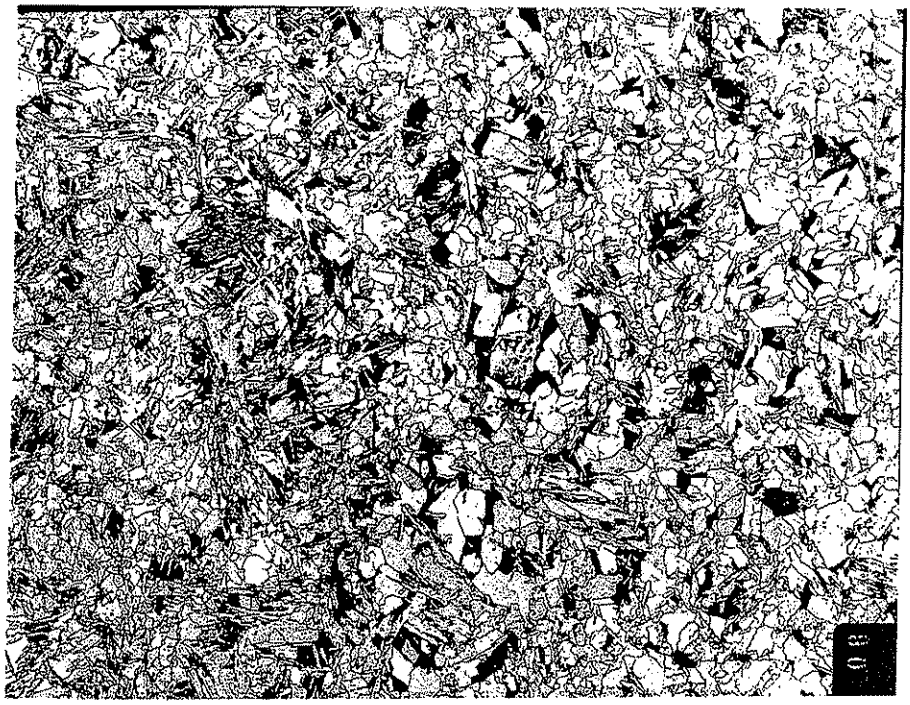

Flange Microstructure at 1/6W-3/4T, Pos.1
Heat No. 89322-9009(100X), [Photo 9/91/55]

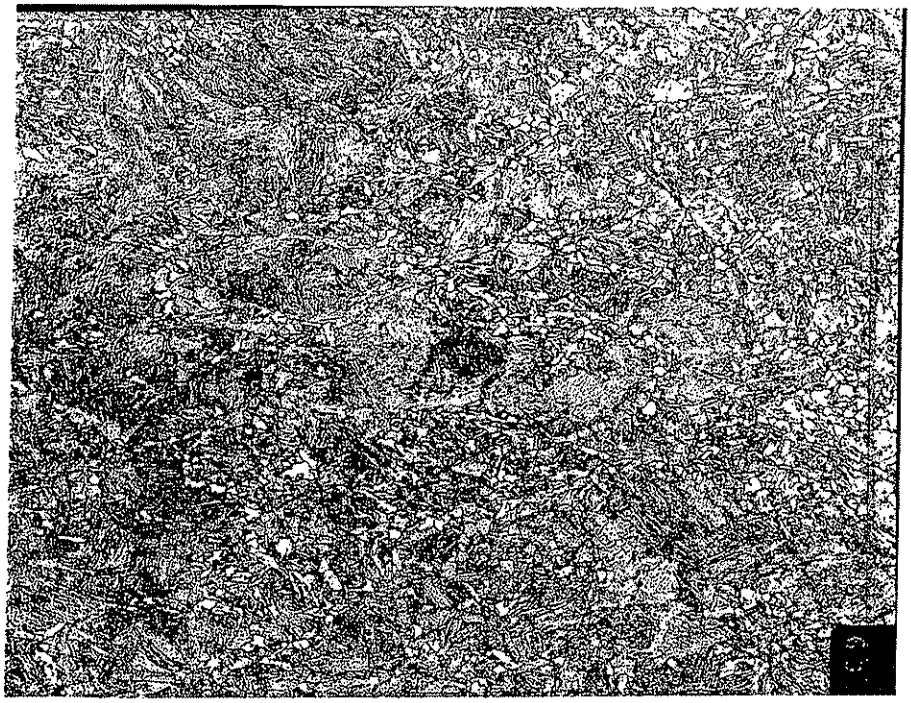

Flange Microstructure at 1/6W-3/4T, Pos.2
Heat No. 89322-9009(100X), [Photo 9/91/56]

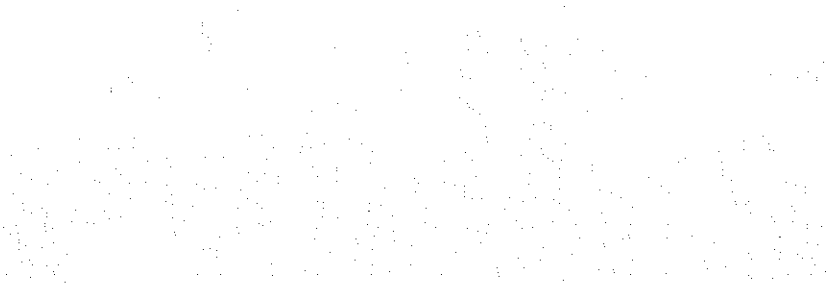

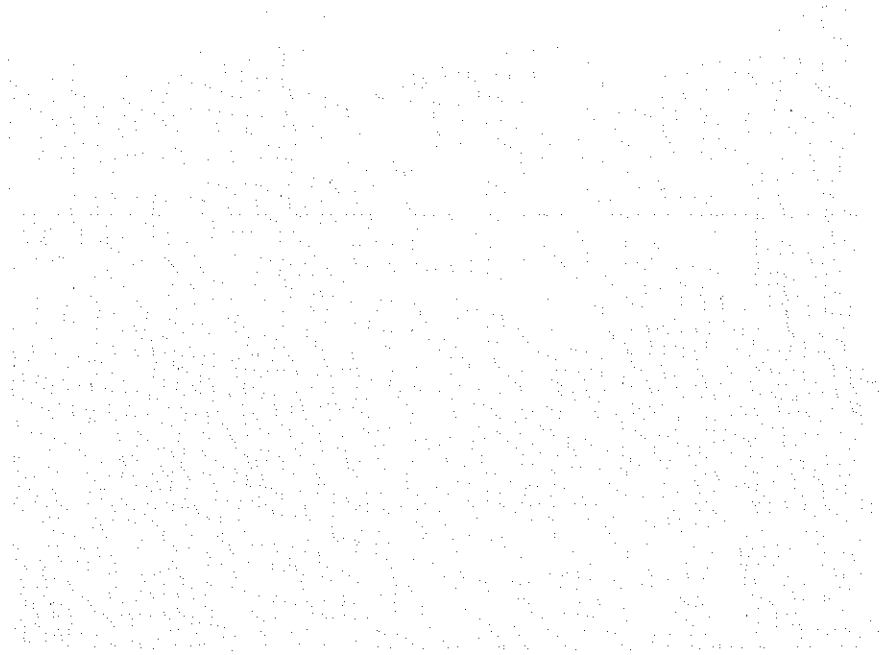

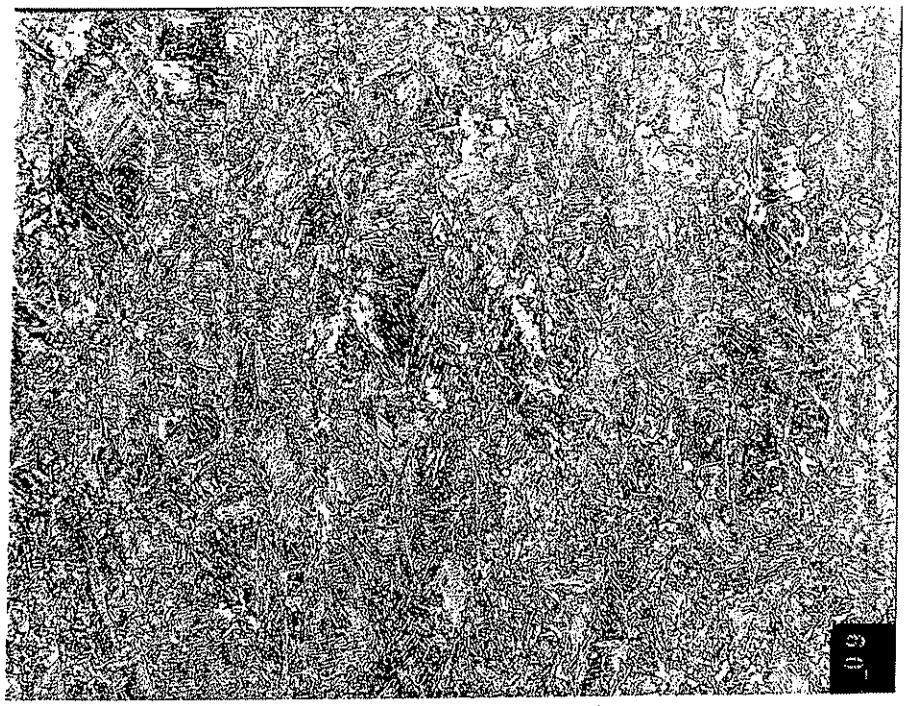

Flange Microstructure at 1/4W-Surface, Pos.1
Heat No. 89322-9009(100X), [Photo 9/91/45]

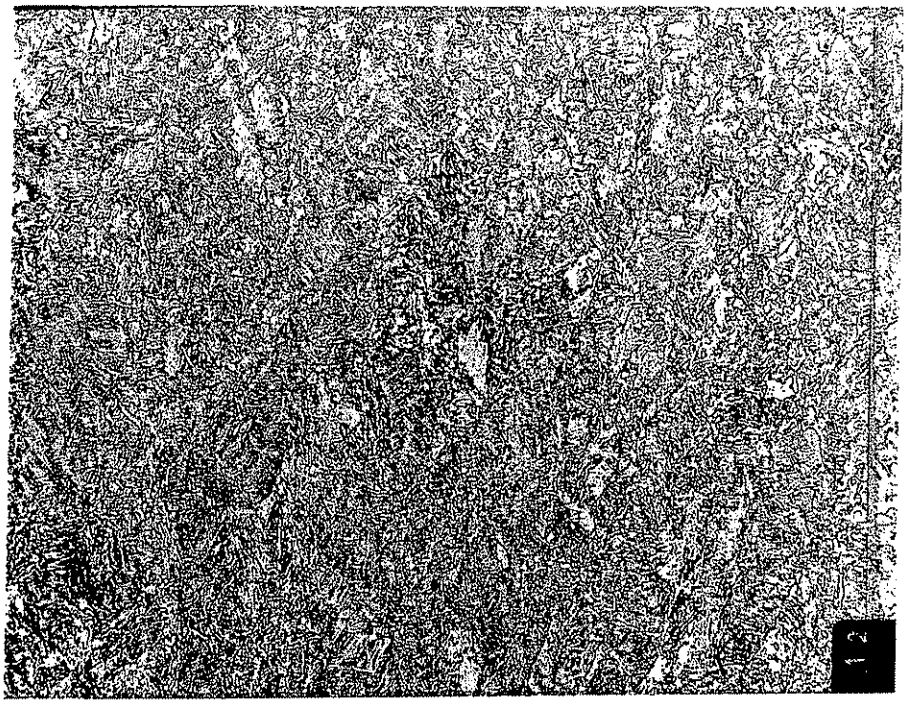

Flange Microstructure at 1/4W-Surface, Pos.2
Heat No. 89322-9009(100X), [Photo 9/91/41]

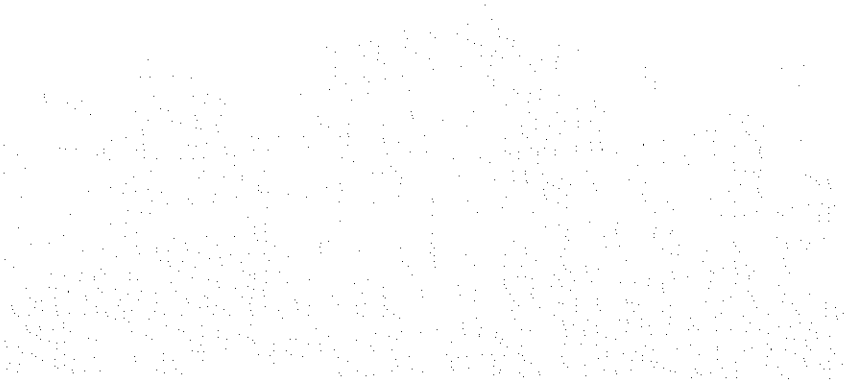

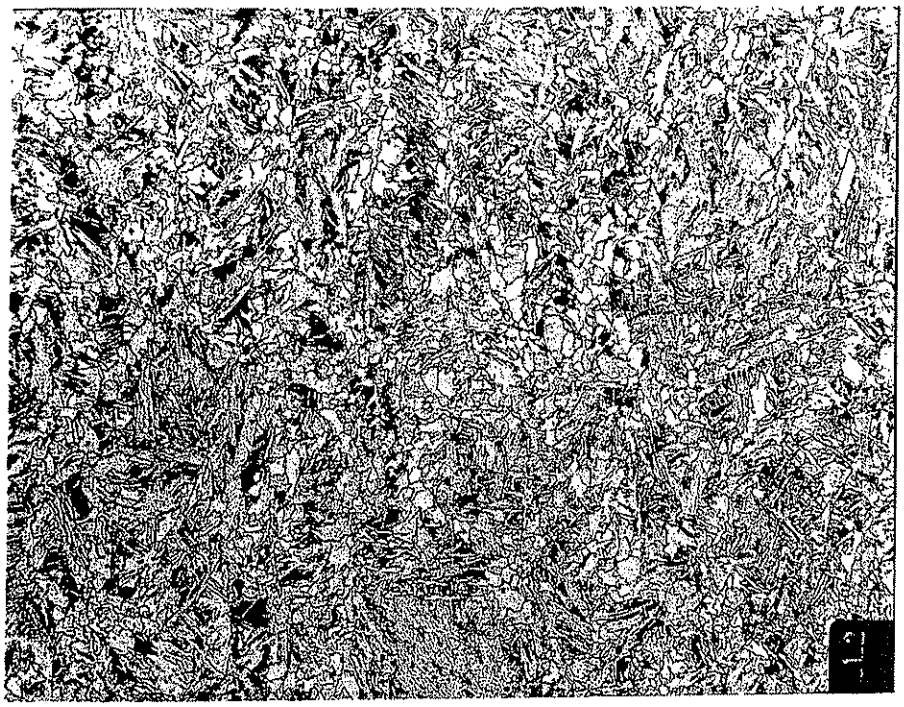

Flange Microstructure at 1/4W-1/4T, Pos.1
Heat No. 89322-9009(100X), [Photo 9/91/46]

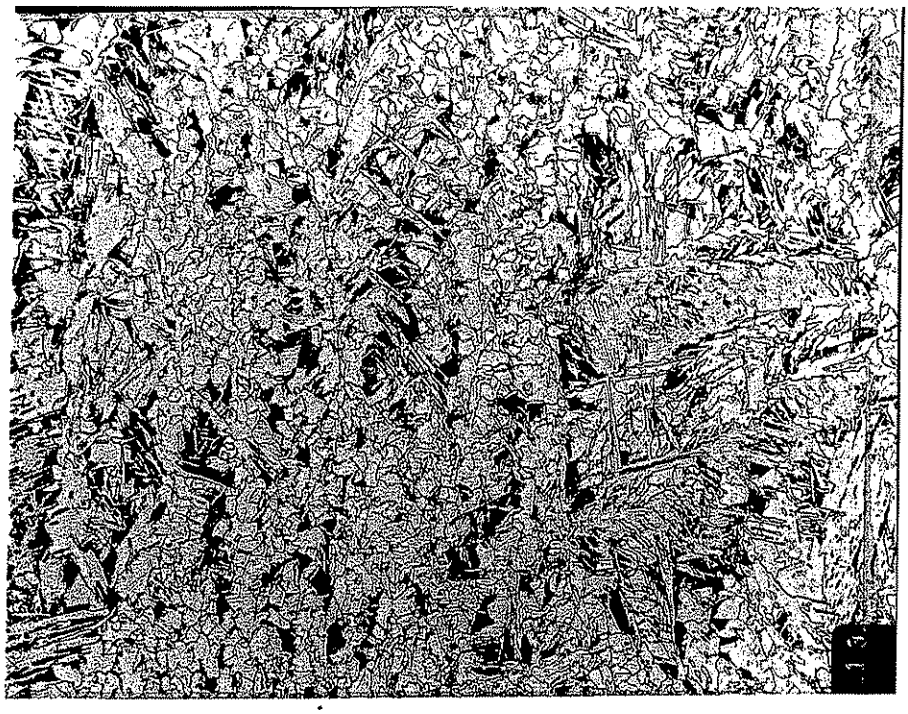

Flange Microstructure at 1/4W-1/4T, Pos.2
Heat No. 89322-9009(100X), [Photo 9/91/42]

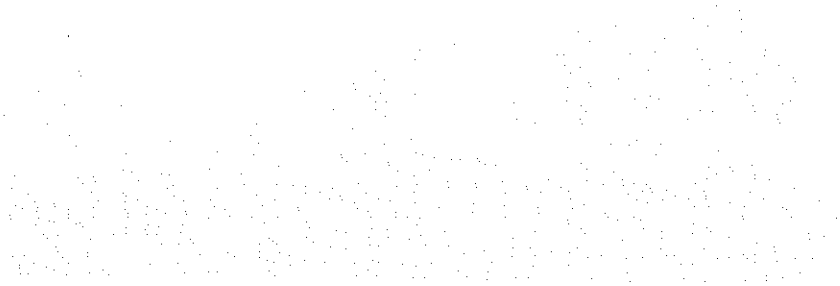

Flange Microstructure at 1/4W-1/2T, Pos.1
Heat No. 89322-9009(100X), [Photo 9/91/47]

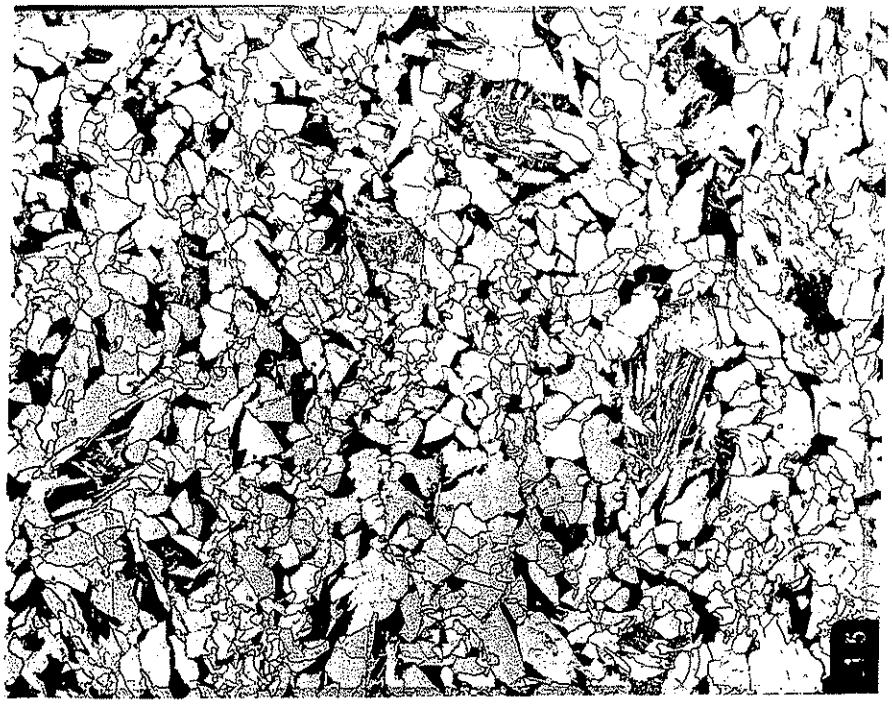

Flange Microstructure at 1/4W-1/2T, Pos.2
Heat No. 89322-9009(100X), [Photo 9/91/43]

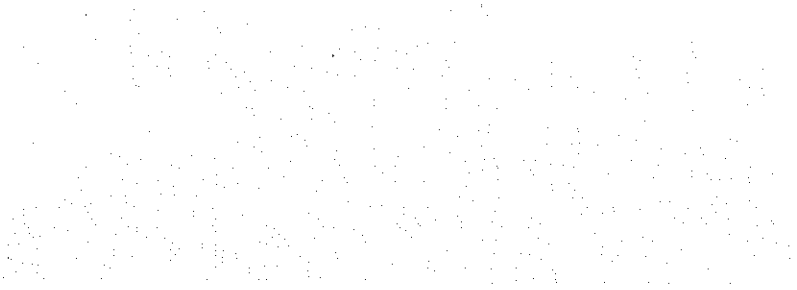

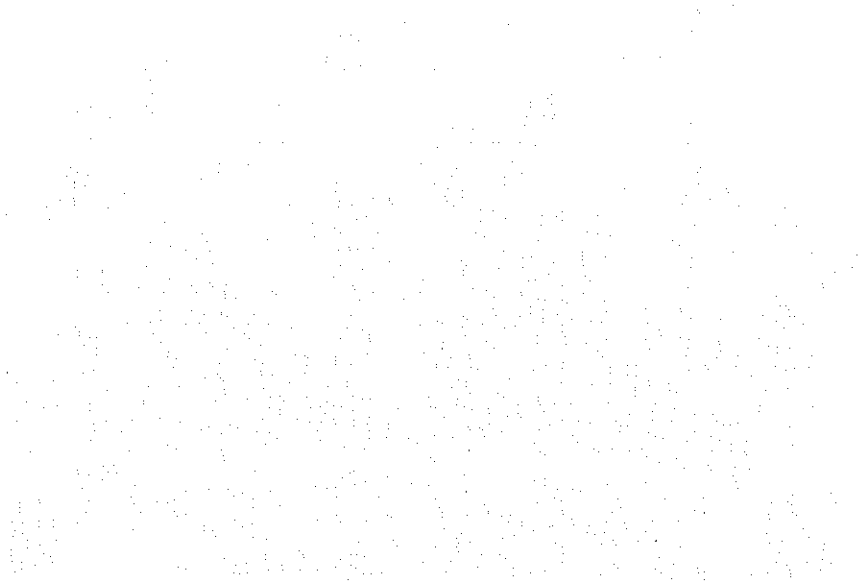

Flange Microstructure at 1/4W-3/4T, Pos.1
Heat No. 89322-9009(100X), [Photo 9/91/48]

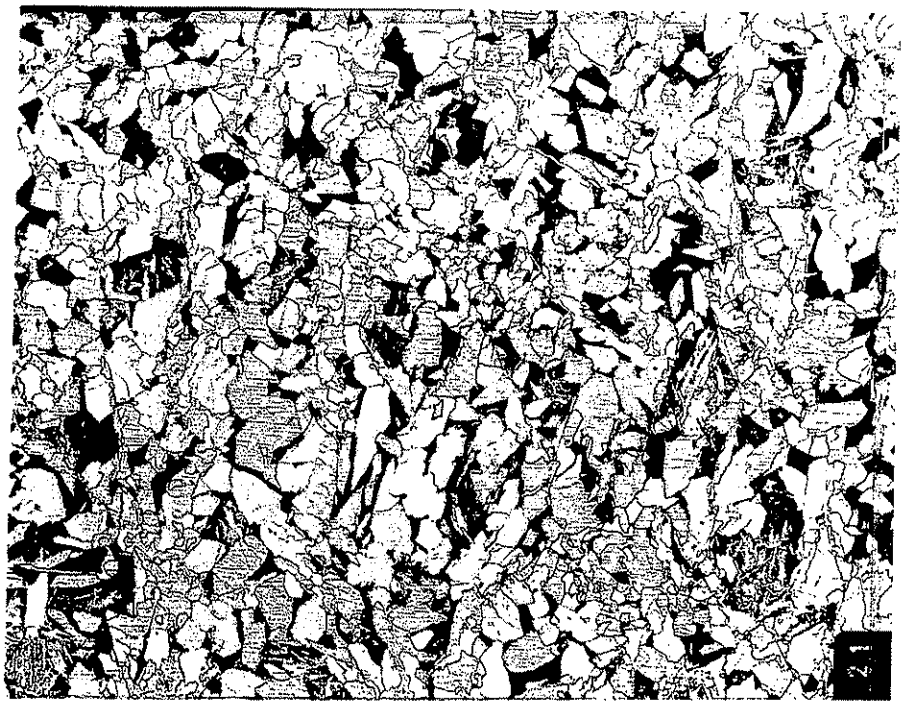

Flange Microstructure at 1/4W-3/4T, Pos.2
Heat No. 89322-9009(100X), [Photo 9/91/44]

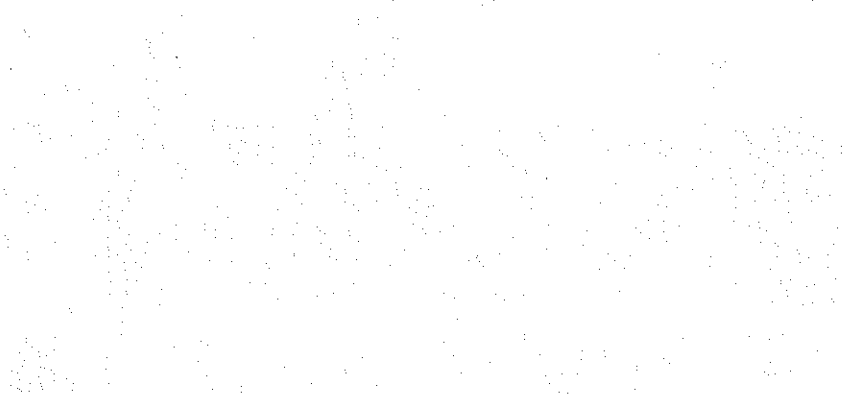

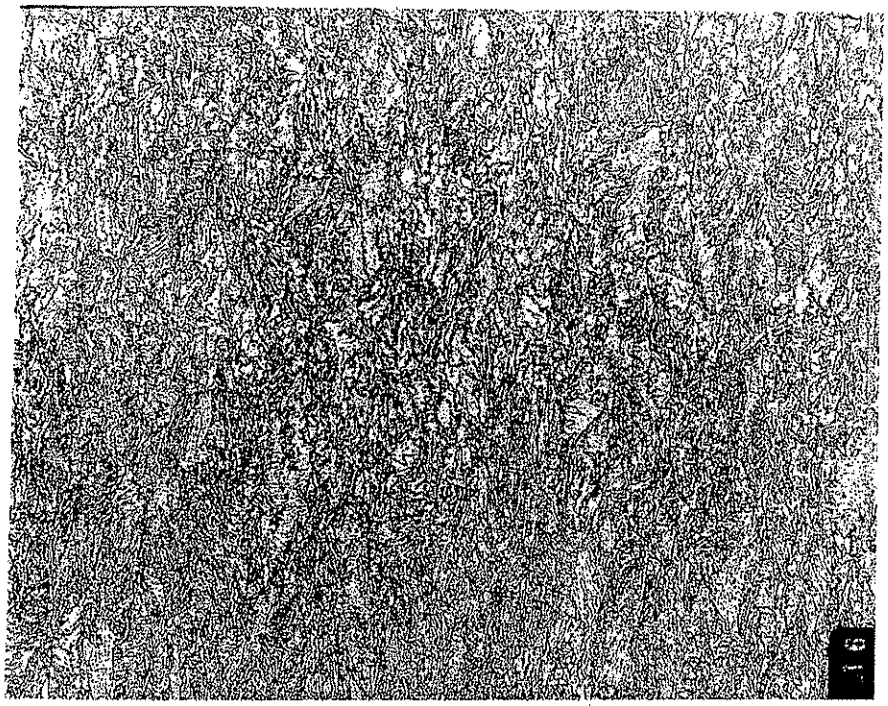

Flange Microstructure at 1/2W-Surface
Heat No. 89322-9009(100X), [Photo 9/91/37]

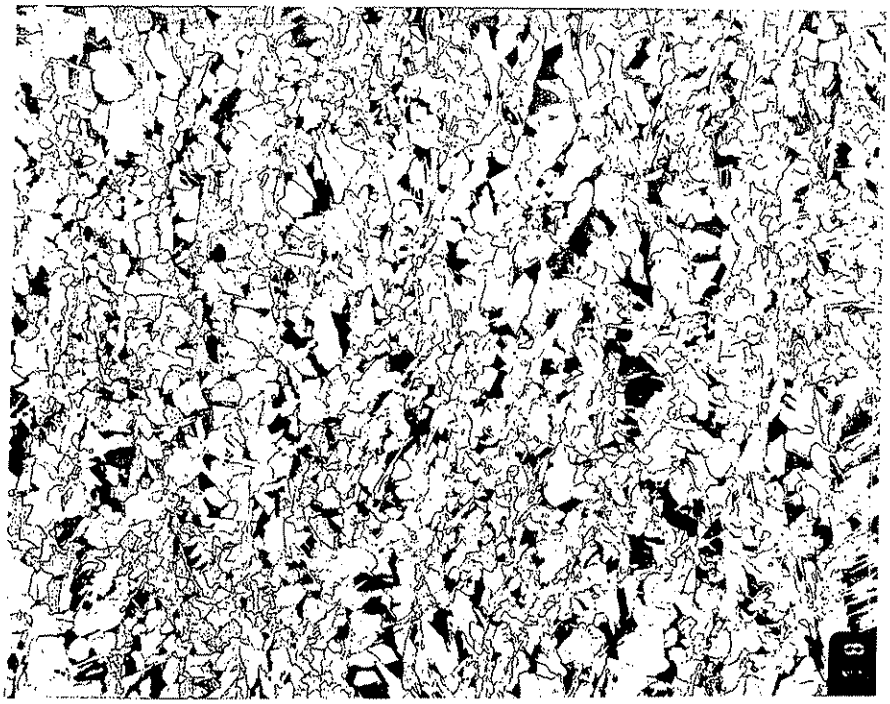

Flange Microstructure at 1/2W-1/4T
Heat No. 89322-9009(100X), [Photo 9/91/38]

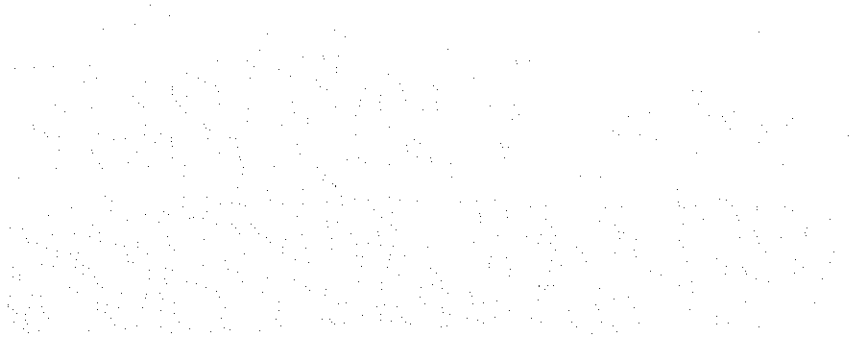

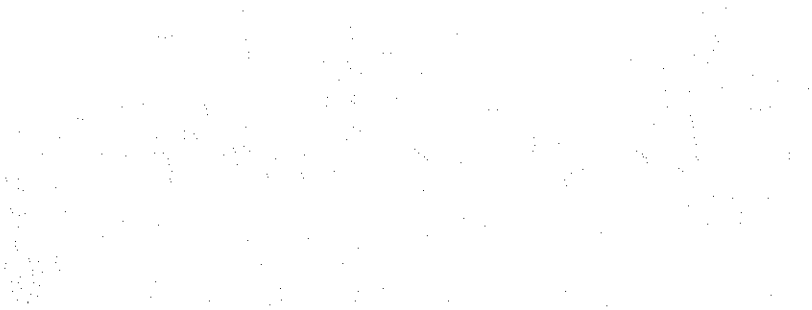

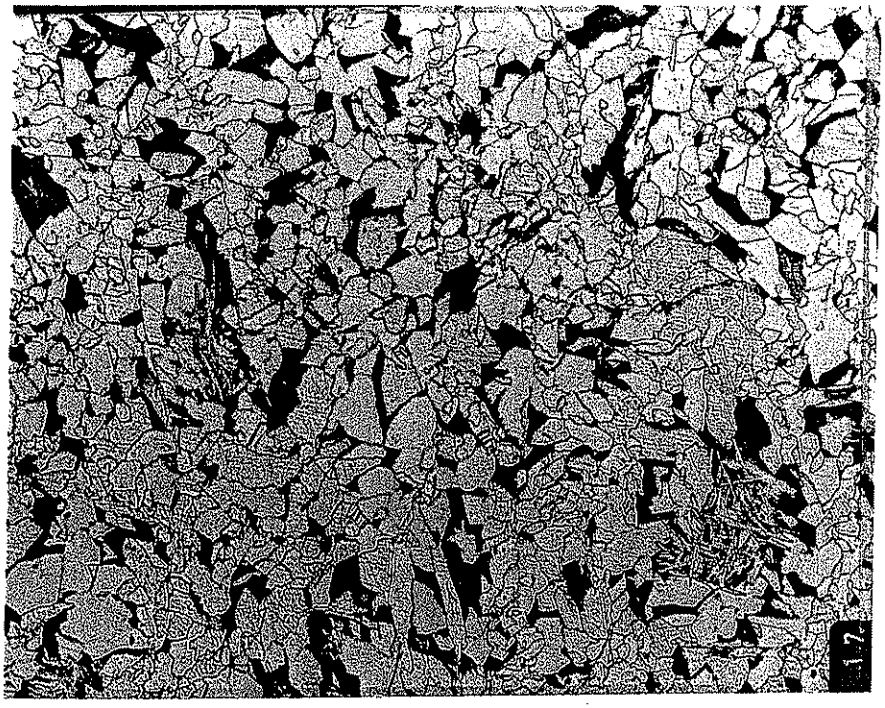

Flange Microstructure at 1/2W-1/2T
Heat No. 89322-9009(100X), [Photo 9/91/39]

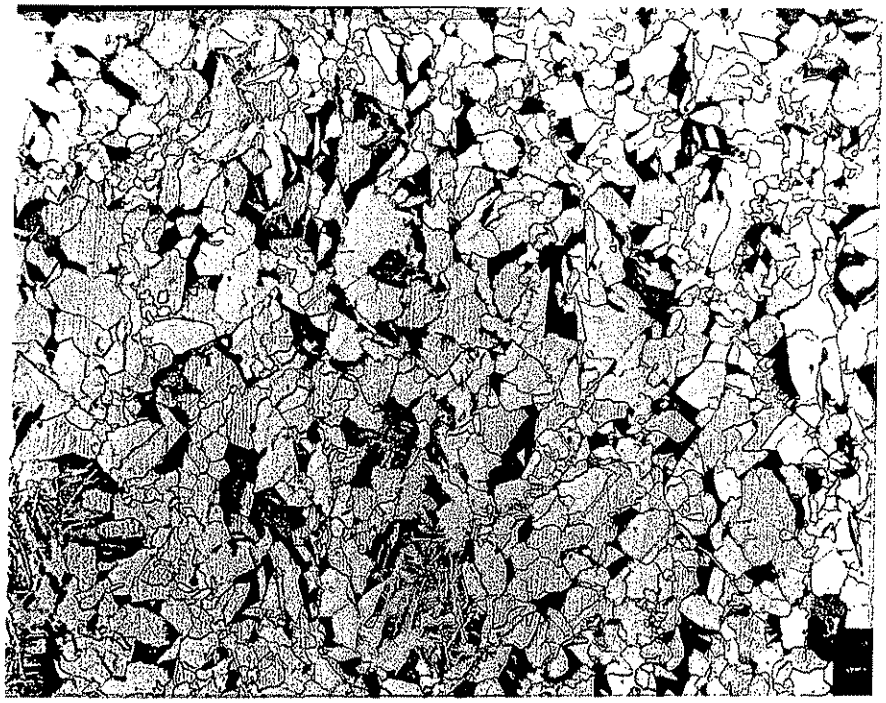

Flange Microstructure at 1/2W-3/4T
Heat No. 89322-9009(100X), [Photo 9/91/40]